

1999

Petrology and petrogenesis of the Cardinal Peak pluton, North Cascades, Washington

Laura A. Parent
San Jose State University

Follow this and additional works at: https://scholarworks.sjsu.edu/etd_theses

Recommended Citation

Parent, Laura A., "Petrology and petrogenesis of the Cardinal Peak pluton, North Cascades, Washington" (1999). *Master's Theses*. 1943.
DOI: <https://doi.org/10.31979/etd.26ya-mcs6>
https://scholarworks.sjsu.edu/etd_theses/1943

This Thesis is brought to you for free and open access by the Master's Theses and Graduate Research at SJSU ScholarWorks. It has been accepted for inclusion in Master's Theses by an authorized administrator of SJSU ScholarWorks. For more information, please contact scholarworks@sjsu.edu.

INFORMATION TO USERS

This manuscript has been reproduced from the microfilm master. UMI films the text directly from the original or copy submitted. Thus, some thesis and dissertation copies are in typewriter face, while others may be from any type of computer printer.

The quality of this reproduction is dependent upon the quality of the copy submitted. Broken or indistinct print, colored or poor quality illustrations and photographs, print bleedthrough, substandard margins, and improper alignment can adversely affect reproduction.

In the unlikely event that the author did not send UMI a complete manuscript and there are missing pages, these will be noted. Also, if unauthorized copyright material had to be removed, a note will indicate the deletion.

Oversize materials (e.g., maps, drawings, charts) are reproduced by sectioning the original, beginning at the upper left-hand corner and continuing from left to right in equal sections with small overlaps.

Photographs included in the original manuscript have been reproduced xerographically in this copy. Higher quality 6" x 9" black and white photographic prints are available for any photographs or illustrations appearing in this copy for an additional charge. Contact UMI directly to order.

Bell & Howell Information and Learning
300 North Zeeb Road, Ann Arbor, MI 48106-1346 USA

UMI[®]
800-521-0600

PETROLOGY AND PETROGENESIS OF THE CARDINAL PEAK PLUTON,
NORTH CASCADES, WASHINGTON

A Thesis

Presented to

The Faculty of the Department of Geology

San Jose State University

In Partial Fulfillment

of the requirements for the Degree

Master of Science

by

Laura A. Parent

December 1999

UMI Number: 1397741

UMI[®]

UMI Microform 1397741

Copyright 2000 by Bell & Howell Information and Learning Company.

All rights reserved. This microform edition is protected against
unauthorized copying under Title 17, United States Code.

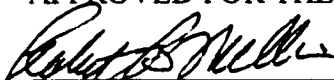
Bell & Howell Information and Learning Company
300 North Zeeb Road
P.O. Box 1346
Ann Arbor, MI 48106-1346

© 1999

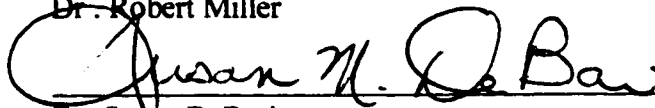
Laura A. Parent

ALL RIGHTS RESERVED

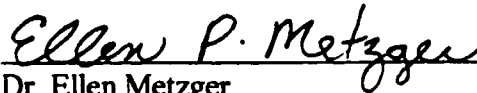
APPROVED FOR THE DEPARTMENT OF GEOLOGY



Dr. Robert Miller



Dr. Susan DeBari



Dr. Ellen Metzger

APPROVED FOR THE UNIVERSITY



ABSTRACT

PETROLOGY AND PETROGENESIS OF THE CARDINAL PEAK PLUTON, NORTH CASCADES, WASHINGTON

by Laura A. Parent

The focus of this study is on the magmatic evolution of the 72 Ma Cardinal Peak pluton. This arc-type pluton is predominantly tonalitic, although its northwest and central sections contain significant quantities of mafic rocks. Field evidence and geochemical data indicate that both fractional crystallization and melting of a mafic lower crust were important processes in the evolution of the pluton, and that all sections of the pluton were constructed by numerous magma pulses. This study concludes that the following sequence of events formed the pluton: 1) Evolved mafic to felsic mantle-derived magmas were emplaced as the northwest and central Border Complex and the northwest Main Phase. 2) Heat from these mantle-derived magmas melted the lower crust and caused production of a tonalitic magma, which was emplaced as the central and southeast Main Phase. 3) Minor mafic magmatism continued during the emplacement of the central and southeast Main Phase.

ACKNOWLEDGEMENTS

This project was supported by grants from both Sigma Xi and the Geological Society of America. Drs. Susan DeBari and Robert Miller introduced me to this project and the North Cascades, I thank them for their enthusiasm and support. Field assistance was provided by Roger Lewis, who always had a helping hand and a funny story. Robert Jones of Stanford was helpful, patient and kind during my visits to his electron microprobe.

TABLE OF CONTENTS

	Page
INTRODUCTION.....	1
Petrologic Models for Formation of Tonalitic Magmas in Arcs.....	2
Magma Chamber Construction.....	3
TECTONIC AND GEOLOGIC SETTING.....	6
DESCRIPTION OF THE CARDINAL PEAK PLUTON.....	12
Previous Work.....	12
Field Descriptions and Petrology.....	13
Holden Assemblage.....	13
General Description of the Cardinal Peak Pluton.....	16
NW Section: from Hilgard Pass to Dole Lakes.....	17
Border Complex.....	17
Main Phase.....	18
Central Section: from Pinnacle Mountain to Cardinal Peak.....	20
Border Complex.....	20
Main Phase.....	21
Southeast Section: from Cardinal Peak to Crow Hill.....	23
Main Phase.....	23
PETROGRAPHY.....	27
Border Complex.....	27

Main Phase	30
WHOLE ROCK CHEMISTRY	36
Previous Work and Scope of Present Study.....	36
Analytical Methods	36
Major Element chemistry.....	39
Trace Element Chemistry	43
Rare Earth Element Chemistry	47
Cumulates	48
Hornblendite	48
Plagioclase accumulation.....	48
Mafic Rocks	48
Northwest.....	48
Central.....	51
Mafic Tonalite (60-65% SiO ₂)	51
Northwest.....	51
Central.....	51
Southeast	53
Felsic Tonalite (>65% SiO ₂)	53
Northwest.....	53
Central.....	53
Southeast	53
MINERAL CHEMISTRY	55

Analytical Methods	55
Plagioclase	55
Amphibole	60
Biotite.....	65
Epidote	65
PRESSURE AND TEMPERATURE CONSTRAINTS ON PLUTON	
CRYSTALLIZATION	71
Constraints on Pressure From Magmatic Epidote	71
Al-in-Hornblende Barometry	71
Hornblende-Plagioclase Thermometry	72
Apatite Saturation Thermometry	75
Zircon Saturation Thermometry	76
Summary of temperature data.....	77
PETROLOGIC PROCESSES.....	80
Origin of the Mafic Rocks	80
Origin of the Tonalite: Fractional Crystallization.....	85
Origin of the Tonalite: Lower-Crustal Melting.....	91
Origin of the Tonalite: Magma Mixing.....	99
Assimilation of Crustal Rocks.....	101
MAGMA CHAMBER CONSTRUCTION	102
CONCLUSIONS.....	107
REFERENCES.....	110

APPENDIX A: CHEMICAL ANALYSES FROM CATER (1982)	118
APPENDIX B: WHOLE ROCK CHEMICAL ANALYSES.....	120
APPENDIX C: PARTITION COEFFICIENTS	129

LIST OF ILLUSTRATIONS

Figure	Page
1. Location Map for the Cardinal Peak Pluton.....	4
2. Map Showing Offset of North Cascades Core From Coast Plutonic Complex.....	7
3. Major Terranes of Northwestern Washington.....	9
4. Geologic Map of the Cardinal Peak Pluton and Surrounding Area.....	10
5. Sample and Geographic Location Map.....	14
6. Photograph of Dikelet of Cardinal Peak Tonalite Intruding Country Rock.....	15
7. Photograph of Contact of Tonalite and Diorite in NW Border Complex.....	15
8. Photograph Illustrating Heterogeneity of NW Main Phase.....	19
9. Photograph of Contact of Tonalite and Diorite in NW Main Phase.....	19
10. Photograph of Holden Assemblage Xenolith.....	22
11. Photograph of Schlieren in Central Main Phase.....	22
12. Photograph Showing Typical SE Main Phase Biotite Tonalite.....	25
13. Photograph of Hornblende-bearing Tonalite Dikes.....	25
14. Photograph of Pegmatite Body.....	26
15. Photomicrograph of Central Border Complex Hornblendite.....	28
16. Photomicrograph of Zoned Plagioclase.....	28
17. Photomicrograph of Magmatic Epidote.....	33
18. Photomicrograph of Zoned Epidote.....	33
19. Photomicrograph of Fractured Plagioclase Grain.....	35

20. Photomicrograph of Recrystallized Quartz	35
21. NW- SE Traverse of Main Phase Rocks Showing Increase in SiO ₂ to SE	40
22. Harker Diagrams for Major Elements	42
23. AFM Diagram	44
24. A/NK and A/CNK Discrimination Diagrams.....	45
25. Harker Diagrams for Trace Elements.....	46
26. REE Diagrams for Cumulate Rocks	49
27. REE Diagrams for Mafic Rocks	50
28. REE Diagrams for Mafic Tonalites (60-65% SiO ₂).....	52
29. REE Diagrams for Felsic Tonalites (>65 % SiO ₂).....	54
30. Traverse Across Plagioclase Grains Showing Variation in Anorthite Content....	58
31. Maximum and Minimum Anorthite Content in Plagioclase in NW-SE traverse	59
32. Leake Nomenclature Diagram for Amphibole.....	62
33. Maximum and Minimum Values for Elements in Amphibole	63
34. Amphibole Mineral Chemistry vs. Whole Rock SiO ₂	64
35. Maximum and Minimum Values for Elements in Biotite	67
36. Biotite Mineral Chemistry vs. Whole Rock SiO ₂	68
37. Maximum and Minimum Pistacite Content in Epidote.....	70
38. Pistacite Content in Traverses Through Epidote	70
39. Pressures Derived From Barometry Along a NW-SE Traverse	74
40. Comparison of Thermometers	78

41. Harker Diagrams Comparing Cardinal Peak, Chilliwack Medium-K Series and Onion Valley Mafic Rocks	82
42. REE Diagram Comparing Cardinal Peak, Chilliwack Medium-K Series and Onion Valley Mafic Rocks	84
43. REE Fractionation Model 1: NW Tonalite.....	88
44: REE Fractionation Model 2: SE Tonalite	90
45. Sr/Y Discrimination Diagram	92
46. Harker Diagrams Comparing Cardinal Peak Tonalite and Melting Experiments Compositions.....	94
47. REE Melting Model 1: NW Tonalite	97
48. REE Melting Model 2: Central Tonalite	98
49: REE Melting Model 3: SE Tonalite.....	100
50: SW-NE Traverses Across the Cardinal Peak Pluton Showing Variations in SiO ₂ and Yb for Whole Rock Compositions	105
51: Cartoon Illustrating Petrogenesis of the Cardinal Peak Pluton	108

LIST OF TABLES

Table	Page
1. Mineral Percentages in Border Complex Rocks.....	27
2. Mineral Percentages in Main Phase Rocks.....	31
3. Representative Plagioclase Analyses.....	56
4. Representative Amphibole Analyses	61
5. Representative Biotite Analyses	66
6. Representative Epidote Analyses.....	69
7. Results of Barometry and Thermometry	73
8. Major Element Fractionation Model 1: NW Tonalite	86
9. Major Element Composition of Parent Rocks for Melting Experiments.....	95

INTRODUCTION

The purpose of this study is to elucidate the magmatic processes that controlled the formation of the Cardinal Peak pluton. The Late Cretaceous [72 Ma, (Haugerud et al., 1991)] Cardinal Peak pluton is a mid-crustal (6-8 kbar), predominantly tonalitic intrusion located in the crystalline core of the North Cascades range (North Cascades core) of Washington State, U.S.A. Tonalitic, calc-alkaline intrusions such as the Cardinal Peak pluton are very common in the Earth's crust, and are a significant component of magmatic arcs (e.g., Barker, 1979; Barker et al., 1981; Beard and Lofgren, 1991). Unlike many other tonalitic plutons, however, the Cardinal Peak pluton also preserves a significant amount of mafic rock that may have played an important role in the genesis of the more felsic main body of the pluton. Hence, study of this pluton can provide constraints on common magma evolution processes in arcs. In addition, the Cardinal Peak pluton is similar to other tonalitic plutons found in the North Cascades core, and therefore the results of this study may have general implications for the regional processes that controlled pluton formation in the Cascades arc during the Late Cretaceous.

The main aspects of this study are: 1) a detailed petrographic, petrologic and geochemical description of the Cardinal Peak pluton, 2) an evaluation of petrologic models for the formation of the tonalitic rocks that make up the bulk of the Cardinal Peak pluton, and 3) an evaluation of processes that were responsible for the distinctive spatial characteristics of the pluton.

Petrologic Models for Formation of Tonalitic Magmas in Arcs

Three models for the generation of tonalitic magmas in continental arcs are considered for the formation of the Cardinal Peak pluton. The first is the traditional view that intermediate or felsic magmas form by fractional crystallization of mafic magmas (e.g., Bowen, 1956; Barker and Arth, 1976). Indeed, the Cardinal Peak pluton contains rock types typically found in a high-aluminum fractionation suite: hornblendite, gabbro, diorite and tonalite (Arth et al., 1978; Arth, 1979). It is possible to determine whether the pluton represents such a suite by the use of geochemical fractionation models that incorporate major, trace and rare earth elements.

A second model for the generation of tonalitic magmas invokes partial melting of the lower crust by underplating of mantle magmas (e.g., Tepper et al., 1993). It is widely accepted that basaltic magmas in arcs are produced by partial melting of an ultramafic mantle parent (e.g., Yoder, 1976; Tatsumi and Eggins, 1995). Melting of the mantle wedge in arc settings is caused by lowering the melting point of the mantle by water influx from dehydration of the subducting slab (e.g., Tatsumi, 1989). If a portion of hot mantle-derived magma stalls beneath the arc's lower crust, this influx of heat can cause partial melting of the lower crust (Tepper et al., 1993). Recent experimental work has shown that melting the types of mafic rocks typically found in the lower crust can produce a tonalitic melt (e.g., Beard and Lofgren, 1991; Winther, 1996). A lower-crustal origin for the tonalitic rocks of the Cardinal Peak pluton can be tested using geochemical models.

A third model is that intermediate magmas (including tonalitic magmas) are the product of mixing felsic lower-crustal melts with mafic mantle melts (e.g., Sisson et al., 1996; Dawes, 1993). Analysis of geochemical data from the pluton can show if a mixing origin is likely for the Cardinal Peak tonalite.

Magma Chamber Construction

Similar to many other plutons in the North Cascades core, the Cardinal Peak pluton has a long, narrow shape in map view and strikes NW-SE (Fig. 1). For the nearby Entiat pluton, Paterson and Miller (1998) propose that this shape and orientation is due to pluton construction by intrusion of arc-parallel diapiric ridges of magma.

The Cardinal Peak pluton also displays marked changes along its strike. Abundant sheets (sub-parallel, tabular magma bodies) and a wide range of rock compositions mark the NW end, while the SE section of the pluton consists of relatively homogenous tonalite. One hypothesis for this along-strike variation is that the pluton is tilted, so that the NW part of the pluton exposes a deeper level of the magma chamber, possibly even the feeder system, and preserves a range of compositions that would have been mixed by convection in higher levels of the chamber. The SE part of the pluton represents the higher levels, which were convectively mixed and homogenized. This hypothesis can be tested in part by geobarometry on rocks from the NW and SE parts of the pluton.

A second hypothesis suggests that the source of magma in the NW was substantially different than that at the SE end of the pluton. In this case, the

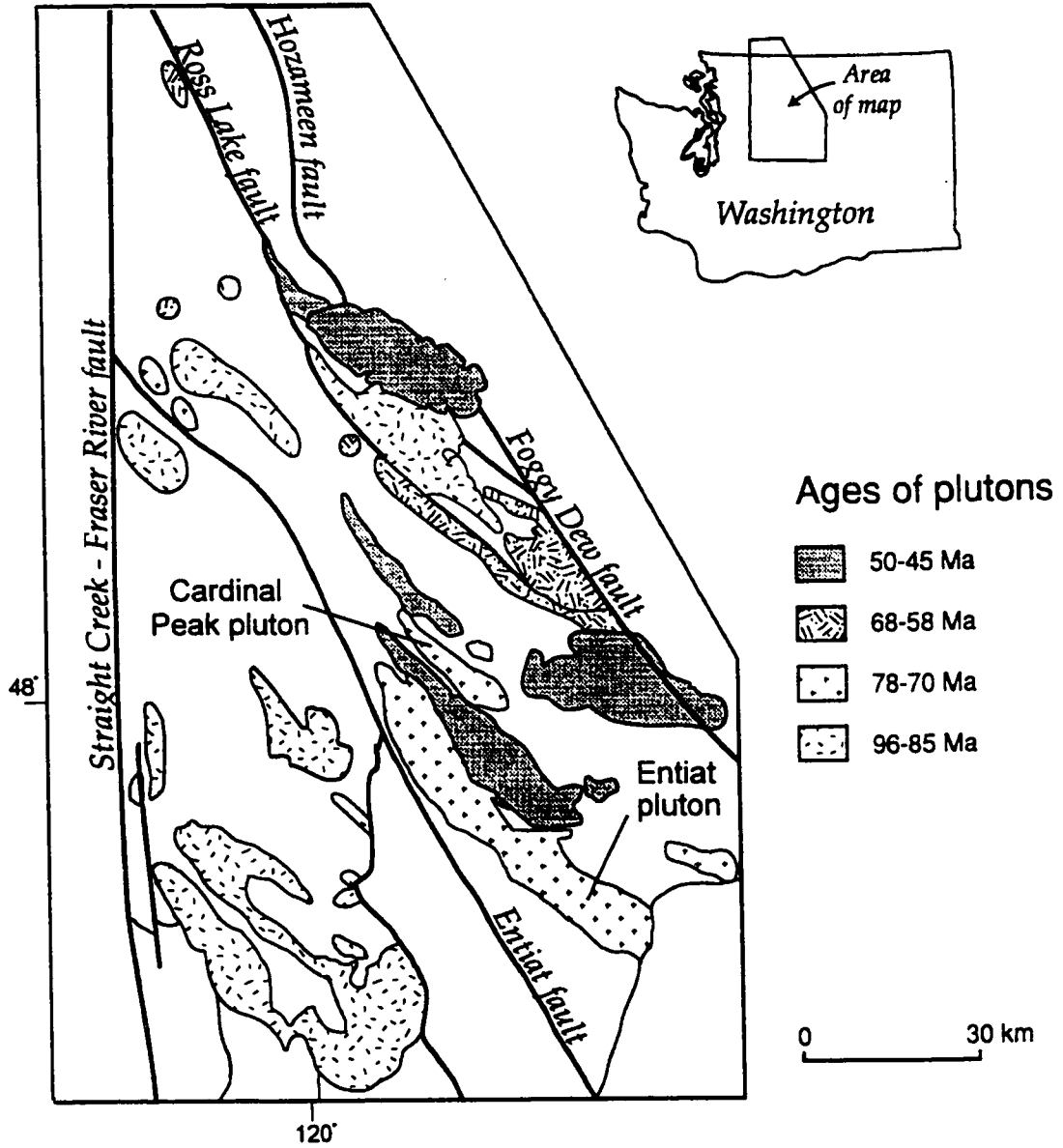


Figure 1. Location map of the Cardinal Peak pluton, showing Cretaceous to Eocene plutons. Modified from Miller et al. (1989).

northwesterly magmatism included a range of mafic to felsic compositions, while the more southeasterly magmatism was mainly tonalitic and was more voluminous and homogeneous. The southeastern part of the magma chamber may have been constructed of multiple sheets of homogenous magma, or one large pulse of magma. This hypothesis is not as easily tested as the tilted-pluton hypothesis, but may be evaluated from geochemical data taken from NE-SW traverses across the pluton.

TECTONIC AND GEOLOGIC SETTING

The Cardinal Peak pluton is located in the North Cascades range of north-central Washington State (Fig. 1). The geology of this area is complex, reflecting accretion of several pre-Late Cretaceous oceanic and arc terranes, a Late Cretaceous to Eocene orogeny which included emplacement of numerous plutons, an Eocene extensional event and the Oligocene to Holocene emergence of the Cascades magmatic arc (Tabor et al., 1989). At various times during the Quaternary, this area was extensively carved by glaciation; as a result the exposure is generally excellent, particularly on the high peaks.

The accreted terranes and younger plutonic rocks in this area are part of the crystalline core of the North Cascades or North Cascades core (Misch, 1966; 1988). The North Cascades core is the southern extension of the Coast Plutonic Complex, but is now offset from it by ~80 to 180 km of right lateral slip along the Straight Creek-Fraser River fault (Vance, 1957; Misch, 1966; Tabor et al., 1989) (Fig. 2). The Coast Plutonic Complex extends for over 1500 km along the northwest coast of North America, and includes many Late Cretaceous tonalitic plutons similar in composition to the Cardinal Peak pluton (e. g., Cui and Russell, 1995).

Final accretion of the terranes of the North Cascades core to the continent occurred in the Late Cretaceous (Tabor et al., 1989). Following accretion these terranes were metamorphosed and significantly thickened by either magma loading (Brown and Walker, 1993), thrust faulting (McGroder, 1991; Miller et al., 1993), or a combination of

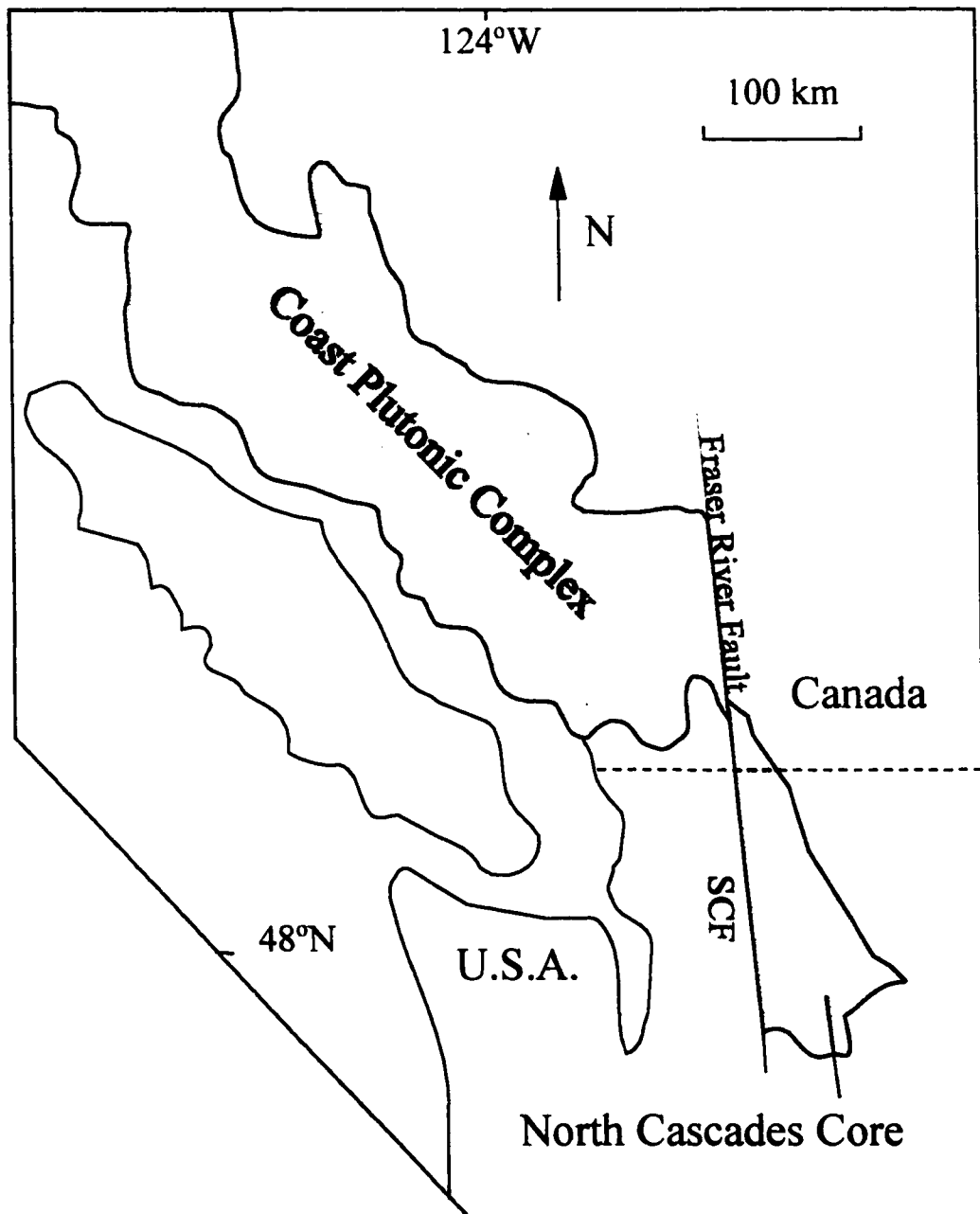


Figure 2. Map showing offset of North Cascades Core from Coast Plutonic Complex. SCF=Straight Creek Fault. Modified from Miller et al. (1993).

these processes. From the Late Cretaceous to the Eocene, tonalitic to granodioritic plutons, including the 72 Ma Cardinal Peak pluton, were intruded into these terranes.

The Cardinal Peak pluton lies within the Chelan Mountains terrane (Fig. 3), which is bounded on the northeast by the Ross Lake fault zone, on the northwest by the Straight Creek-Fraser River fault, on the southeast by the onlapping Miocene Columbia River Basalt, and on the southwest by the Entiat fault and the Nason and Swakane terranes. The Chelan Mountains terrane is comprised of two major supracrustal units: the Napeequa unit and the Cascade River unit (Tabor et al., 1989; Miller et al., 1994), both of which have been intruded by post-accretion Late Cretaceous and younger plutons. The Napeequa unit consists of siliceous schist, quartzite and amphibolite, with less abundant metapelite, marble and minor greenschist and metagabbro, reflecting a chert-basalt marine protolith (Tabor et al., 1989). The Cascade River unit is thought to be an island arc sequence, consisting of metamorphosed intermediate volcanic rocks, greywacke, and minor conglomerate (Tabor et al., 1989). Dragovich et al. (1989) dated a metadacite within this unit at 220 Ma (Late Triassic). A correlative to the Cascade River unit is the Holden assemblage (Miller et al., 1994), which forms the country rock to the Cardinal Peak pluton in most locations (Fig. 4). The Holden assemblage is intruded by the Late Triassic Dumbell plutons, which constrain the age of the Holden as Triassic or older.

The Holden assemblage consists of amphibolite, hornblende-biotite schist, calc-silicate rock, leucocratic gneiss, and rare pelitic schist and is metamorphosed to middle amphibolite facies (Cater and Crowder, 1967; Cater and Wright, 1967; Miller et al., 1994; Murphy, 1996). The protoliths of the Holden assemblage are interpreted by Miller

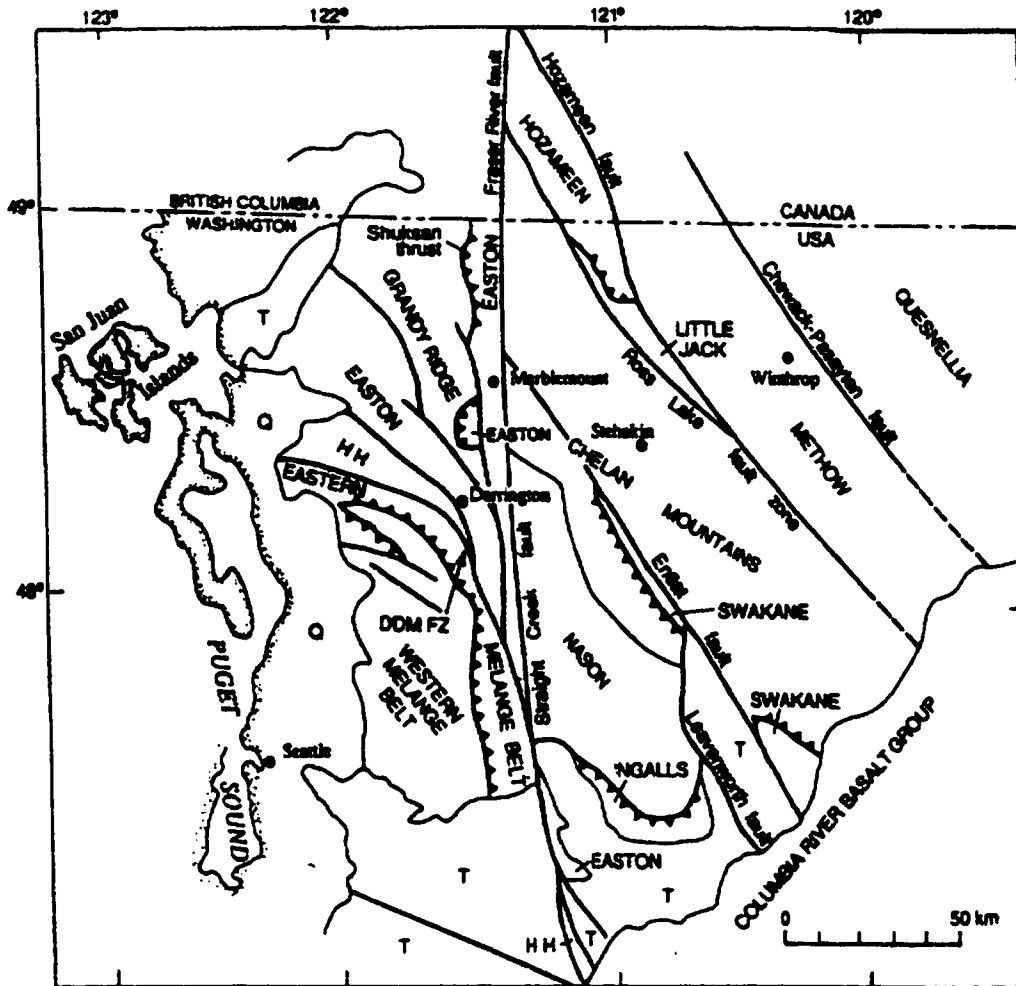


Figure 3. Major terranes of northwestern Washington. The Cardinal Peak pluton is located in the Chelan Mountains terrane. Note that HH=Helena-Haystack Melange Belt, DDM FZ=Darrington-Deviils Mountain Fault Zone, T=Tertiary sediments and volcanics, Q=Unconsolidated sediments. Taken from Tabor et al. (1989).

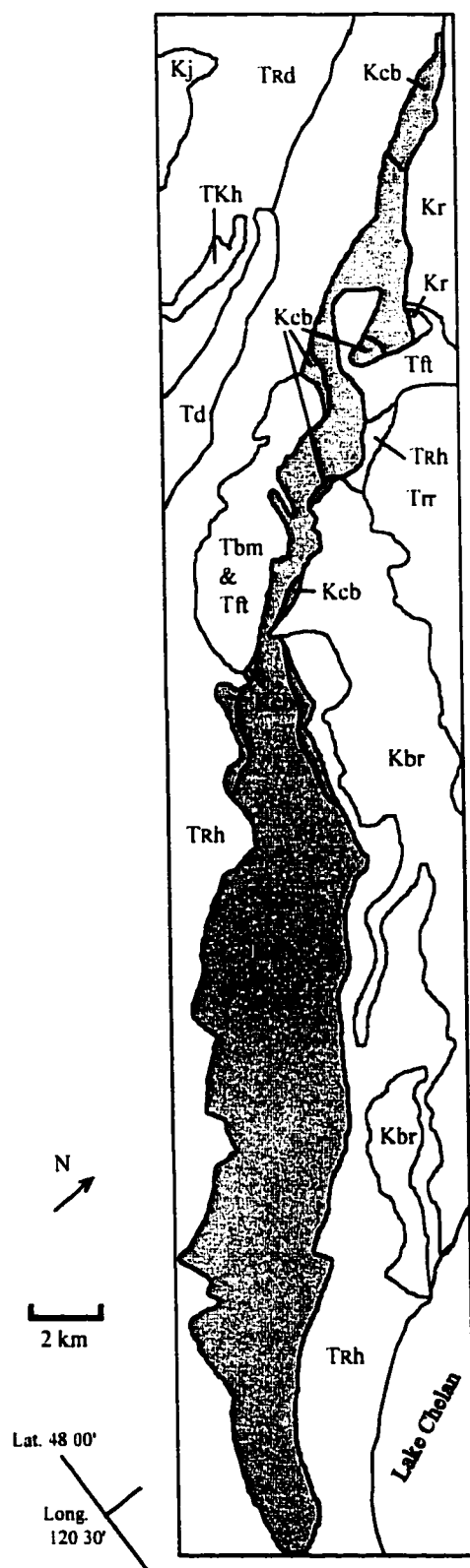


Figure 4. Geologic map of the Cardinal Peak pluton and surrounding area. Modified from Cater and Crowder (1967) and Cater and Wright (1967).

Legend

Trr	Railroad Creek Pluton
Tbm	bioite monzonite
Tft	felsic tonalite
Td	Duncan Hill Pluton
Kc	Cardinal Peak Pluton-Main Phase
Kcb	Cardinal Peak Pluton-Border Complex
Kr	Riddle Peak Pluton
Kj	Seven Fingred Jack Pluton
Kbr	Bearcat Ridge Orthogneiss
Trd	Dumbell Mountain Pluton
Trh	Holden Assemblage

et al. (1994) to be sedimentary and volcanic island arc rocks: basalt, andesite, marl, sandstone and limestone. These rocks are intensely deformed, with foliation and lineation varying in intensity from strong to mylonitic (Miller et al., 1994). Metamorphism in the Holden assemblage appears in part to predate the intrusion of the Cardinal Peak pluton (Murphy, 1996). The intrusion of this pluton produced only local deformation, and did not increase the metamorphic grade of its host rocks (Miller and Paterson, 1995). In the southern part of the Chelan Mountains terrane, the Holden assemblage and the Dumbell plutons are intruded by numerous small leucotonalite dikes and sills, which mark the contact with the Early Cretaceous Chelan Migmatite Complex (Hopson and Mattinson, 1994).

The Cardinal Peak pluton also intrudes the 89 Ma Bearcat Ridge orthogneiss. This intrusion consists of hornblende- and biotite-bearing tonalite and granodiorite, and has been extensively deformed since emplacement (Cater, 1982). In addition, the NW tip of the Cardinal Peak intrudes layered gabbro of the pre-latest Cretaceous Riddle Peaks pluton. In the Eocene, the Cardinal Peak pluton was intruded by the Railroad Creek pluton (Cater and Wright, 1967; Cater, 1982), and it is also intruded by other undated Tertiary plutons.

DESCRIPTION OF THE CARDINAL PEAK PLUTON

Previous Work

The Cardinal Peak pluton was mapped at a scale of 1:62,500 by Cater and Crowder (1967) and Cater and Wright (1967) as part of the Holden and Lucerne Quadrangle geologic maps. These maps show the elongate nature of the pluton, and delineate the extent of the Border Complex (referred to as the Contact Complex by Cater and coworkers). The geologic maps also delineate a hornblende-biotite-quartz diorite to leucocratic biotite granodiorite unit and a separate calcic hornblende diorite to quartz diorite unit, which are together referred to as the Main Phase in this paper. It should be noted that quartz diorite, as used by Cater and coworkers, is equivalent to the IUGS classification for tonalite [$>20\%$ and $<60\%$ quartz, $<10\%$ K-feldspar (Streckeisen, 1976)].

The petrology of the Cardinal Peak pluton was later described in detail by Cater (1982) in a study of the intrusive rocks of the Holden and Lucerne Quadrangles. Based on field relationships, he determined that the Border Complex (his Contact Complex) was intruded prior to and coeval with the Main Phase. He also raises some of the questions that are addressed in this study, such as the petrogenetic relationship between the Border Complex and the Main Phase.

Miller and Paterson (e.g., 1995) have focused on the structure of the Cardinal Peak pluton in their ongoing work. Paterson et al. (1998) describe foliation patterns in the pluton. Hurban (1991) detailed the structure of the northwestern tip of the Cardinal

Peak pluton, as part of a structural study of rocks in the Holden area. Haugerud et al. (1991) determined U-Pb ages of zircons from the Cardinal Peak pluton at 72.5 ± 0.4 Ma (uncertainty is the 95% confidence limit), with an inherited component resulting from the entrainment of ~ 2.0 Ga zircons. The degree of discordance indicates that only 0.03% - 0.12% of the Pb in the Cardinal Peak pluton is Precambrian (Haugerud et al., 1991). White et al. (1988) reported oxygen isotope values for the pluton as part of a Glacier Peak wilderness study.

Field Descriptions and Petrology

Holden Assemblage

The contact of the Cardinal Peak pluton with the Holden assemblage was observed in three locations, two in the SE part of the pluton (Fig. 5, locations A and B), and one in the central segment (Fig. 5, location C). The country rock type observed at all three locations was amphibolite. Dikelets (typically 5 to 15 cm wide) of Cardinal Peak tonalite commonly intrude into the Holden assemblage next to the contact, extend for meters or tens of meters into the country rock, and generally crosscut the foliation of the Holden rocks (Fig. 6). These dikelets make up 1% or less of the country rock. There is no evidence of partial melting or increase in metamorphic grade at the contact.

Inclusions of Holden assemblage are commonly found within the Cardinal Peak pluton, especially near the outer contacts of the pluton and at the NW end. These inclusions are most commonly amphibolite, although leucogneiss inclusions are also found. The inclusions range in size from a few decimeters to tens of meters, and are

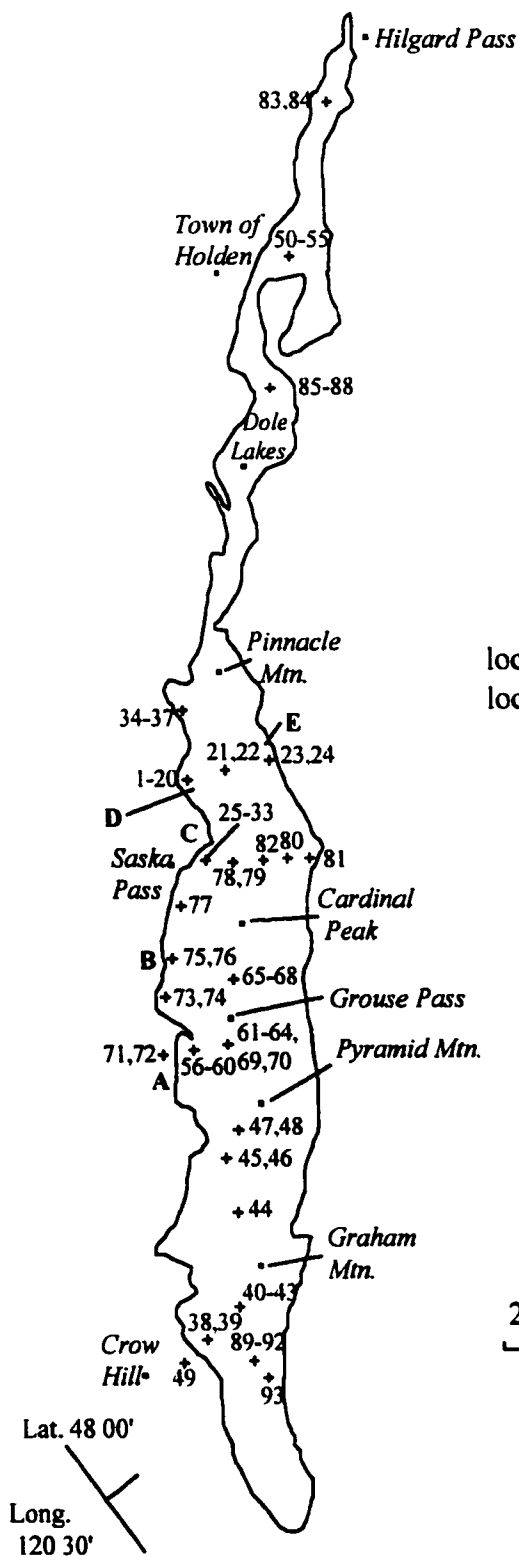


Figure 5. Sample and geographic location map. Bold letters indicate locations referred to in the text.

Explanation
 + Sample location
 • Feature location



Figure 6. Dikelet of Cardinal Peak tonalite (light-center) intruding Holden amphibolite near pluton contact.

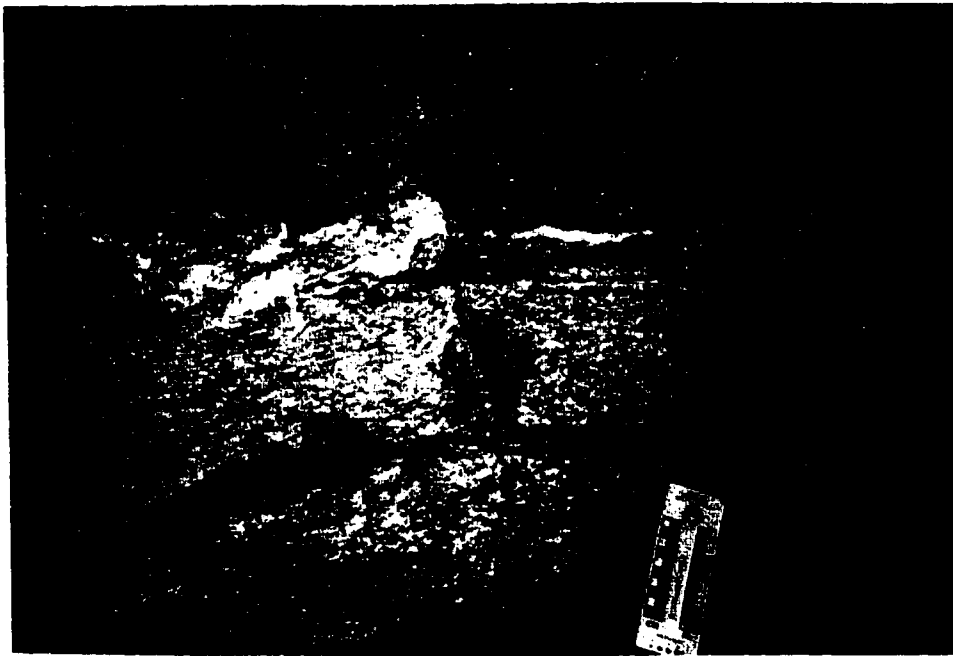


Figure 7. Contact of tonalite (light-bottom) with diorite (darker-top) in the NW Border Complex. The contact is concordant to foliation. The scale at the bottom right of the picture is 16.5 cm long.

generally elongate, with the long axis parallel or sub-parallel to the lineation in the pluton.

General Description of the Cardinal Peak Pluton

In map view, the Cardinal Peak pluton is less than 4 km wide and approximately 35 km long (Fig. 4). The exact length of the pluton is not known, as the SE termination is covered by vegetation along the steep slopes adjacent to Lake Chelan (Miller and Paterson, unpublished manuscript). The pluton is narrower in the NW than in the SE (roughly 0.5 km vs. 4 km), and the NW end terminates in a narrow tip. The extent of the pluton below the surface is unknown, however the exposed relief is ~ 2.3 km.

The composition of the pluton varies from ultramafic to intermediate, but is mainly biotite \pm hornblende tonalite. The pluton can be separated into two major lithologic phases: the Main Phase, which makes up most of the southeastern two thirds of the pluton and the interior of the northwestern third, and the Border Complex, which lies along the margins of the northwestern third of the pluton (Cater, 1982; Cater and Crowder, 1967; Cater and Wright, 1967) (Fig. 5). The Main Phase is generally much more homogeneous than the Border Complex, especially towards the SE, and consists mainly of biotite \pm hornblende tonalite with volumetrically minor amounts of granodiorite and hornblende diorite. Magmatic epidote is present in all varieties of tonalite from the Main Phase, but is especially common in biotite tonalite. The mafic to locally ultramafic Border Complex is a heterogeneous unit of hornblendite, hornblende gabbro, hornblende diorite, hornblende \pm biotite tonalite and leucotonalite. The Border

Complex is most commonly intruded by the Main Phase, but in some locations the Border Complex and the Main Phase are mutually intrusive.

The pluton shows a general trend of increasing heterogeneity to the NW, along strike. The NW part of the pluton consists of Border Complex gabbro, diorite and tonalite, and Main Phase diorite and tonalite. Because the Main Phase is more mafic in the NW than it is elsewhere, and because the Main Phase and the Border Complex both show centimeter- to meter-scale mingling of different lithologies, these units can be difficult to distinguish. The central section of the pluton consists of a clearly delineated rim of Border Complex, and an interior of Main Phase tonalite. The SE section of the pluton is composed of Main Phase biotite tonalite. The following descriptions present each section in more detail.

NW Section: from Hilgard Pass to Dole Lakes (Fig. 5)

Border Complex. As described by Miller and Paterson (1995), the Border Complex in the northwesternmost tip of the pluton consists of hundreds of centimeter- to meter-scale sheets that range from gabbro to tonalite. Farther south, but still in the NW section of the pluton, the Border Complex is less clearly sheeted, but is heterogeneous on the outcrop scale, varying both in grain size and mineral modal content (Fig. 7).

The Border Complex in this area consists of gabbro, quartz diorite and tonalite with hornblende as the dominant mafic phase. These rocks are medium- to fine-grained, and have hypidiomorphic granular texture. Strong magmatic lineation defined by alignment of hornblende and plagioclase is present in some locations.

Main Phase. The Main Phase in this area is lithologically variable. Several different rock types are commonly mingled together in a single outcrop (Fig. 8) and show cross cutting relationships (Fig. 9). Compositional changes are gradational in some places, and rocks may grade from coarse- to fine-grained in a single outcrop. Sharp contacts are also seen, as are mutually intrusive relationships between centimeter- to meter-wide dikes of tonalite and diorite.

The Main Phase in this region includes diorite, quartz diorite, biotite tonalite and hornblende tonalite. Mafic rocks form a much greater percentage of the pluton here than in the central and SE Main Phase. Most rocks are medium- to fine-grained, but some tonalite is coarse grained. Textures range from hypidiomorphic granular to protomylonitic, and some rocks show very strong magmatic lineation defined by alignment of hornblende and plagioclase.

Rare, late-stage aplite dikes are also found in this portion of the pluton. These dikes are fine-grained, centimeters to tens of centimeters in width, and cut sharply across all the Main Phase rock types.

Inclusions of Holden assemblage are meters to tens of meters in length, and tens of centimeters to meters in width. They are generally oriented with their long axes parallel to the lineation in the Main Phase. In some areas inclusions make up approximately 5% of the outcrop, but more commonly are less than 1%. Even rarer than the inclusions are centimeter-scale enclaves of hornblendite, which resemble central Border Complex hornblendite. The hornblendite enclaves have rounded and embayed contacts that suggest they were not fully solidified during injection of the tonalite.



Figure 8. Typical heterogeneity found in the NW Main Phase. Tonalite and diorite are mingled together in a single outcrop. Scale is 16.5 cm long.



Figure 9. Contact of tonalite (light) and diorite (dark), with tonalite dikelets intruding diorite in bottom half of picture. The contact, and the edges of the dikelets have been traced with a black line.

Central Section: from Pinnacle Mountain to Cardinal Peak (Fig. 5)

Border Complex. The Border Complex is lithologically distinct from the much more homogenous Main Phase in this area. The Border Complex is heterogeneous at outcrop scale, and contains hornblendite, gabbro, diorite, quartz diorite, tonalite and leucotonalite. Volumetrically, diorite is the most common phase. The rock types found in the Border Complex in this region are the most varied in the pluton, whereas the Main Phase consists almost exclusively of biotite \pm hornblende tonalite.

In some areas, the different rock types of the Border Complex are intermingled chaotically, and in other areas there is a clear sheeting relationship of meter-scale parallel bodies of mafic to felsic lithology. Hornblendite bodies, ranging from centimeters to tens of centimeters in scale, appear to be the oldest phase, and they are broken up and intruded by gabbro and diorite, which are in turn intruded by tonalite that appears to be identical to the Main Phase tonalite in this area. The sharp contacts between the hornblendite and the other phases suggest that the hornblendite was solid or semi-solid before intrusion of the gabbro and diorite. Rare, fine-grained leucocratic aplite dikes also intrude the Border Complex. These dikes are centimeter-scale in width and cut sharply across all rock types.

The contact of the Border Complex and the Main Phase varies between localities in this part of the pluton. In many areas, the contact is marked by local centimeter- to meter-wide and several meter-long intrusions of Main Phase tonalite into Border Complex diorite, and, rarely, intrusions of Border Complex diorite into Main Phase tonalite. In one location, a 65 to 100 meter-wide intermingled zone of tonalite, mafic enclaves and country rock, including a 10 meter-wide inclusion of Holden assemblage,

marks the contact (Fig. 5, location D). In another location, the contact between Border Complex rocks and Main Phase tonalite is sharp and planar (Fig. 5, location E).

The outer contact of the pluton, which in this area juxtaposes the Holden assemblage and Border Complex, is fairly sharp. However, centimeter-scale dikes of Border Complex commonly intrude the country rock, in some cases making up 20% of the outcrop.

Main Phase. Main Phase rocks in the central section consist almost exclusively of biotite \pm hornblende tonalite. This section is compositionally and texturally more homogenous than the NW section, especially south of Saska Pass (Fig. 5). In particular, there is little difference in grain size or mafic content at outcrop scale. However, where contacts between bodies of different grain size and/or composition are seen, they are usually sharp. Biotite-rich schlieren, which extend for several meters (Fig. 10), and mafic enclaves are common in a few locations. Mafic enclaves make up 5% or less of most outcrops and are absent or rare in most places. These mafic enclaves consist of fine-grained biotite \pm hornblende tonalite or quartz diorite and have the same mineralogy as the host, but contain a larger percentage of mafic minerals (up to 40% mafic minerals in some enclaves) and are finer-grained.

Inclusions of Holden assemblage amphibolite, meter-scale in length and width, are also very common in this section of the pluton, especially towards the external contacts of the pluton. These inclusions comprise 10% or more of the outcrop in some

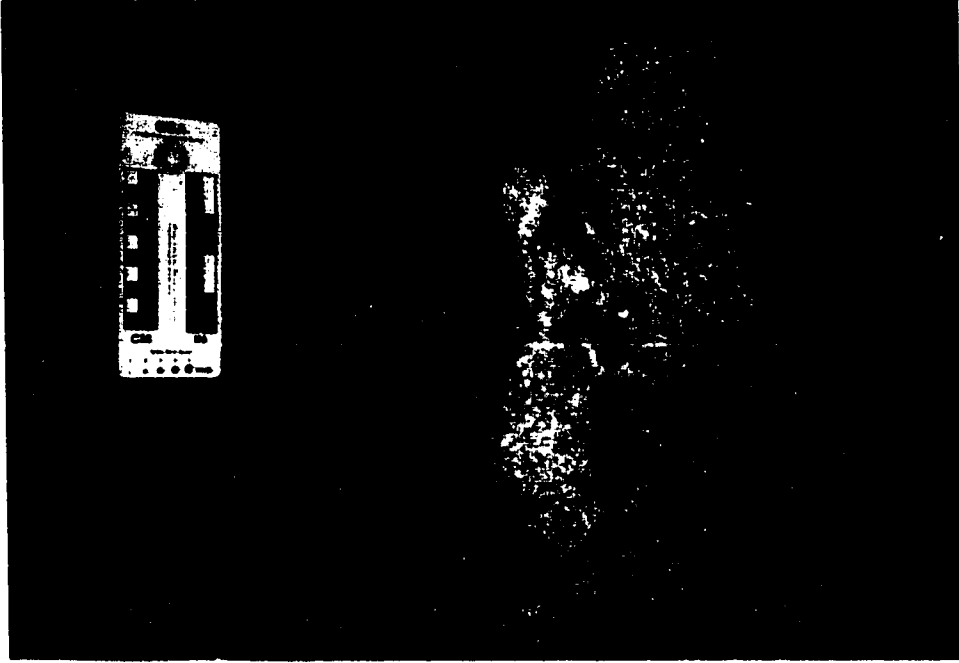


Figure 10. Xenolith of Holden Assemblage amphibolite (dark) intruded and disrupted by Cardinal Peak tonalite.



Figure 11. Biotite-rich schlieren in tonalite from central Main Phase. Scale is 16.5 cm long.

areas. Most inclusions have sharp contacts and show no evidence of partial melting, and are commonly intruded by dikelets of Main Phase tonalite and broken up into blocks (Fig. 11). Inclusions of amphibolite and leucogneiss in one area directly north of Cardinal Peak are tens of meters in length and width. The leucogneiss inclusions exhibit more ductile-appearing contacts with the host pluton than the amphibolite inclusions. The long axis of most of the larger inclusions parallels the external contacts of the pluton. Very fine-grained aplite dikes that are centimeter-scale in width occur rarely, and crosscut the foliation in the Main Phase.

Hornblende abundance in the Main Phase in this segment of the pluton is lower than in the NW (0-15% compared to up to 47% in the NW) and biotite abundance is proportionately higher. The hornblende content gradually decreases southeastwards until hornblende is completely absent or only a minor component in Main Phase rocks south of Saska Pass. Mafic contents range from 10%-25%; the most mafic samples also contain the highest hornblende/biotite ratio. The grain size of these rocks is predominantly coarse to medium, but a few samples are fine-grained. Most rocks in this area have a protomylonitic texture, consisting of relatively large feldspar and hornblende grains in a variably recrystallized groundmass of quartz, plagioclase and biotite. Some of the strongly deformed samples with large, rounded feldspars take on an appearance called "popcorn" by Cater (1982).

Southeast Section: from Cardinal Peak to Crow Hill (Fig. 5)

Main Phase Most of the Main Phase in the SE part of the pluton consists of coarse

biotite tonalite, which is generally homogenous in grain size and mineral mode at outcrop scale (Fig. 12). However, locally between Pyramid Mountain and Graham Mountain, changes in mineral proportion and grain size are evident across a single outcrop. The contacts between these phases are mutually interfingered.

Hornblende is almost non-existent in the SE Main Phase. However, it is present at the western margin of the pluton directly south of Cardinal Peak, and fine- to medium-grained hornblende bearing tonalite dikes (centimeter-scale in width) occur at Grouse Pass (Fig. 13). A large (several tens of meters-wide) hornblende tonalite enclave is located east of Grouse Pass (R. B. Miller pers. comm., 1998).

Very coarse-grained, meter- to tens of meters-wide pegmatite bodies are found north of Grouse Pass. The mineralogy of these bodies is similar to that of the Main Phase, consisting of plagioclase, biotite and quartz. Biotite crystals in these pegmatites can reach several centimeters in length (Fig. 14).

The textures of the Main Phase rocks range from protomylonitic to hypidiomorphic granular. Most samples from this section contain about 30% quartz, but this increases to 40% at the SE end. Mafic content varies from 10% to 30%, with an average of 15%.

In this section the Main Phase is in contact with the Holden assemblage. Centimeter-scale dikes of the Main Phase tonalite intrude the country rock, making up 5% or less of the outcrop.

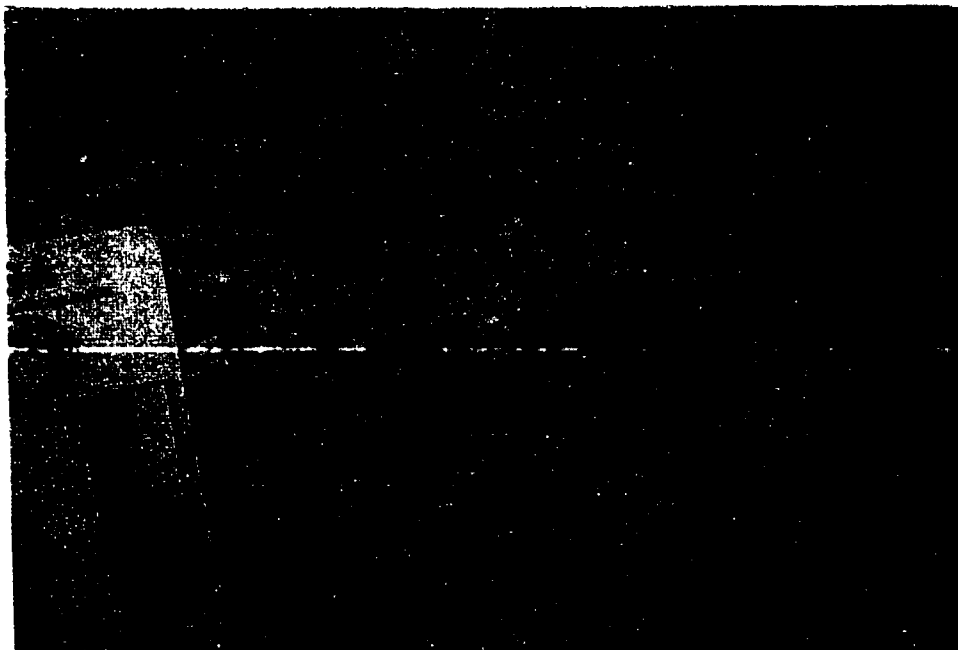


Figure 12. Typical biotite tonalite from the SE Main Phase. The scale shows inches on the right.

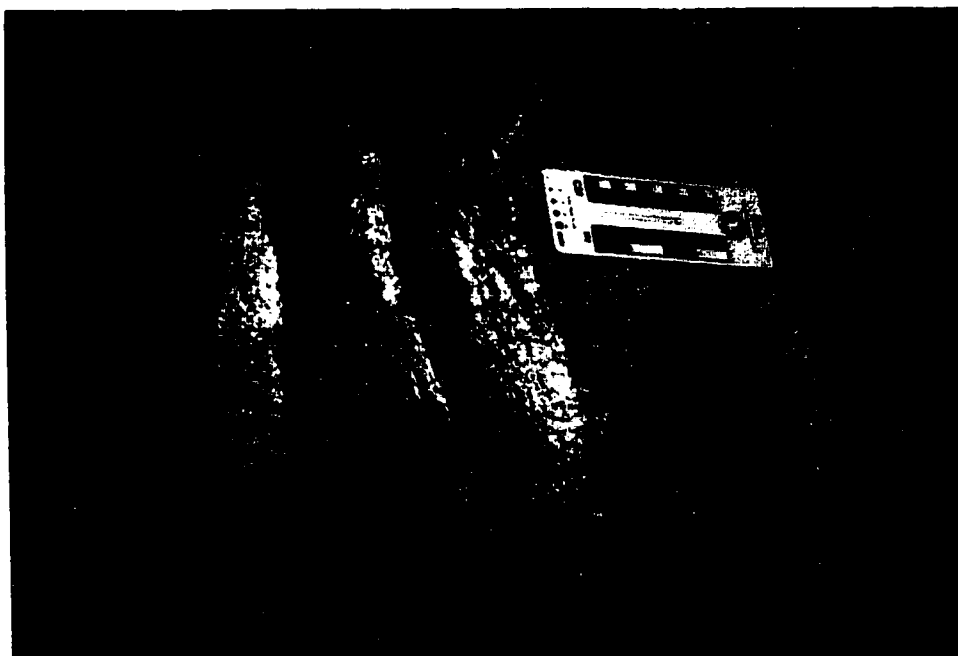


Figure 13. Hornblende-bearing tonalite dikes (darker) intruding biotite tonalite (lighter). The scale is 16.5 cm long.

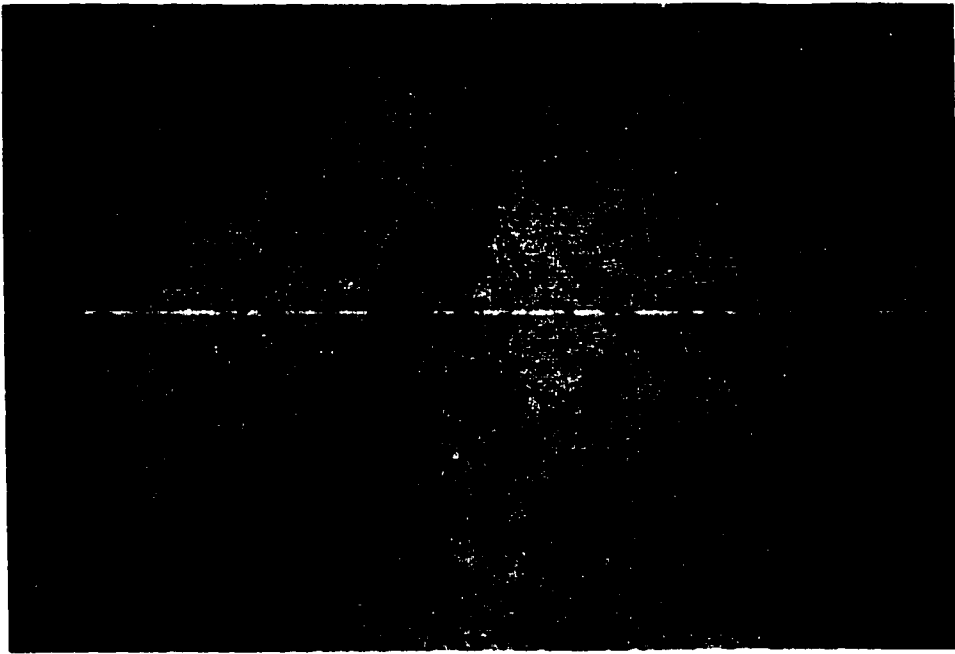


Figure 14. Pegmatite body in SE Main Phase containing large biotites. Scale is 16.5 cm long.

PETROGRAPHY

One hundred forty eight samples of the Cardinal Peak pluton were examined in thin section for this study. The goal of this chapter is to characterize the rock types, minerals and textures of Cardinal Peak rocks.

Border Complex

The lithologies found in the Border Complex are hornblendite (Fig. 15), hornblende gabbro, diorite, quartz diorite, tonalite and leucotonalite. Percentages of primary minerals are given in Table 1. Most rocks also contain chlorite and secondary epidote, which are alteration products of biotite and hornblende; and sericite, which is an alteration product of plagioclase.

Table 1: Mineral percentages in Border Complex rocks

<u>Rock type</u>	<u>Hblde</u>	<u>Biotite</u>	<u>Plag</u>	<u>Quartz</u>	<u>Accessory minerals</u>
hornblendite	90-100	trace	0-10	0-5%	apatite, sphene, epidote, oxides
hblde gabbro	40-50	0-10	45	trace	apatite, sphene, oxides
diorite	30-40	0-5	55-60	0-5	apatite, sphene, oxides
quartz diorite	5-30	15-30	50-60	10-15	apatite, sphene, epidote, oxides
tonalite	0-30	5-15	40	25	apatite, sphene, epidote, oxides
leucotonalite	0	5	60	35	muscovite, apatite, oxides

The mineral descriptions that follow are for the mafic and ultramafic rocks of the Border Complex. The mineral descriptions for the Border Complex tonalite are identical to those of the Main Phase tonalite, and are found in the following section.



Figure 15. Photomicrograph of central Border Complex hornblendite. This hornblendite is almost 100% hornblende, with very little interstitial plagioclase. Width of view is approximately 8 mm.



Figure 16. Plagioclase with an oscillatory zoned core, embayed and mantled by a normally zoned rim. The grain is surrounded by recrystallized quartz. The width of view is approximately 4 mm.

Hornblende is found in most of the Border Complex (Table 1). In hornblendite, hornblende tends to be bimodal in size: most is very coarse (up to 1 centimeter), but some is fine. The coarse grains are subhedral to anhedral, and the fine grains are subhedral. Pleochroism is from pale brown to green. Some larger grains have light patches in their cores that show higher birefringence than the surrounding parts of the grain. These patches were first thought to represent remnant pyroxene not completely replaced by hornblende. However, microprobe analyses of these patches showed they are actinolite.

Locally, plagioclase-rich veinlets (70-80% plagioclase, 20-30% hornblende) intrude hornblendite, and in these samples the hornblende grains in the host appear partially resorbed and are fractured near the veinlets.

In gabbro and diorite samples, hornblende is medium- to fine-grained, generally subhedral, but also can be anhedral, and is pleochroic from light green to dark green. Based on its subhedral shape, it is an early crystallizing phase. Hornblende rims are commonly altered to chlorite.

Plagioclase is medium- to fine-grained, and subhedral to anhedral. In hornblendite, plagioclase is an interstitial, late-crystallizing phase, whereas in gabbro and diorite its occurrence as subhedral grains indicates that it is an early crystallizing phase. Oscillatory zoning and patchy zoning are common, as is alteration of cores to sericite. Large plagioclase grains generally show evidence of brittle deformation in the form of fractures.

Biotite in gabbro and diorite samples is medium- to fine-grained, subhedral to anhedral, and shows straw yellow to brown pleochroism. It can be found rimming

hornblende; thus it crystallized after hornblende. Biotite rims are commonly altered to chlorite.

Where present, quartz is fine-grained and interstitial. Its interstitial habit indicates that it is a late crystallizing phase.

Border Complex rocks show evidence of both magmatic and solid state deformation. Magmatic deformation takes place while the magma was in a partially liquid state, and is most commonly shown by the alignment of minerals, such as plagioclase and hornblende, with high-aspect ratio primary shapes (e.g., Paterson et al., 1998). Solid state deformation, on the other hand, takes place after the magma has fully crystallized. This deformation is commonly shown by ductile strain of late-crystallizing minerals such as quartz, or by brittle or ductile deformation of other minerals.

In these samples, aligned hornblende and plagioclase record magmatic deformation. Solid state deformation is marked by undulose extinction, recrystallized grains and subgrains in quartz, and fractures in plagioclase. The extent of solid state deformation is somewhat less in these rocks than in most of the Main Phase rocks, especially from the central and SE Main Phase.

Main Phase

The rock types found in the Main Phase are diorite, quartz diorite, tonalite and aplite. Mineral percentages are shown in Table 2. Most rocks also contain chlorite, an alteration product of biotite and hornblende, and sericite, an alteration product of plagioclase.

Table 2. Mineral percentages in Main Phase rocks

<u>Rock type</u>	<u>Hblde</u>	<u>Biotite</u>	<u>Plag</u>	<u>Quartz</u>	<u>Accessory minerals</u>
diorite	5-45	0-30	50-65	trace	apatite, oxides
quartz diorite	5-20	5-30	50-65	10-20	apatite, sphene, oxides
tonalite	0-30	0-25	30-75	20-40	epidote (0-10%), k-feldspar (0-5%), oxides, apatite, sphene
aplite	0	trace	60	35	apatite, muscovite ± garnet

Plagioclase is very coarse- to fine-grained; the largest grains are found in the central and SE Main Phase. It is generally subhedral, but most of the very coarse grains are anhedral. Oscillatory, normal and patchy zoning are all common, and normally zoned rims with oscillatory zoned cores are found locally (Fig. 16). Cores of plagioclase are commonly altered to sericite. Based on its subhedral shape and large size, plagioclase was the first phase to crystallize in Main Phase rocks. Most of the larger plagioclase grains show extensive fractures.

Hornblende is present in all of the NW Main Phase samples, but is absent in samples from the SE part of the pluton. It is predominantly euhedral to subhedral, and coarse- to medium-grained. The coarsest grains are found in NW samples. Medium-sized hornblendes tend to be euhedral, and the coarser grains are subhedral. Coarser grains commonly show embayed edges and quartz inclusions. Hornblende shows pale to dark green or brown pleochroism; some grains have straw yellow pleochroism. Based on its euhedral to subhedral shape, hornblende was an early crystallizing mineral. Locally, hornblende rims have undergone extensive alteration to chlorite and oxides. In rocks with extensive solid state deformation (e.g., quartz subgrains, fractured plagioclase), hornblende is commonly found only as fine, anhedral, recrystallized grains.

Biotite is the most common mafic mineral in the central and SE Main Phase, but is also found locally in the NW Main Phase. It is coarse- to fine-grained, and generally subhedral to anhedral, with straw yellow to brown or light brown to reddish brown pleochroism. It is commonly altered to chlorite and oxides. Where biotite co-exists with hornblende it most commonly mantles the hornblende; thus, biotite crystallized after hornblende. In rocks with substantial amounts of solid state deformation biotite is found only as small, anhedral, recrystallized grains.

Quartz in the NW and central Main Phase is interstitial and medium- to fine-grained. In the SE Main Phase, quartz is coarse- to fine-grained, and coarsens toward the southeastern end of the pluton. Based on its interstitial character, it is a late crystallizing phase.

Epidote is fine- to medium- grained, with green to light brown pleochroism. It is anhedral to subhedral, and is most common in the SE Main Phase (up to 5-10% in some samples). In some grains, contacts against plagioclase and quartz are embayed, but are euhedral against biotite (Fig. 17). This texture suggests that these epidote grains are magmatic (Zen and Hammarstrom, 1984). Secondary epidote is also found; some euhedral grains are wholly surrounded by, and may have replaced, plagioclase. Epidote also forms replacement rims around some hornblende grains. Optical oscillatory zoning is common in larger grains (Fig. 18), and some cores are probably allanite.

K-feldspar is found in tonalite samples toward the SE end of the pluton. It is medium-grained, subhedral, and shows microcline twinning.

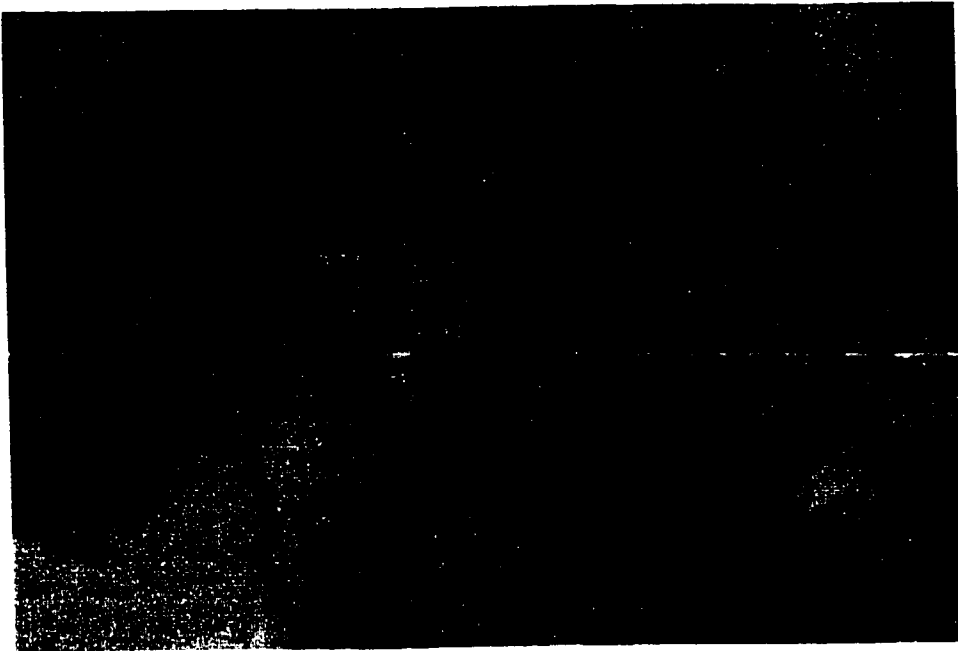


Figure 17. Epidote (blue) showing magmatic texture under crossed polars. Magmatic texture is defined by the euhedral contact of epidote with hornblende and the embayed contact with quartz. Width of view is approximately 4 mm.

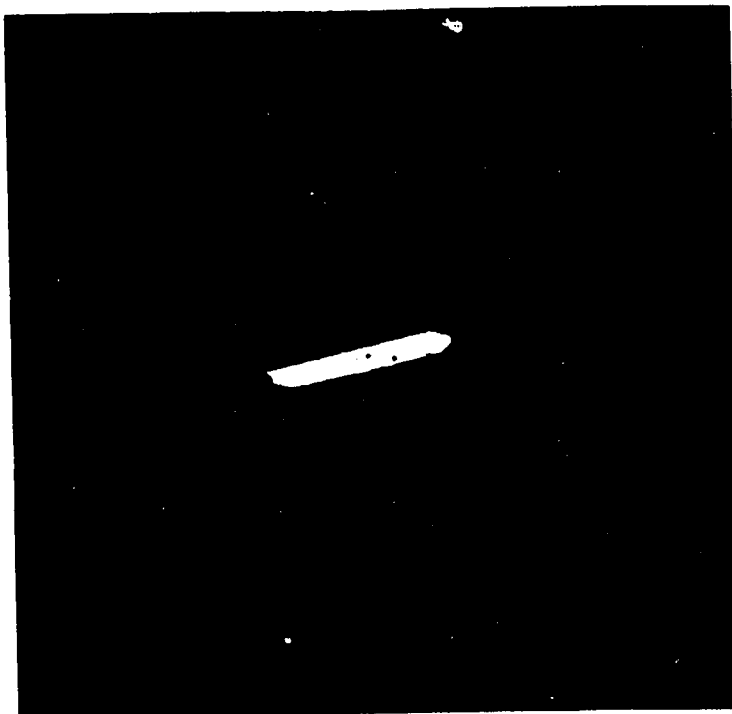


Figure 18. Oscillatory zoned epidote in tonalite. Width of view is approximately 1 mm.

Muscovite is found rarely in tonalite samples near the SE end of the pluton. These samples also have more quartz and less biotite than other Main Phase samples. Muscovite is medium- to fine-grained, and euhedral to subhedral. Based on its euhedral to subhedral shape and lack of replacement textures, this muscovite may be primary.

Rocks from the NW Main Phase show strong magmatic deformation, defined by aligned plagioclase and hornblende. Rocks from the central and SE Main Phase do not display evidence of extensive magmatic deformation.

Solid state deformation in these rocks is indicated by broken and rotated plagioclase (Fig. 19), and recrystallized grains, subgrains, "ribbons" (Fig. 20), and undulose extinction of quartz. Biotite commonly wraps around plagioclase and is recrystallized. Solid state deformation, although present in all samples to some degree, decreases towards the SE end of the pluton. At this end, the only evidence of solid state deformation is undulose extinction of quartz, and local quartz subgrains and fractured plagioclase.

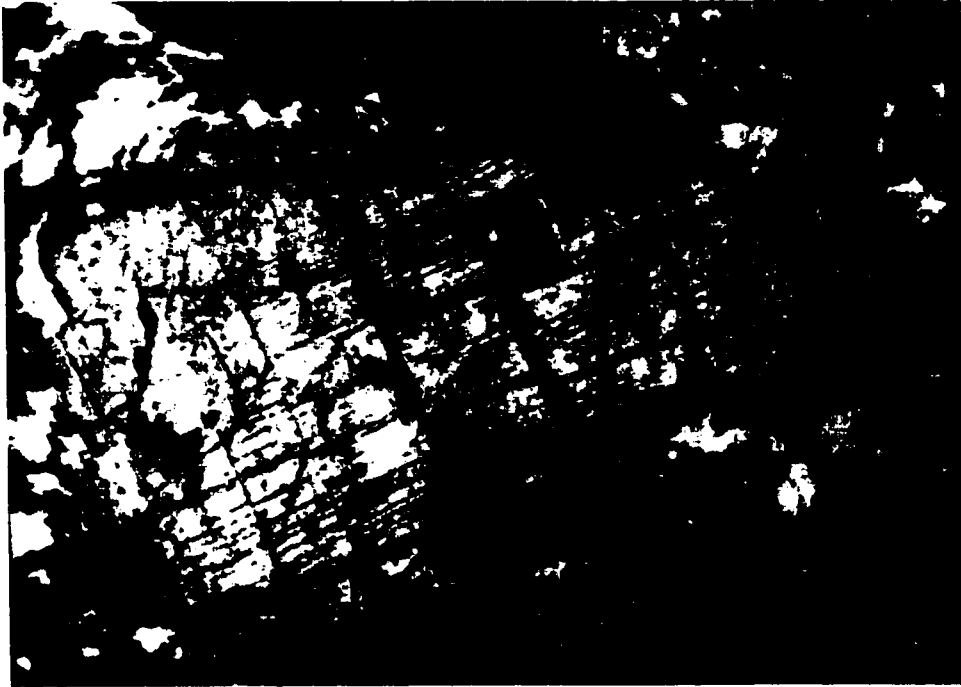


Figure 19. Microfractured plagioclase grain surrounded by recrystallized quartz in tonalite. Width of view is approximately 4 mm.



Figure 20. Quartz showing recrystallization and subgrain formation in tonalite. Width of view is approximately 4 mm.

WHOLE ROCK CHEMISTRY

Previous Work and Scope of Present Study

Cater (1982) performed major element and semiquantitative trace element analyses on two samples from the Cardinal Peak pluton. The results of these analyses are shown in Appendix A.

In this study, 45 samples were analyzed for major elements, 38 samples for selected trace elements, and 47 samples for rare earth elements in order to provide constraints on petrologic processes operative in the Cardinal Peak pluton. Samples were chosen to represent the range of rock compositions in the pluton and to provide along and across strike spatial coverage.

Analytical Methods

Samples prepared for geochemical analyses were first cleaned of obvious weathering or alteration products by removing the affected portions with a steel hydraulic press at San Jose State University (SJSU). The samples were then broken into 1 inch³ (16 cm³) chips in the hydraulic press, and fed into a table-top jaw crusher with tungsten carbide plates. The crushed chips were inspected for weathering and contamination, and discarded if contaminated. The crushed chips were then ground into a fine powder using tungsten carbide containers in a shatterbox mill.

Major and trace elements (including rare earth elements), were determined by several methods. Twenty-three samples were analyzed for major and some trace elements using an automated Rigaku 3370 X-ray fluorescence spectrometer (XRF) at the

Washington State University (WSU) GeoAnalytical Laboratory. These samples were ground into powder at SJSU using the method described above, and then sent to WSU. Fused pellets were prepared at WSU by heating one part of rock powder with two parts of lithium tetraborate to 1000°C. Each element analysis was corrected for line interference and matrix effects. The samples were compared with eight United States Geological Survey (USGS) standards (PCC-1, BCR-1, BIR-1, DNC-1, W-2, AGV-1, GSP-1 and G-2). Accuracy and precision are given in Johnson et al. (1998). This method reports the following major oxides in weight percent (wt. %): SiO₂, Al₂O₃, TiO₂, FeO, MnO, CaO, MgO, K₂O, NaO, and P₂O₅. Trace elements are reported in parts per million (ppm): Ni, Cr, Sc, V, Ba, Rb, Sr, Zr, Y, Nb, Ga, Cu, Zn, Pb, and Th.

Major element analyses of 20 additional samples were performed using the Kevex Model 700 energy-dispersive XRF at SJSU. These samples were ground into powder using the method described above, and then pressed into pellets using a mixture of 1.2 g boric acid to 3.8 g rock powder. X-ray intensity measurements were converted to oxide weight % using a best-fit line from known standards [USGS standards G-2, AGV-1, BCR-1 and GSP-1 (Flanagan, 1976)]. This method reports the major oxides in wt. %: SiO₂, Al₂O₃, TiO₂, FeO, MnO, CaO, MgO, K₂O, NaO, and P₂O₅, and produces results with estimated errors from 10-40%, relative to concentration.

Rare earth element analyses for 47 samples were obtained using Instrumental Neutron Activation Analysis at both the Oregon State University Reactor Center and the Phoenix Memorial Laboratory at the University of Michigan. The samples sent to Oregon State University were powdered at SJSU according to the above procedure. The

samples were irradiated in the reactor for 6 hours at 1 megawatt. One count was taken at 4-5 days after irradiation for short-lived isotopes and a second count was taken at 3-4 weeks for long-lived isotopes. Counts were standardized to a National Bureau of Standards coal fly ash and 4 internal standards. Reported elements are: Sc, Cr, Zn, Rb, Ba, Th, La, Ce, Nd, Sm, Eu, Tb, Yb and Lu (in ppm). The accuracy for these elements is 5%, except for the following: 3% for Sc and La, 10% for Cr, Rb and Ba, and 15% for Zn.

Samples sent to the Phoenix Memorial Laboratory were also powdered at SJSU. They were first irradiated at 2 megawatts for one minute, and counts were taken for short-lived isotopes at 10 minutes and at 2 hours after irradiation. The samples were then irradiated for a second time at 2 megawatts for 6-20 hours, and counts were taken for long-lived isotopes at one week and at five weeks. Counts were standardized to a National Bureau of Standards coal fly ash. Analyses obtained were for rare earth elements La, Ce, Sm, Eu, Dy, Yb and Lu. The reported accuracy varies from 1 to 10%, and depends on the relative concentration of the element.

Two samples were sent to WSU GeoAnalytical Laboratory for major oxide, trace element and REE analysis using a Sciex Elan Model 250 inductively coupled plasma-mass spectrometer (ICP-MS). These samples were sent as whole rocks. At WSU, the rocks were ground into powder using an iron container in a shatterbox mill. The powder was mixed with lithium tetraborate, then heated in a carbon crucible. The resulting glass was ground again in the shatterbox and this powder was heated and dissolved with a mixture of HF, HNO₃, and HClO₄. The sample was dried, then HClO₄ was added, after which the sample was dried again and mixed with HNO₃, H₂O₂, and HF. In addition, an

internal standard containing In, Re, and Ru was added to the sample. The samples were run with an acid blank and USGS standards BCR-P, GMP-01, and MON-01. This method reports SiO₂, Al₂O₃, TiO₂, FeO, MnO, CaO, MgO, K₂O, NaO, and P₂O₅ in wt. %, trace elements Ni, Cr, Sc, V, Ba, Rb, Sr, Zr, Y, Nb, Ga, Cu, Zn, Pb, and Th as ppm and rare earth elements from La to Lu, as elements ppm. The accuracy varies from 1.5% to 6%, depending on the amount of the element relative to total weight.

Major element chemistry

This section presents the results of major element analyses from 45 samples from the Cardinal Peak pluton. These data are shown in Appendix B.

The most mafic samples (<55% SiO₂) occur in the NW and central Border Complex, and the NW Main Phase. Hornblendite samples from the central Border Complex contain SiO₂ from 52-60%; the high value of 60% SiO₂ reflects the relatively large percentage of quartz (5%) in this sample. The most felsic samples (SiO₂ >70) are from the NW Main Phase, central Border Complex and SE Main Phase, while the largest variation in SiO₂ content is found in the NW Main Phase and the central Border Complex.

A traverse along the axis of the pluton from NW to SE for Main Phase samples shows an increase in SiO₂ content towards the SE (Fig. 21). NW Main Phase samples show a wider range of SiO₂ content, while samples from the central and SE Main Phase are generally clustered between 63 and 69% SiO₂.

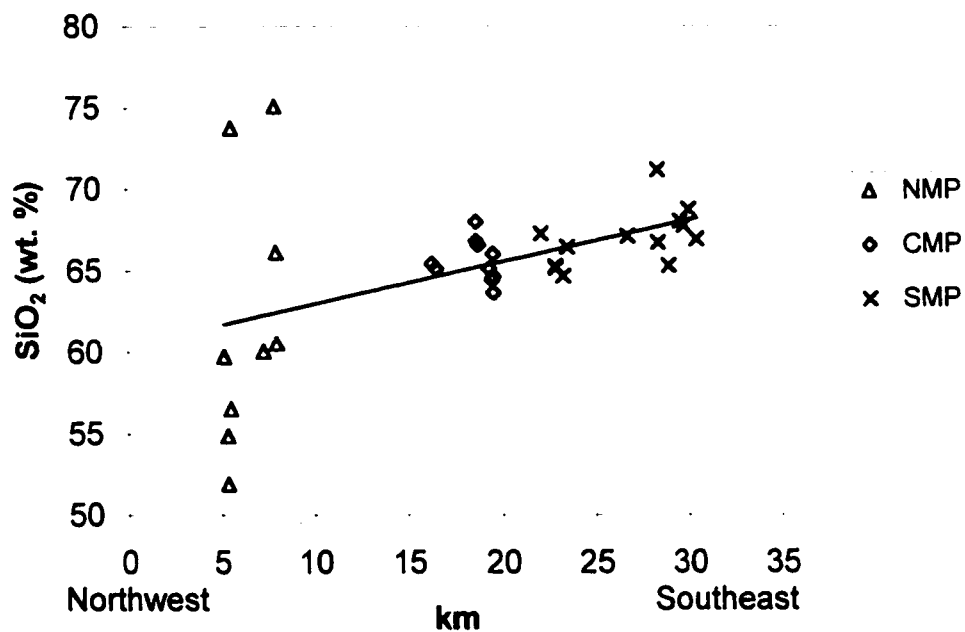


Figure 21. Northwest-southeast traverse of Main Phase rocks showing increasing SiO₂ towards the SE, and scatter in SiO₂ values in the NW Main Phase. The x-axis denotes the distance of the sample from the northwest tip of the pluton. Abbreviations used: NMP=NW Main Phase, CMP=central Main Phase, SMP=SE Main Phase.

Harker diagrams for the Cardinal Peak samples are shown in Figure 22. The samples are divided into six groups: NW and central Border Complex, central Border Complex hornblendites, and NW, central and SE Main Phase.

In general, central and SE Main Phase samples are tightly clustered, and usually form well-defined differentiation trends; however mafic samples (<60% SiO₂) and felsic Border Complex and NW Main Phase samples are more scattered. CaO is the only major element to show a very well-defined linear trend of compatible behavior for all pluton locations and rock types except hornblendite. MgO, FeO, TiO₂, and MnO also show compatible behavior, but the trends are clearly linear only for samples with greater than 60% SiO₂. P₂O₅ displays compatible behavior in felsic samples, but shows scatter below 60% SiO₂. The compatible trend for P₂O₅ above 60% SiO₂ may reflect the fractionation of apatite, however, this does not explain the scatter seen in mafic samples. Al₂O₃ exhibits a compatible trend above 70% SiO₂, constant values between 70 and 60% SiO₂, and scatter below 60% SiO₂. The trend for K₂O shows incompatible behavior with some scatter. Most samples from the NW Main Phase appear to have higher K₂O for a given wt. % SiO₂, than other samples, while central Border Complex samples have less K₂O. Na₂O shows a slight increase with respect to SiO₂; however, most felsic NW samples have less Na₂O for a given wt. % SiO₂ than SE or central samples. For CaO, MgO, Al₂O₃, FeO and TiO₂, most SE and central Main Phase samples are tightly clustered, showing little variation in SiO₂ or major oxide. As expected, Mg# [Mg/(Mg+Fe)*100] decreases with increasing SiO₂. Hornblendite samples (all from the central Border Complex) are higher in MgO and CaO and lower in Al₂O₃ relative to the

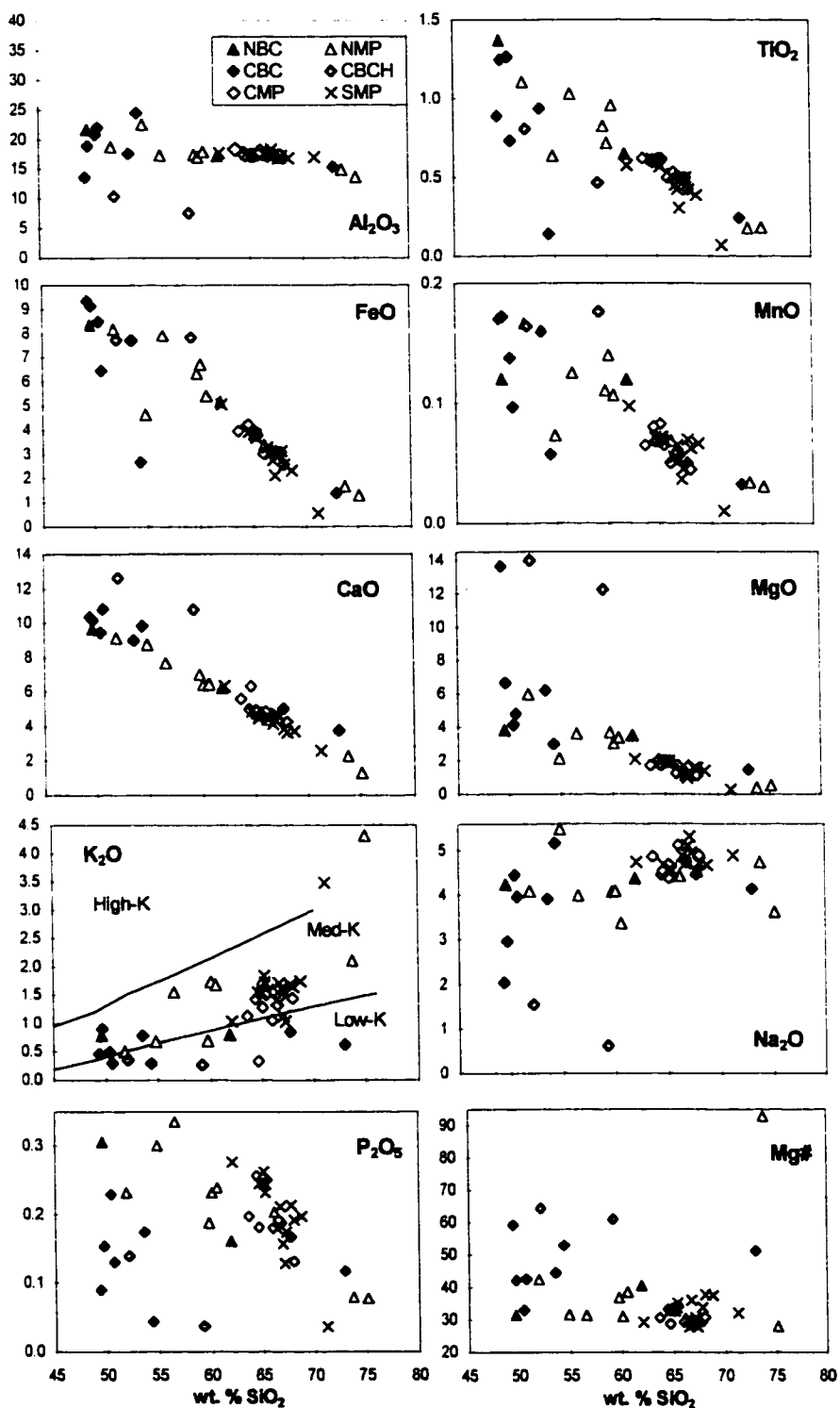


Figure 22. Harker Diagrams for major elements. Y-axis is oxide weight percent. Abbreviations used as in Figure 21, except NBC=NW Border Complex, CBC=central Border Complex, CBCH=central Border Complex hornblende.

rest of the samples, and lie outside the linear trends shown by the rest of the samples for these oxides.

Using the classification of Peccerillo and Taylor (1976), most samples fall within the medium-K trend on a K_2O Harker diagram (Fig. 22); although central Border Complex rocks define a low-K sequence, as do some of the NW Border Complex and NW Main Phase rocks. Other NW Main Phase rocks define a relatively high-K trend. Two samples, both SiO_2 -rich, plot in the high-K field.

Cardinal Peak rocks show a calc-alkaline trend on an AFM diagram (Fig. 23). On A/NK and A/CNK discrimination diagrams, samples are metaluminous to slightly peraluminous (Fig. 24). No samples are peralkaline.

Trace Element Chemistry

This section presents the results of whole rock trace element analyses of 38 Cardinal Peak samples. These data are displayed in Appendix B. Figure 25 shows Harker diagrams, in which samples are divided into the same six groups as in Figure 22.

These diagrams show both compatible and incompatible trends, and samples from different locations in the pluton define differing trends for some elements. As on the major element Harker diagrams, mafic samples (<60% SiO_2), Border Complex and NW Main Phase samples are much more scattered than central and SE Main Phase felsic samples.

Ni, Cr and V have compatible trends, decreasing with increasing SiO_2 , however, some NW Main Phase samples exhibit a more enriched trend for these elements than

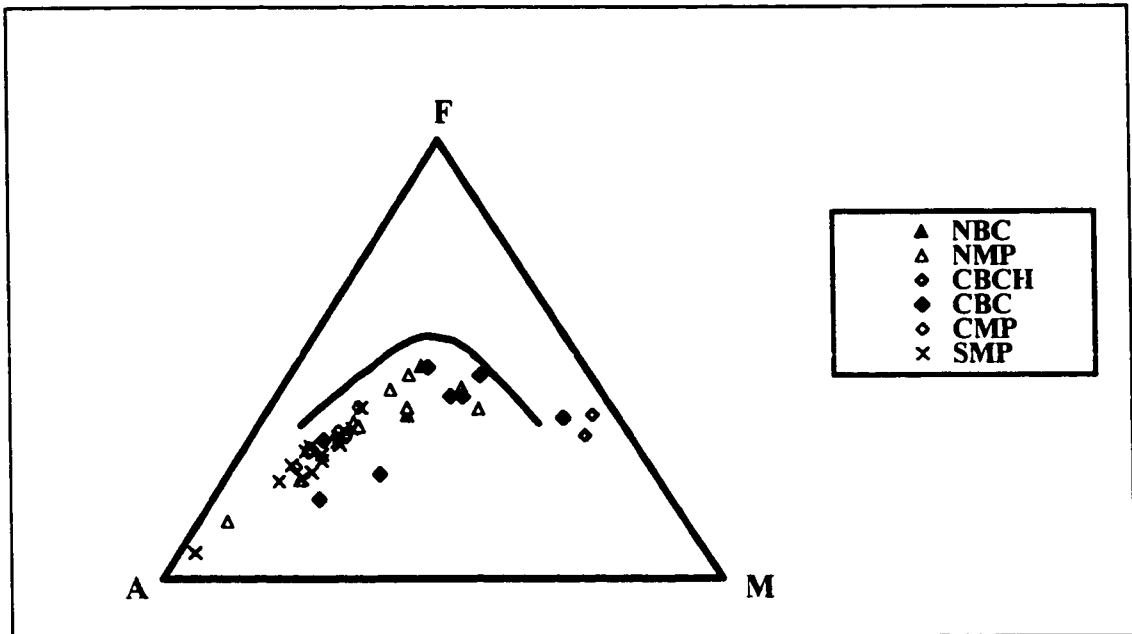


Figure 23. AFM diagram for Cardinal Peak samples. Abbreviations used as in Figure 22. The curve is from Irvine and Baragar (1971).

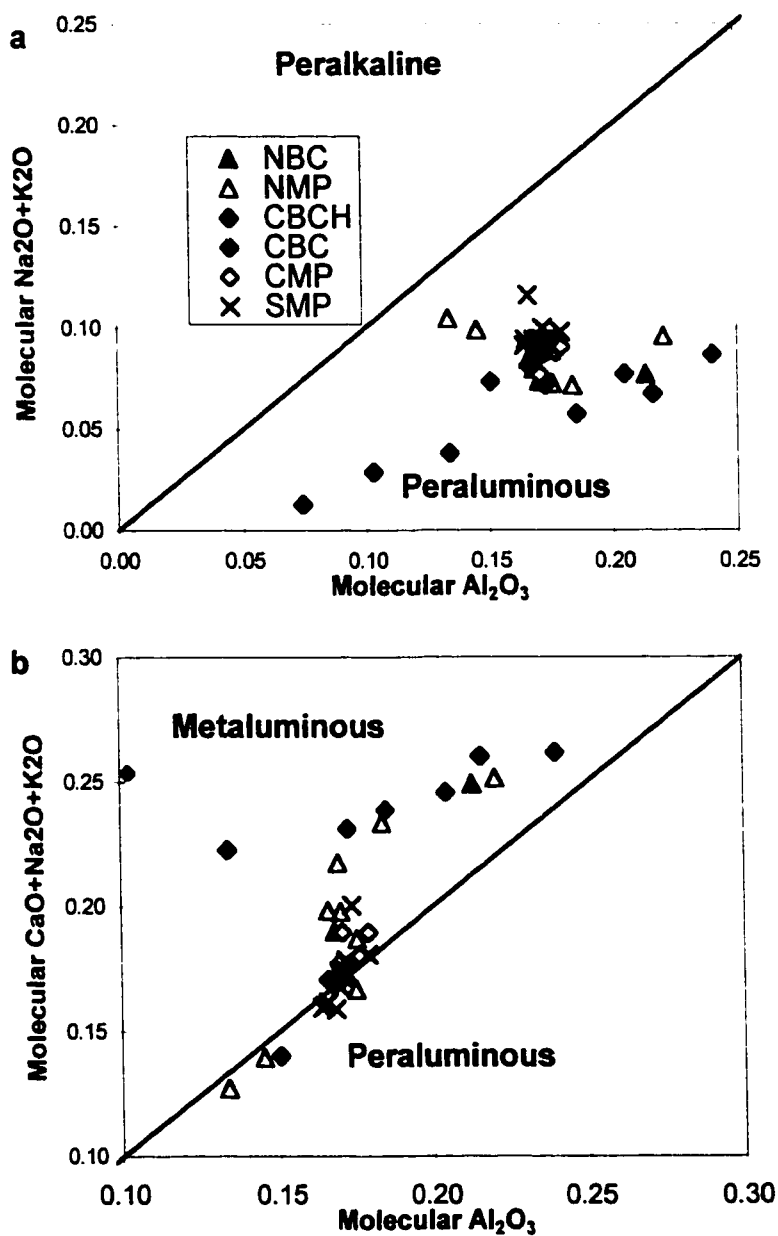


Figure 24. a) A/NK discrimination diagram. b) A/CNK discrimination diagram. Peraluminous samples from the A/NK diagram are plotted on the A/CNK diagram to determine if they are metaluminous or peraluminous. Abbreviations used as in Figure 22.

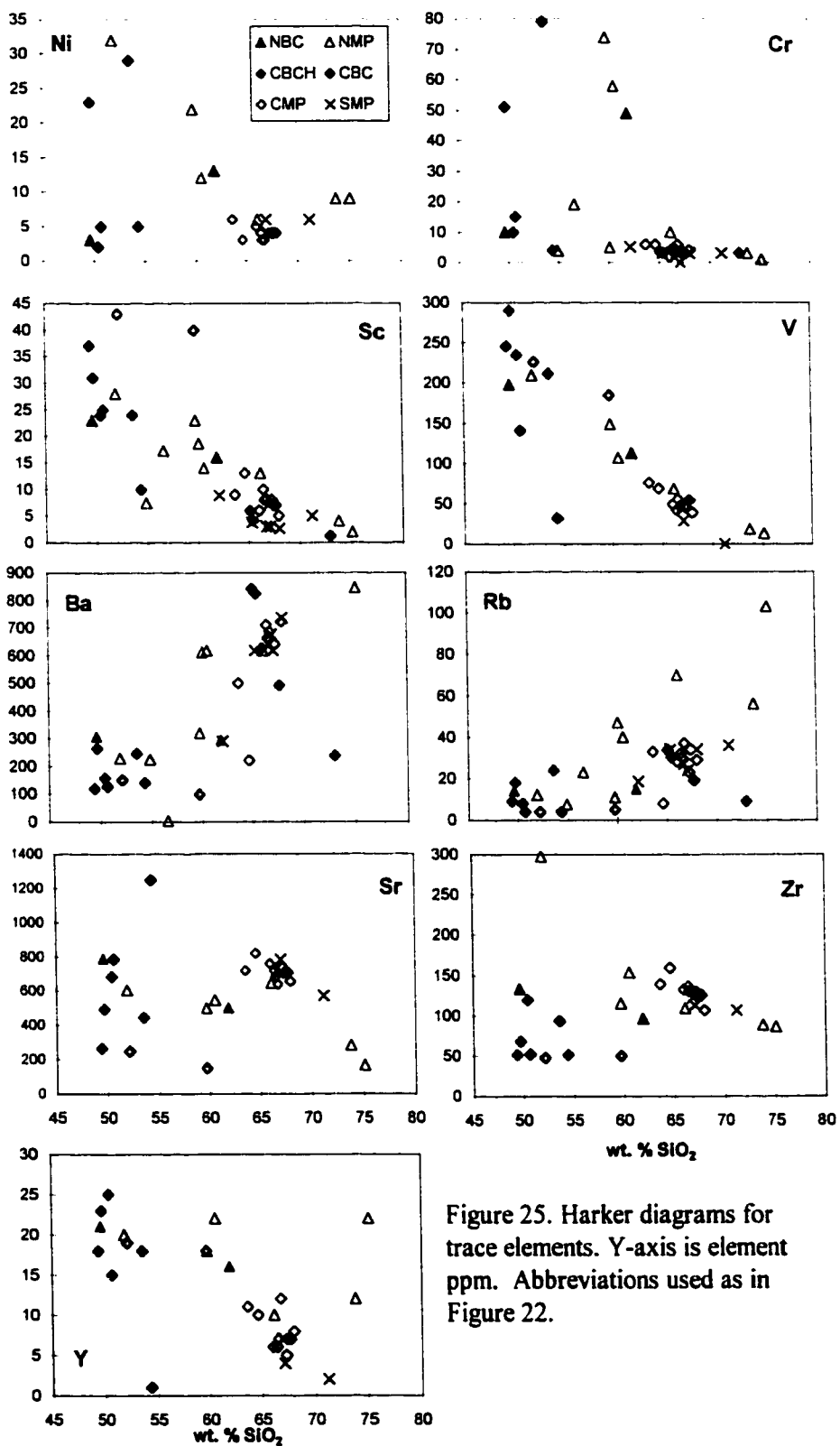


Figure 25. Harker diagrams for trace elements. Y-axis is element ppm. Abbreviations used as in Figure 22.

their central and SE counterparts. Both of the hornblendite and two of the gabbro samples plot off the scale of the Ni and Cr diagrams, with Ni > 35 and Cr > 80. Sc also shows a compatible trend for all rock types and pluton locations. Ba and Rb display incompatible behavior, but these trends are scattered. This scatter might be due to low grade alteration of the samples. NW Main Phase samples with SiO₂ > 61% show a trend of higher Rb for a given SiO₂ than central and SE samples. Sr and Zr are incompatible in samples with less than 65% SiO₂, and then behave compatibly above 65% SiO₂. Y is compatible for central and SE samples, especially among samples with >60% SiO₂, but is higher for a given SiO₂ for most NW samples. This compatible behavior may be caused by Y substituting for Ca in minerals such as plagioclase (Krauskopf and Bird, 1995).

Hornblendite samples are very high in Ni and Cr relative to the rest of the samples, and are also high in Sc. They are low in Sr, Zr and Rb.

Rare Earth Element Chemistry

Rare earth element (REE) data for 47 samples from the Cardinal Peak pluton are presented in Appendix B. Chondrite-normalized REE diagrams are shown in Figures 26 through 29. Samples are divided into four groups: cumulates, mafic rocks (gabbro and diorite), mafic tonalite and felsic tonalite.

REE patterns for Cardinal Peak samples are typical of continental arc plutons, with LREE enriched relative to HREE for non-cumulate samples (Wilson, 1989).

Several of the mafic samples are strongly affected by accumulation of hornblende (bowed

upward pattern), and several mafic to felsic samples display accumulation of plagioclase (strong positive Eu anomaly).

Cumulates

Hornblendite (Fig. 26a). Three hornblendites from the central Border Complex (52-60% SiO₂) show a convex upward pattern that indicates hornblende accumulation. La/Yb ranges from 1.3 to 2.0.

Plagioclase accumulation (Fig. 26b). Two samples from the central Border Complex and one sample from the SE Main Phase show the strong positive Eu anomaly indicative of plagioclase accumulation, and have lower total REE compared to other samples from the Cardinal Peak pluton. These rocks vary from 53 to 74% SiO₂. Rock types are diorite (one sample) and leucotonalite with less than 5% mafic minerals (two samples). There is no correlation of REE with SiO₂ or abundance of plagioclase in these samples.

Mafic Rocks (47-60% SiO₂)

Northwest (Fig. 27a). Six mafic rocks (50-60% SiO₂) from the NW Main Phase and Border Complex are plotted on this diagram. The rock types represented are gabbro, diorite and quartz diorite. These samples generally exhibit slight enrichment in light REE compared to heavy REE with (La/Yb)_{CN} at 2.4 to 4.2. The exception is one sample which is more depleted in heavy REE (4x chondrite for Lu), and has a correspondingly steeper

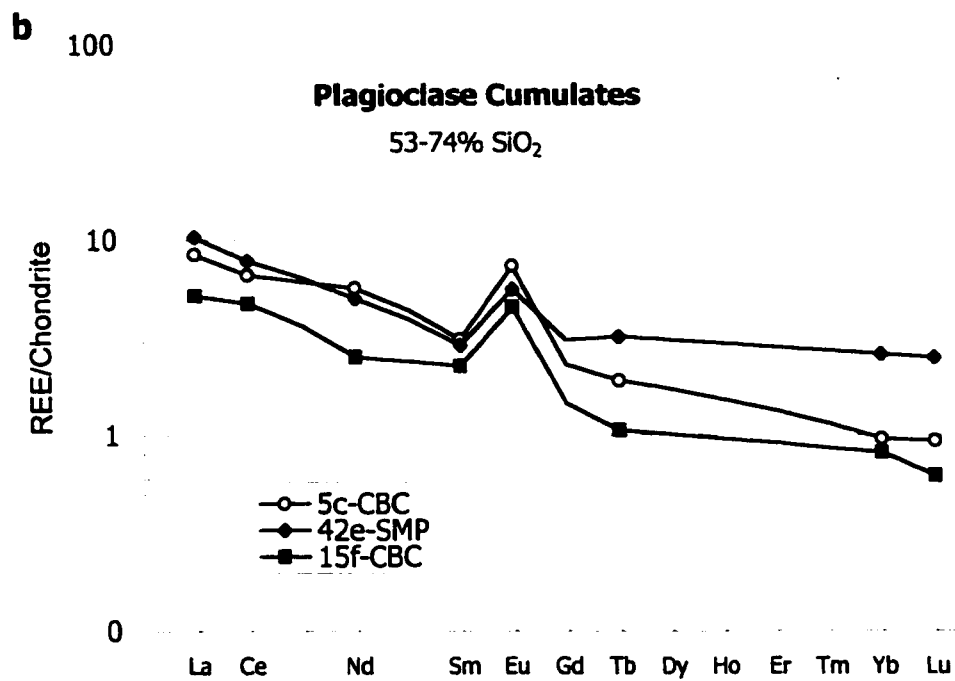
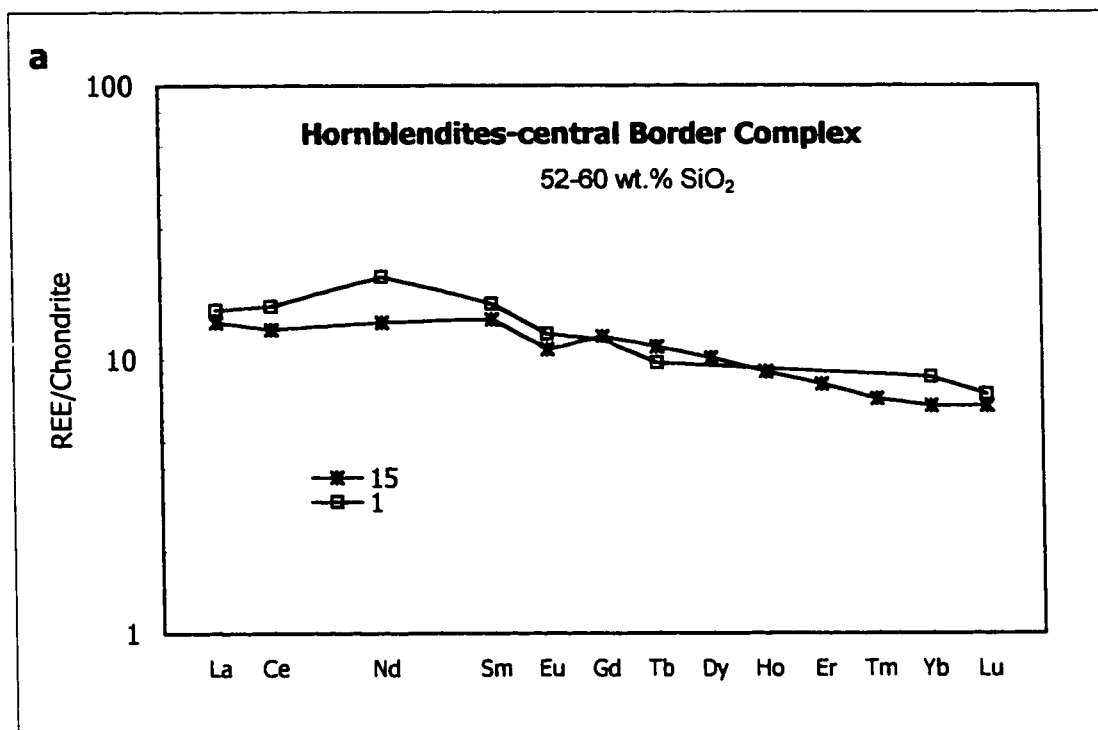


Figure 26. a) REE patterns for hornblendites from the central Border Complex. b) REE patterns for rocks with plagioclase accumulation. Note the change of scale. Abbreviations used as in Figure 22. Sample locations can be found on Figure 5.

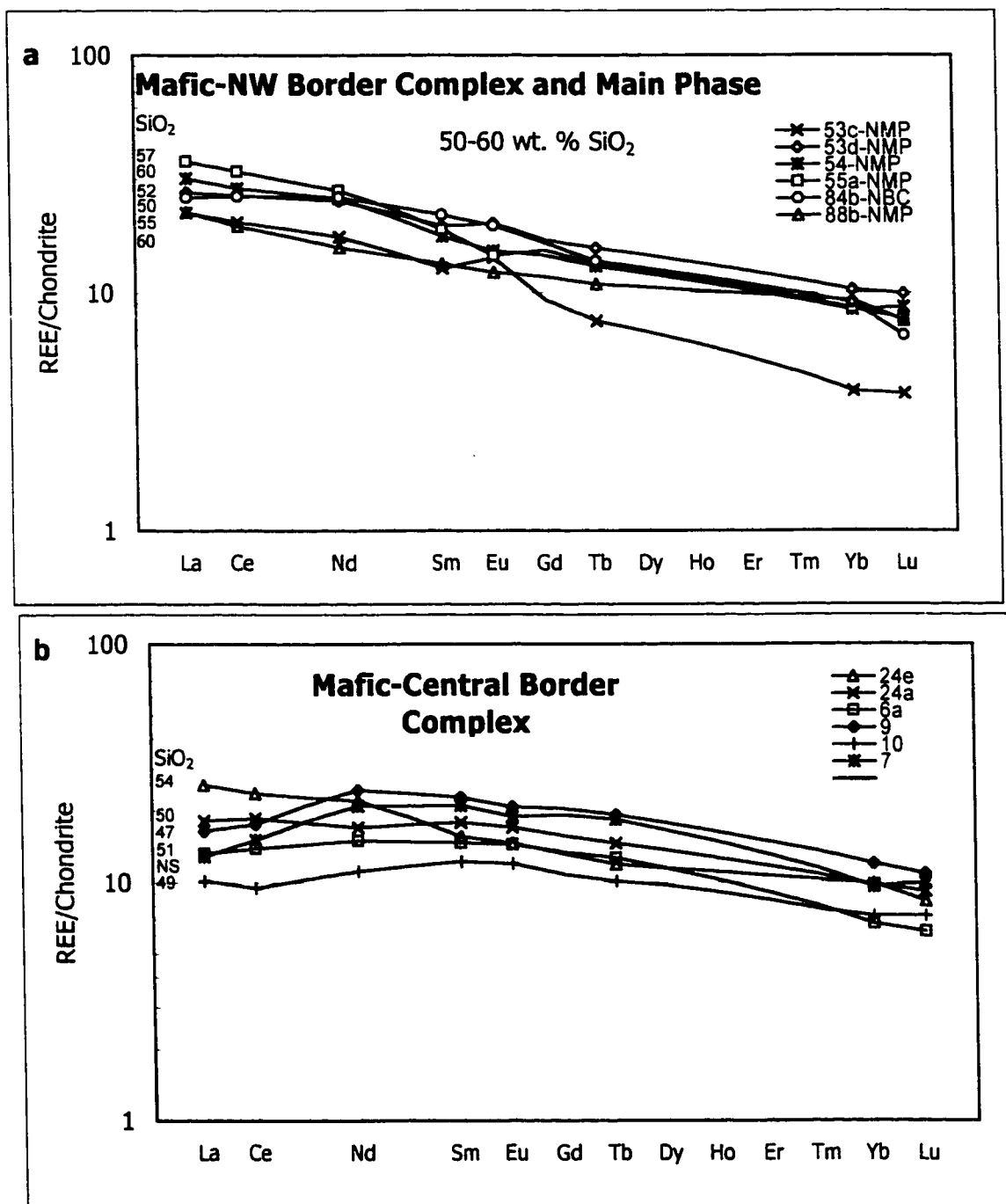


Figure 27. a) REE patterns for mafic rocks from the NW Border Complex and Main Phase. b) REE patterns for mafic rocks from the central Border Complex. Sample locations can be found on Figure 5.

slope ($(La/Yb)_{CN}=5.6$). Two of the samples display slight positive Eu anomalies, while one displays a slight negative Eu anomaly. Two gabbro samples show the bowed upward pattern indicating hornblende accumulation. There is no correlation of REE with SiO_2 .

Central (Fig. 27b). Six mafic rocks (47-54% SiO_2) from the central Border Complex are presented here. These rocks are gabbro, diorite and quartz diorite. Most of these samples show the bowed-up pattern indicative of hornblende accumulation, and also exhibit a very slight enrichment in light REE compared to heavy REE with $(La/Yb)_{CN}$ at 1.4 to 2.6. None of the samples display Eu anomalies. There is no correlation of REE with SiO_2 or abundance of hornblende in these samples.

Mafic Tonalite (60-65% SiO_2)

Northwest (Fig. 28a). Three tonalite samples from the NW Main Phase fit in this category with 60-64% SiO_2 . They are slightly more enriched in LREE (20-50x chondrite for La) and more depleted in HREE (4-8x chondrite for Lu) than the mafic samples, and their REE patterns show correspondingly steeper slopes with $(La/Yb)_{CN}$ at 4.1 to 6.5. Both slightly negative and slightly positive Eu anomalies are apparent in these samples.

Central (Fig. 28b). Six tonalite samples from the central Main Phase are presented here. These rocks have 64-65% SiO_2 . LREE values are 40-60x chondrite for La, and HREE are 1-3x chondrite for Lu, with $(La/Yb)_{CN}$ at 8.0 to 36.6. Most of these samples show slight positive Eu anomalies.

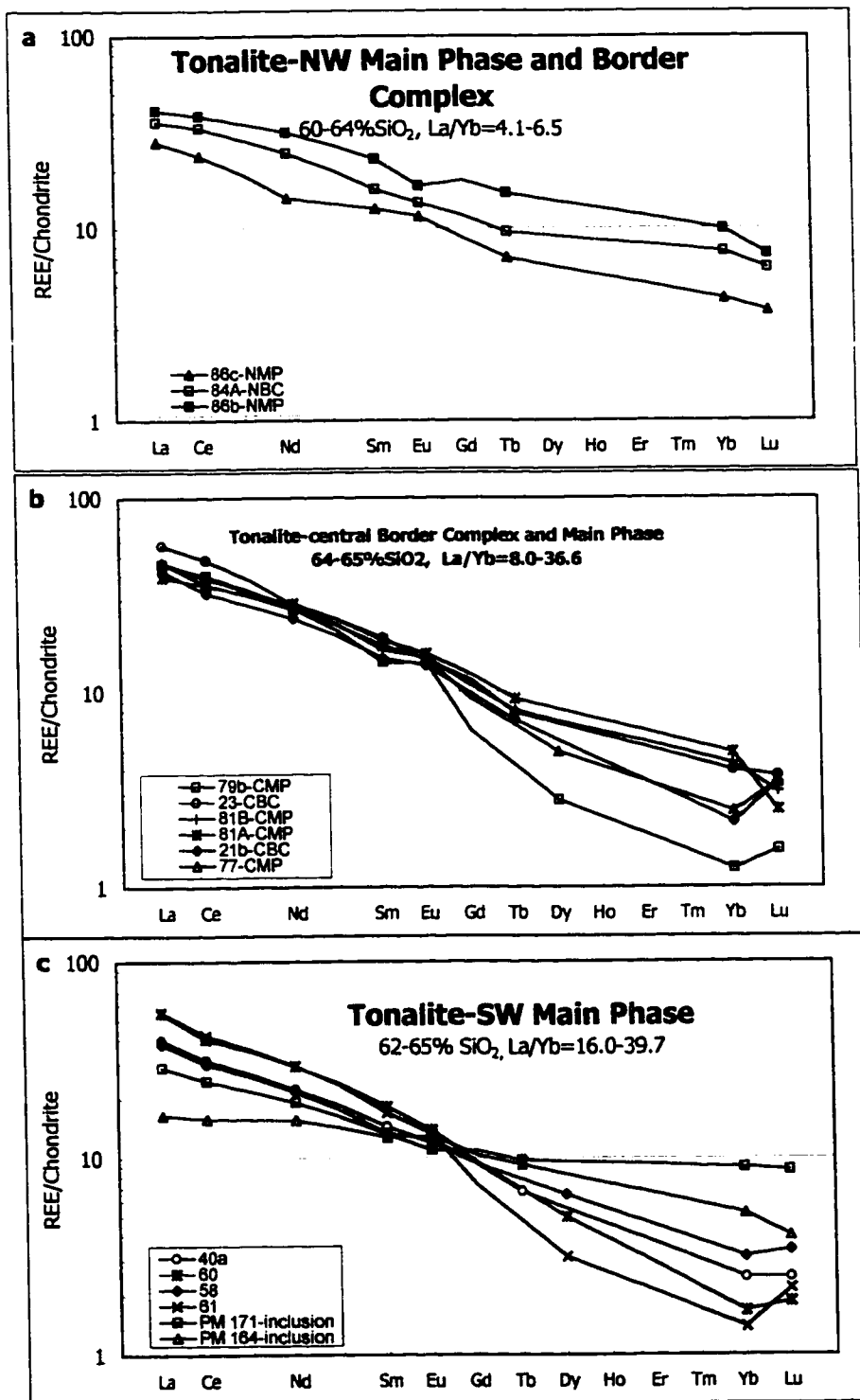


Figure 28. REE patterns for tonalites with 60 to 65% SiO₂. a) Samples from northern Main Phase and Border Complex. b) Samples from central Main Phase and Border Complex. c) Samples from southern Main Phase and hornblende-bearing enclaves. Sample locations may be found on Figure 5. Abbreviations used as in Figure 22.

Southeast (Fig. 28c). Six tonalite samples from the SE Main Phase have 62-65% SiO₂. Two are from the large hornblende-bearing inclusions found south of Grouse Pass. For the non-inclusion samples, LREE values are 40-60x chondrite for La, and HREE are 1-3x chondrite for Lu, with (La/Yb)_{CN} at 16 to 39.7. One of the samples shows a slight positive Eu anomaly. Rocks from the inclusions have LREE values at 17-30x chondrite for La, and HREE at 4-9x chondrite for Lu, and (La/Yb)_{CN} at 3.1-3.2.

Felsic Tonalite (>65% SiO₂)

Northwest (Fig. 29a). Two samples from the NW Main Phase are felsic tonalite. These samples have a slightly convex REE pattern and moderate slopes with (La/Yb)_{CN} from 6.8 to 8.6. They comprise the most felsic tonalite (70-75% SiO₂), but display the lowest (La/Yb)_{CN}.

Central (Fig. 29b). Four tonalite samples from the central Main Phase and one sample from the central Border Complex have from 66 to 74% SiO₂. They have subparallel REE patterns with fairly constant slopes from LREE to HREE, with (La/Yb)_{CN} from 24.6 to 42.1. One of the samples shows a slight negative Eu anomaly.

Southeast (Fig. 29c). These eight samples from the SE Main Phase show REE patterns that are roughly parallel from La to Sm, but have a marked inflection or “dogleg” after Eu. They have the highest (La/Yb)_{CN} at 15.5 to 58.9, and do not exhibit Eu anomalies. SiO₂ content ranges from 66 to 70% SiO₂

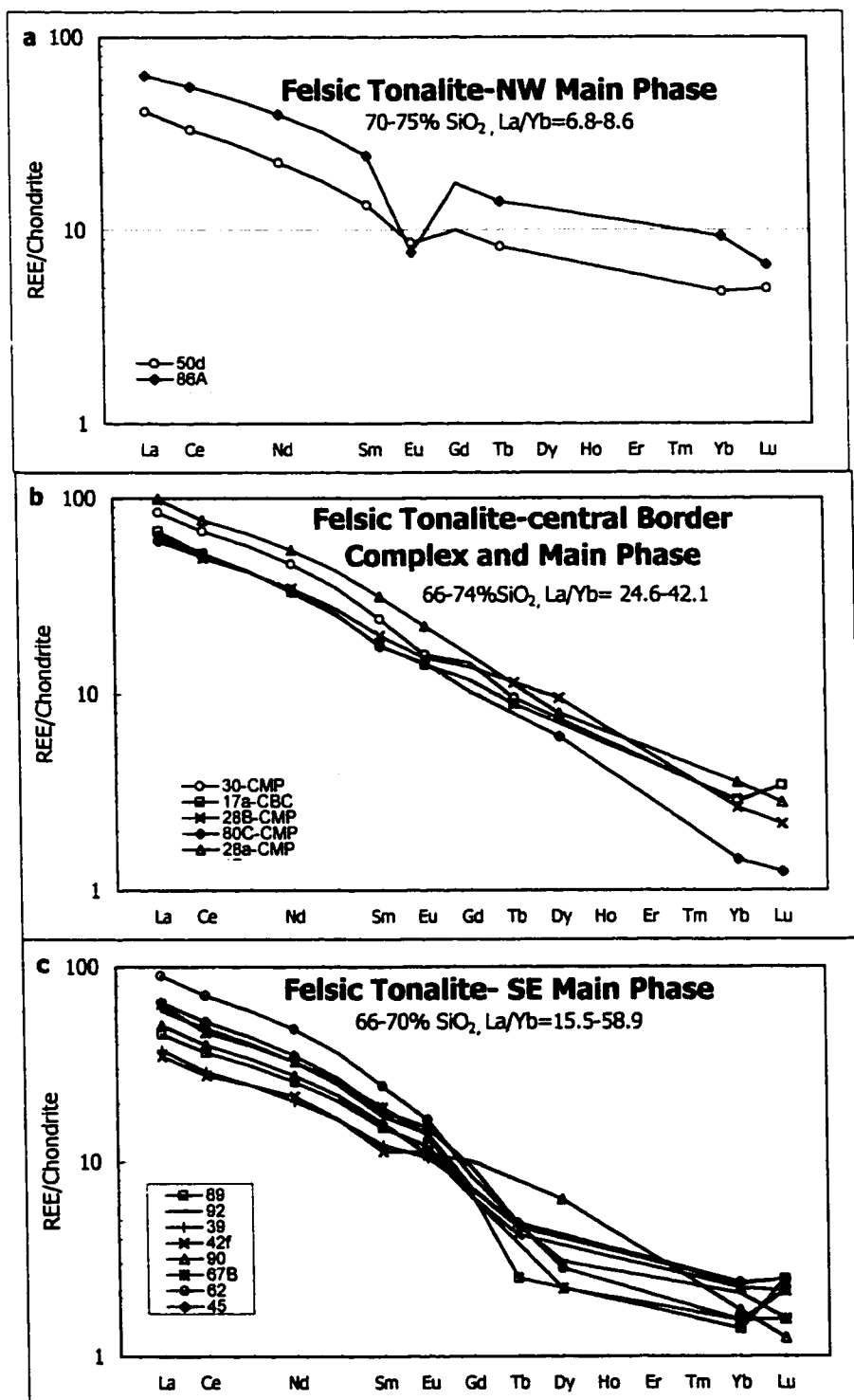


Figure 29. REE patterns for tonalites with >65% SiO₂. a) Samples from NW Main Phase. b) Samples from central Main Phase and Border Complex. c) Samples from SE Main Phase. Sample locations can be found on Figure 5. Abbreviations used as in Figure 22.

MINERAL CHEMISTRY

This section describes the chemistry of three of the major minerals found in the Cardinal Peak pluton: plagioclase, amphibole and biotite; and one accessory mineral: epidote. Spatial variations in mineral chemistry may give clues to the petrologic processes that took place in the pluton. In addition, mineral chemistry is necessary for the fractional crystallization modeling discussed in a subsequent section, while epidote chemistry is necessary to determine whether it has a magmatic origin. Finally, plagioclase and amphibole chemistry is needed for barometry and thermometry.

Analytical Methods

Mineral chemistry was determined by the author, using the JEOL 733 Superprobe electron microprobe at Stanford University. The electron beam was set with an accelerating voltage of 15 kV and the current at 15 nA. Beam size was set at 10 μm for plagioclase, and 1 μm for other minerals. Count time for each element was 20 seconds, and data were reduced using the CITZAF corrections (Armstrong, 1995). A set of internal mineral standards prepared by Stanford University was used for calibration.

Plagioclase

Representative plagioclase analyses for 14 samples are shown in Table 3. Five of these samples are from the Border Complex, and 9 from the Main Phase. In all samples,

anorthite (An) content of plagioclase has a range of An₁₄ to An₅₉, while Or content ranges from Or₀ to Or₁₂.

Rocks from the Border Complex generally show higher An values than rocks from the Main Phase. Plagioclase from a single sample of NW Border Complex has An₃₉₋₅₆, while central Border Complex samples show An₃₅₋₅₂. A core-rim traverse through a plagioclase grain from the central Border Complex (Fig. 30a) reveals a steady decline from An₅₀ in the core to An₄₁ in the rim.

In the Main Phase, the An content of plagioclase varies with location in the pluton, generally decreasing from NW to SE (Fig. 31a). This trend inversely follows the trend of increasing whole rock SiO₂ (Fig. 31b, c). Plagioclase in the NW Main Phase is An₃₀₋₅₀. A rim-rim traverse through a plagioclase grain from the NW Main Phase (Fig. 30a) shows the core at An₅₀, but, halfway to the edge of the grain, a sharp decline to An₃₅ takes place. Optically, this same grain displays a core with strong oscillatory zoning, mantled by a normally zoned rim (Fig. 16). A quartz diorite from the NW Main Phase has the highest Or content measured, Or₁₋₁₂.

The central Main Phase has lower values of An than the NW Main Phase, ranging from An₂₅ to An₅₂, and SE Main Phase samples have the lowest overall An values at An₁₄₋₃₉. The greatest range of An occurs in a sample from the central Main Phase (An₃₁₋₅₂). Core to rim traverses through 2 plagioclase grains in SE Main Phase samples (Fig. 30c, d) display an overall drop in An content from core to rim; however, both grains show zones with increasing An on core to rim traverses. Optical oscillatory zoning also occurs in both of these grains.

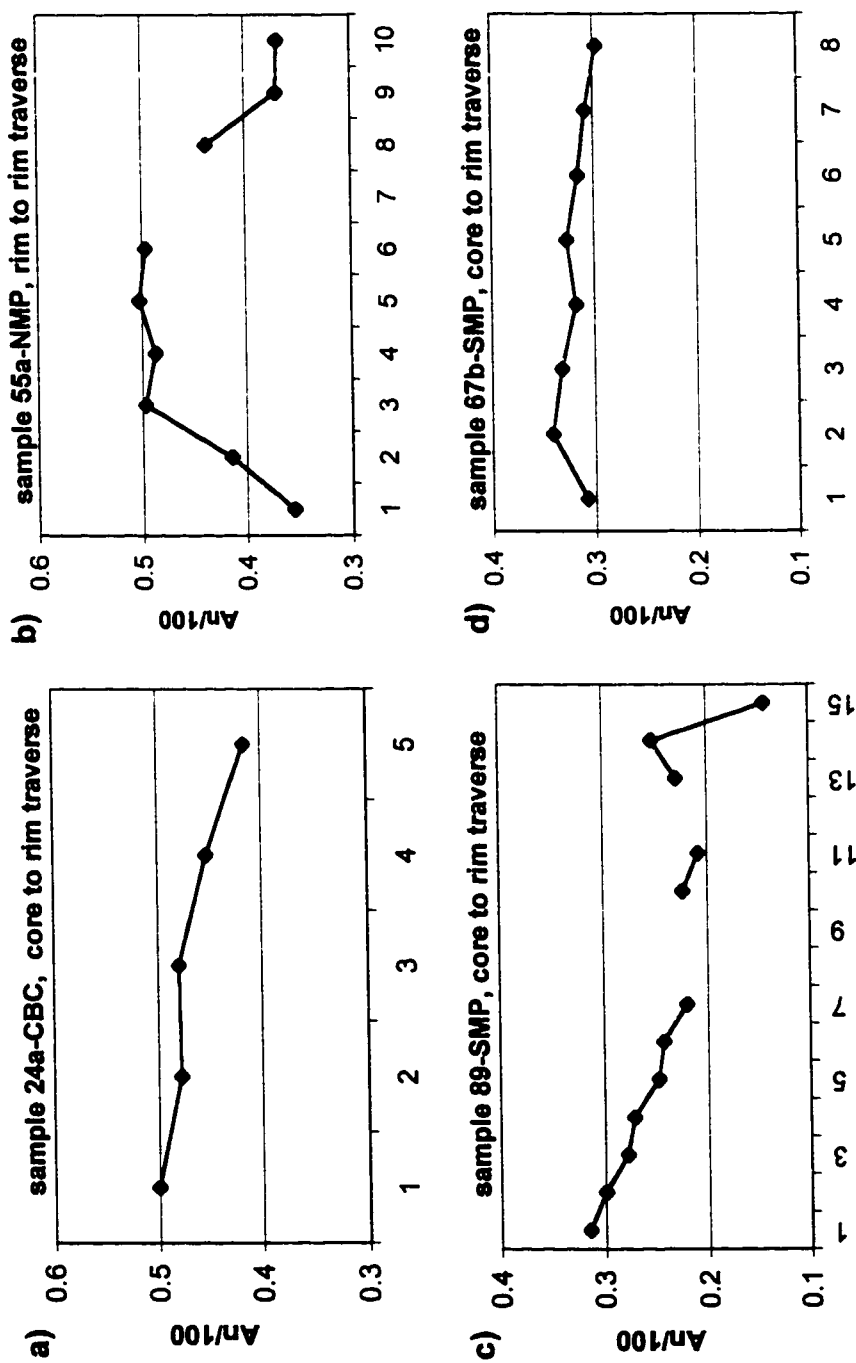


Figure 30. Traverses across plagioclase grains. Y-axis is An content and x-axis is step number. Note the scale change from the top two charts to the lower two charts. Abbreviations used as in Figure 22.

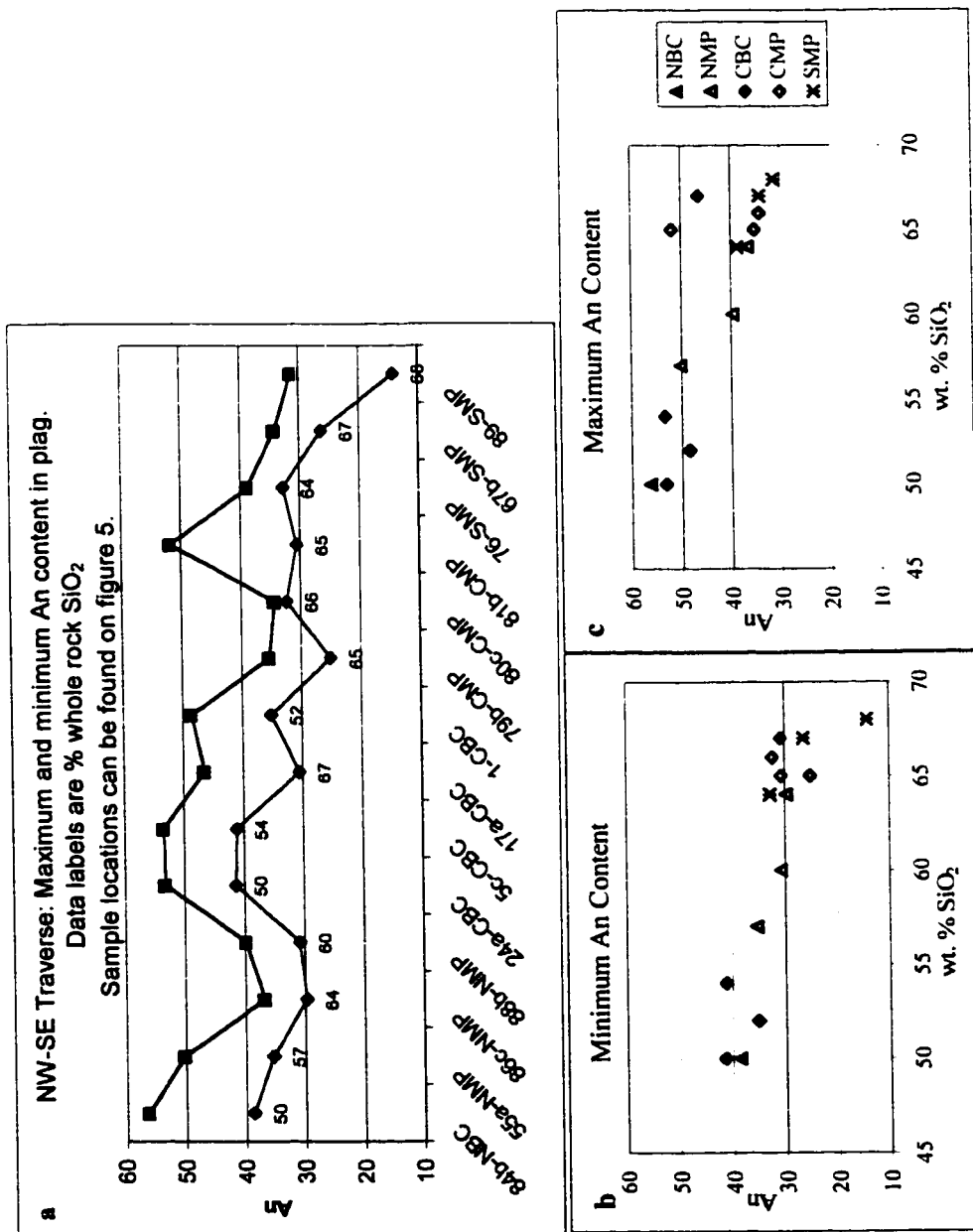


Fig 31. a: Maximum and Minimum An content in a NW-SE traverse. b: Minimum An content plotted against whole rock wt. % SiO₂. c: Maximum An content plotted against whole rock wt. % SiO₂. Abbreviations used: NBC=NW Border Complex, CBC=central Border Complex, NMP=NW Main Phase, CMP=central Main Phase, SMP=SE Main Phase.

Amphibole

Representative amphibole analyses are shown in Table 4. Amphibole is calcic, and ranges from tschermakite to actinolite (Fig. 32), using the nomenclature of Leake (1978). A majority of the samples contain magnesio-hornblende to tschermakite. Actinolite and actinolic hornblende are found only in the central Border Complex hornblendite sample, which also has magnesio-hornblende. The SE Main Phase sample contains mostly tschermakite.

Changes in amphibole mineral chemistry are evident from NW to SE along the strike of the pluton (Fig. 33). Overall, there is a decrease in Mg# [$Mg/(Mg+Fe)$] and an increase in Na+K. Al and Si are generally constant throughout the pluton

Variation diagrams (Fig. 34) show changes in amphibole mineral chemistry as a function of whole rock SiO_2 . These diagrams illustrate that most of the variations in amphibole chemistry correlate with increasing differentiation of the rock. Mg# decreases with increasing differentiation, although central Border Complex samples have high Mg#'s for their whole rock SiO_2 . Na+K increases with increasing SiO_2 , although the single central Main Phase sample has low Na+K. Both Al and Si are constant with respect to whole rock SiO_2 . Amphibole from the central Border Complex hornblendite has high Mg#, low Na+K, low Al and high Si compared to the rest of the samples. This might reflect a different origin for these amphiboles.

Table 4. Representative amphibole analyses. Sample locations can be found on Fig. 5. Abbreviations used as in Figure 31.

	<u>84b-NBC</u>	<u>55a-NMP</u>	<u>88b-NMP</u>	<u>24a-CBC</u>	<u>1-CBC</u>	<u>5c-CBC</u>	<u>17a-CBC</u>	<u>81b-CMP</u>
Oxides (%)								
SiO ₂	43.30	42.38	44.95	42.43	48.07	45.75	42.60	43.82
TiO ₂	1.00	0.78	0.79	0.41	0.42	0.28	0.77	0.89
Al ₂ O ₃	12.65	11.36	8.11	14.36	7.49	11.07	10.26	11.54
FeO	16.05	16.59	17.09	14.60	9.08	11.22	18.39	17.52
MnO	0.27	0.33	0.68	0.25	0.18	0.27	0.55	0.41
Cr ₂ O ₃	0.01	0.00	0.00	0.00	0.06	0.00	0.00	0.00
MgO	10.16	10.64	10.81	10.34	15.84	13.86	9.57	9.43
CaO	10.69	11.29	11.69	11.26	12.50	11.92	11.59	10.71
Na ₂ O	1.47	1.32	0.81	1.19	0.75	1.12	0.99	1.39
K ₂ O	0.34	0.56	0.62	0.33	0.34	0.28	0.90	0.40
Total	95.95	95.24	95.55	95.17	94.71	95.78	95.62	96.12
Formula Atoms								
Si	6.54	6.51	6.89	6.41	7.10	6.75	6.60	6.65
Ti	0.11	0.09	0.09	0.05	0.05	0.03	0.09	0.10
Al	2.25	2.06	1.46	2.56	1.30	1.93	1.87	2.06
Fe	2.03	2.13	2.19	1.85	1.12	1.39	2.38	2.22
Mn	0.04	0.04	0.09	0.03	0.02	0.03	0.07	0.05
Cr	0.00	0.00	0.00	0.00	0.01	0.00	0.00	0.00
Mg	2.29	2.44	2.47	2.33	3.49	3.05	2.21	2.13
Ca	1.73	1.86	1.92	1.82	1.98	1.88	1.92	1.74
Na	0.43	0.39	0.24	0.35	0.21	0.32	0.30	0.41
K	0.07	0.11	0.12	0.06	0.06	0.05	0.18	0.08
Total	38.47	38.62	38.47	38.47	38.34	38.44	38.62	38.46

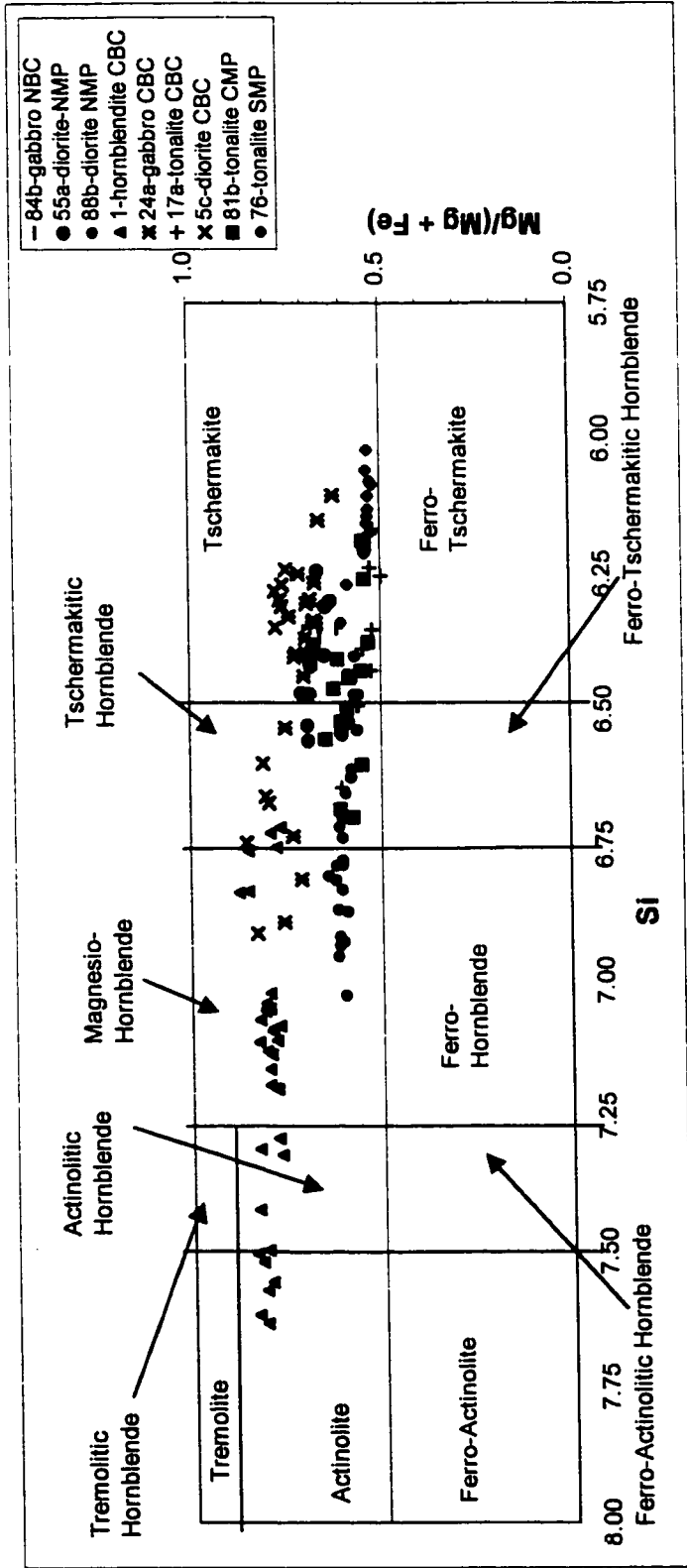


Figure 32. Leake (1978) nomenclature diagram for hornblende in Cardinal Peak samples. Abbreviations used as in Figure 31.

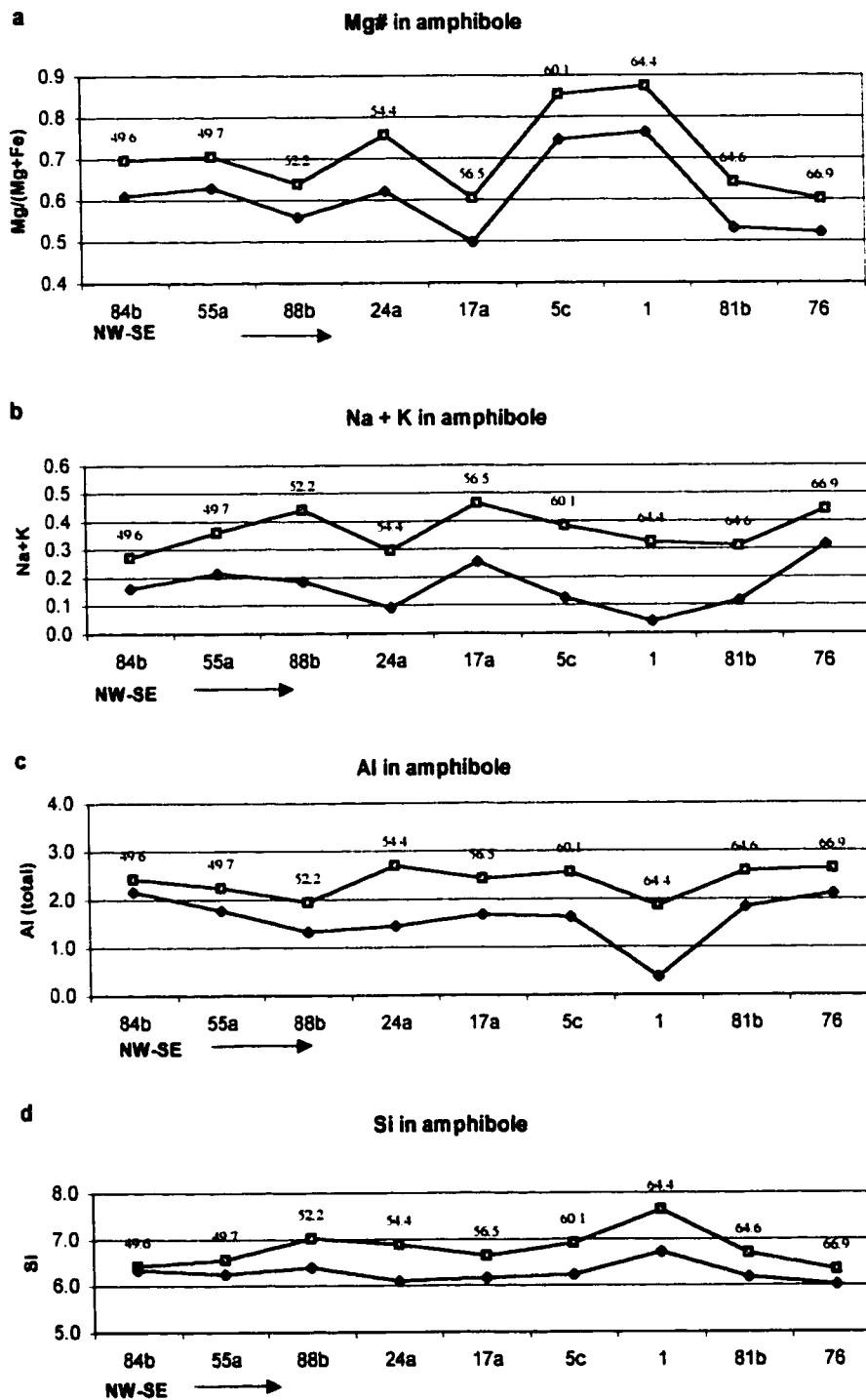


Figure 33. Maximum and minimum values for elements in amphibole along NW to SE traverses. Data labels are whole rock SiO_2 for the sample. Samples locations can be found on Figure 5.

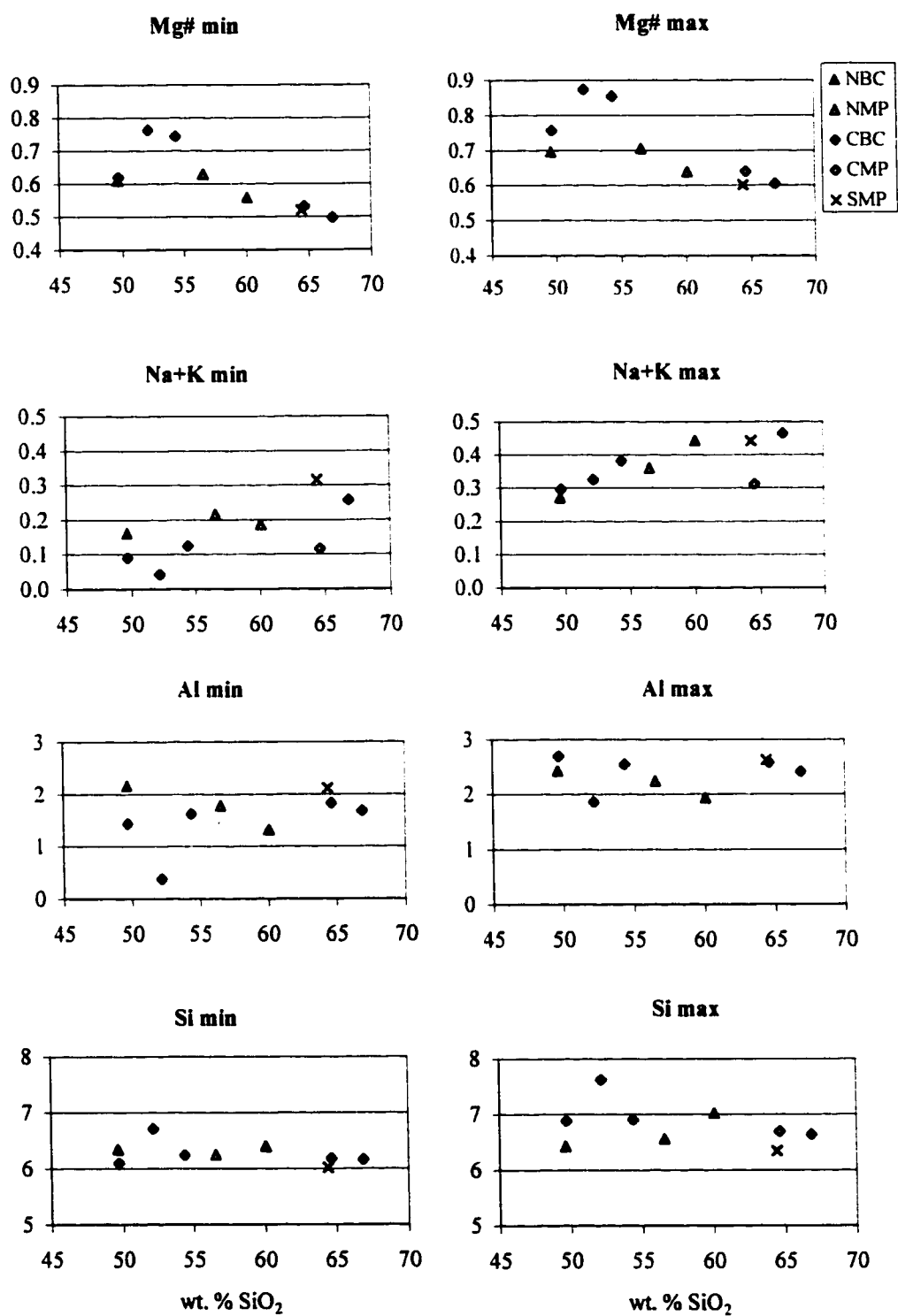


Fig 34. Amphibole mineral chemistry vs. whole rock wt. % SiO₂.

Biotite

Representative biotite analyses are shown in Table 5. Mg content of biotite ranges from 0.85 to 1.68 formula atoms (f.a.), Fe content from 0.87 to 1.41 f.a., and Al content from 1.35 to 1.62 f.a. As with amphibole, changes in biotite chemistry are evident along strike from NW to SE (Fig. 35), reflecting the increasing differentiation of the pluton (Fig. 36). The Mg content of biotite decreases from NW to SE, while Fe content increases. Al generally increases from NW to SE, but shows scatter.

Epidote

Representative epidote analyses from 6 samples are listed in Table 6. Pistacite $[100 \cdot \text{Fe}^{3+} / (\text{Fe}^{3+} + \text{Al})]$ content of epidote ranges from Ps_{24} to Ps_{39} (Fig. 37). Note that some analyses were taken from cores, and others were taken from traverses across grains. The traverses across grains record the most variability in pistacite content. These traverses show that epidote can have either high Ps cores and lower Ps rims (Fig. 38a), or lower Ps cores and higher Ps rims (Fig. 38b).

Table 5. Representative biotite analyses. Sample locations are shown on Figure 5. Abbreviations used as on Figure 31.

	<u>86c-NMP</u>	<u>88b-NMP</u>	<u>55a-NMP</u>	<u>17a-CBC</u>	<u>24a-CBC</u>	<u>79b-CMP</u>	<u>67b-SMP</u>	<u>89-SMP</u>
Oxide (%)								
SiO ₂	35.12	35.08	36.33	36.64	36.33	35.40	35.93	36.05
TiO ₂	2.83	3.77	2.75	3.49	2.42	3.50	2.37	3.17
Al ₂ O ₃	17.19	15.72	15.15	15.69	16.43	17.44	16.72	16.69
FeO	20.03	19.62	16.89	19.19	14.43	19.50	18.73	20.89
MnO	0.34	0.31	0.17	0.23	0.09	0.30	0.23	0.59
Cr ₂ O ₃	0.00	0.00	0.00	0.00	0.01	0.00	0.00	0.02
MgO	8.86	10.16	13.76	10.76	14.62	9.42	10.04	8.15
CaO	0.00	0.01	0.04	0.01	0.02	0.00	0.00	0.00
Na ₂ O	0.11	0.07	0.14	0.09	0.14	0.09	0.09	0.08
K ₂ O	9.50	9.06	8.85	9.09	9.23	9.35	9.44	9.42
Total	93.98	93.79	94.10	95.19	93.72	95.00	93.55	95.05
Formula Atoms								
Si	2.73	2.73	2.77	2.79	2.75	2.71	2.78	2.78
Ti	0.17	0.22	0.16	0.20	0.14	0.20	0.14	0.18
Al	1.58	1.44	1.36	1.41	1.47	1.57	1.53	1.52
Fe	1.30	1.28	1.08	1.22	0.91	1.25	1.21	1.35
Mn	0.02	0.02	0.01	0.01	0.01	0.02	0.01	0.04
Cr	0.00	0.00	0.00	0.00	0.00	0.00	0.00	0.00
Mg	1.03	1.18	1.56	1.22	1.65	1.08	1.16	0.94
Ca	0.00	0.00	0.00	0.00	0.00	0.00	0.00	0.00
Na	0.02	0.01	0.02	0.01	0.02	0.01	0.01	0.01
K	0.94	0.90	0.86	0.88	0.89	0.91	0.93	0.93
Total	18.79	18.78	18.83	18.75	18.84	18.76	18.79	18.75

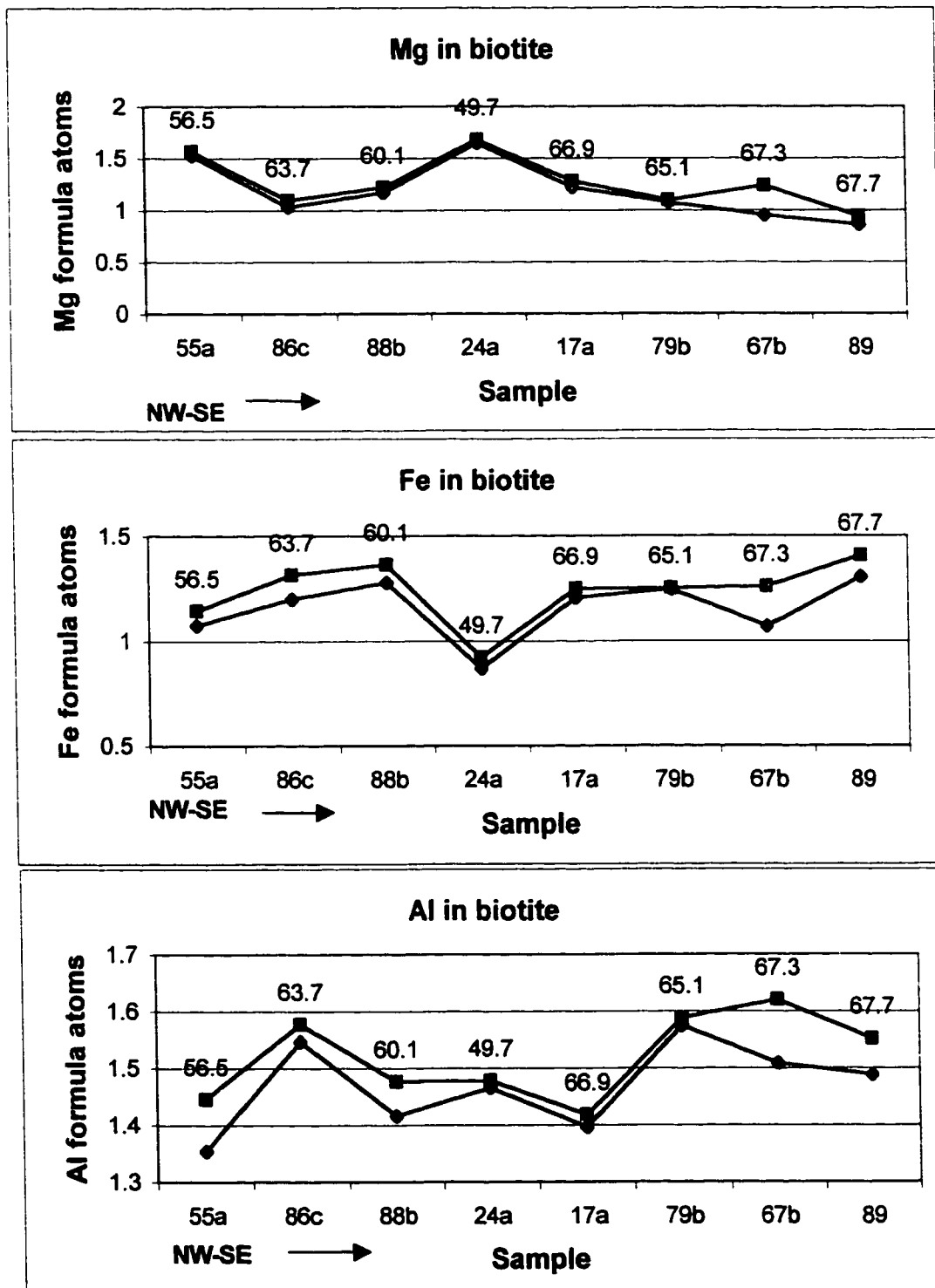


Figure 35. Maximum and minimum values for elements in biotite along NW-SE traverses. Data labels are whole rock SiO₂.

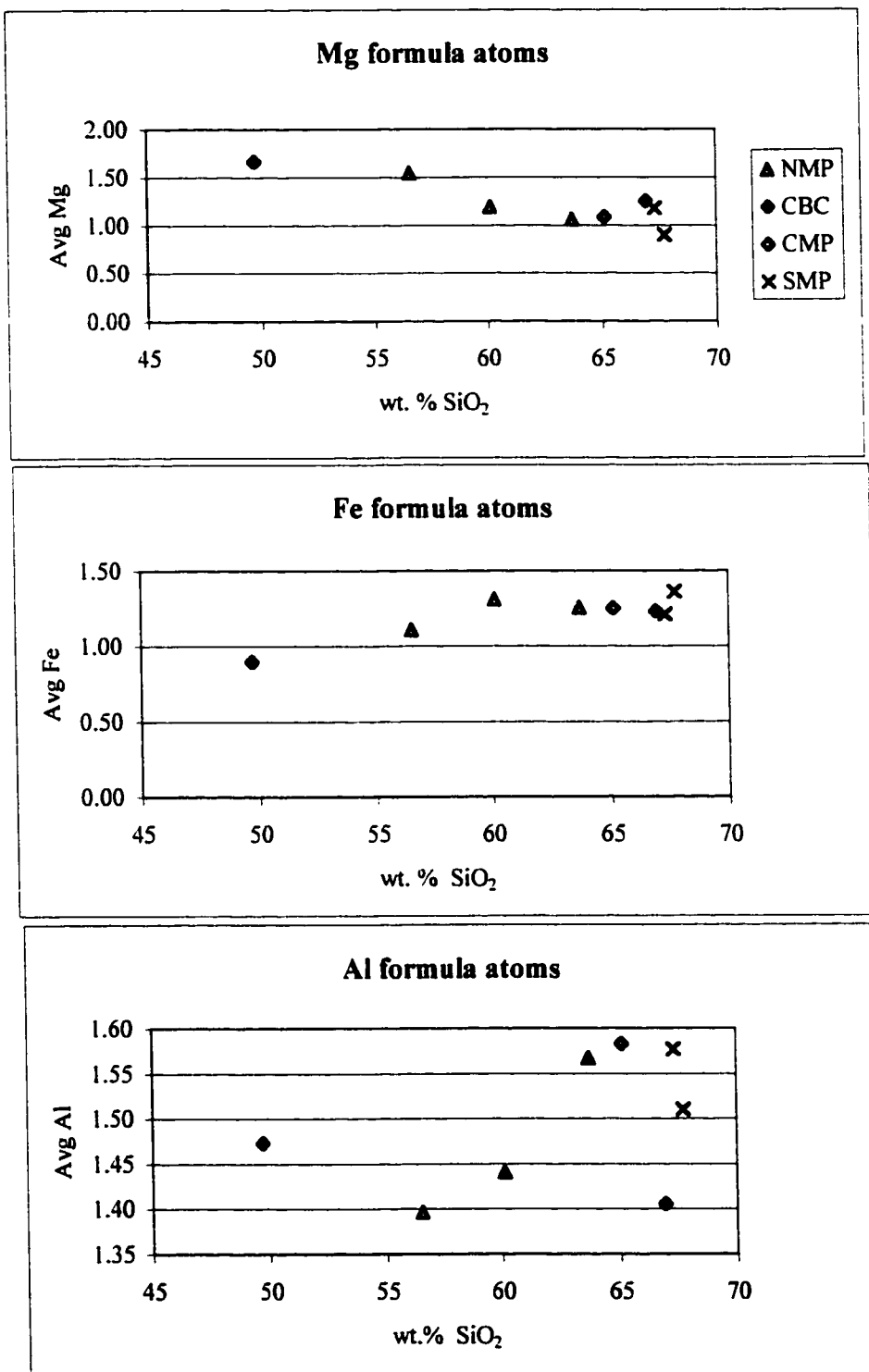


Fig 36. Biotite mineral chemistry vs. whole rock wt. % SiO₂.
Abbreviations used as in Figure 31.

Table 6. Representative epidote analyses. Sample locations are on Figure 5. Abbreviations as on Figure 31.

	<u>17a-CBC</u>	<u>79b-CMP</u>	<u>80c-CMP</u>	<u>76-SMP</u>	<u>67b-SMP</u>	<u>89-SMP</u>
Oxide (%)						
SiO ₂	30.06	32.95	31.17	37.16	37.90	37.78
TiO ₂	37.83	0.30	0.47	0.10	0.23	0.18
Al ₂ O ₃	1.33	18.81	15.98	24.83	23.80	24.22
Fe ₂ O ₃	0.69	13.81	15.01	10.64	13.05	12.69
MnO	0.09	0.44	0.66	0.26	0.22	0.43
Cr ₂ O ₃	0.00	0.17	0.30	0.00	0.02	0.00
MgO	0.00	0.41	0.57	0.02	0.03	0.03
CaO	28.94	17.15	13.67	23.44	22.73	22.65
Na ₂ O	0.00	0.04	0.04	0.00	0.00	0.01
K ₂ O	0.00	0.01	0.02	0.00	0.00	0.00
Totals	98.93	84.08	77.88	96.46	97.99	97.99
Formula Atoms						
Si	2.59	3.06	3.12	3.17	3.01	3.00
Ti	2.45	0.02	0.04	0.01	0.01	0.01
Al	0.13	2.06	1.89	2.49	2.23	2.26
Fe	0.05	0.96	1.13	0.76	0.78	0.76
Mn	0.01	0.03	0.06	0.02	0.01	0.03
Cr	0.00	0.01	0.02	0.00	0.00	0.00
Mg	0.00	0.06	0.08	0.00	0.00	0.00
Ca	2.67	1.70	1.47	2.14	1.93	1.92
Na	0.00	0.01	0.01	0.00	0.00	0.00
K	0.00	0.00	0.00	0.00	0.00	0.00
Totals	20.90	20.41	20.32	21.58	20.48	20.48
Pistacite	0.27	0.32	0.37	0.23	0.26	0.25

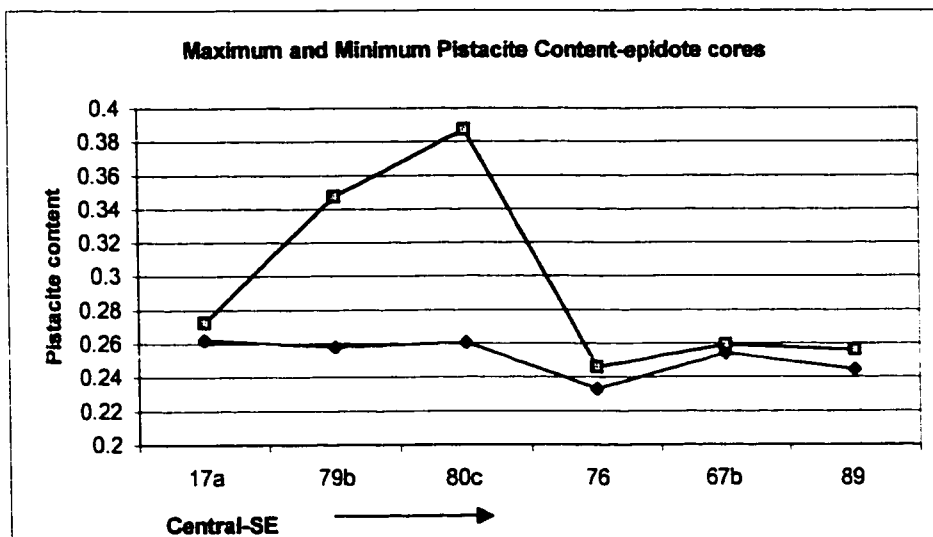


Figure 37. Maximum and minimum pistacite content in epidote for a central to SE traverse along the pluton. Sample locations can be found on Figure 5.

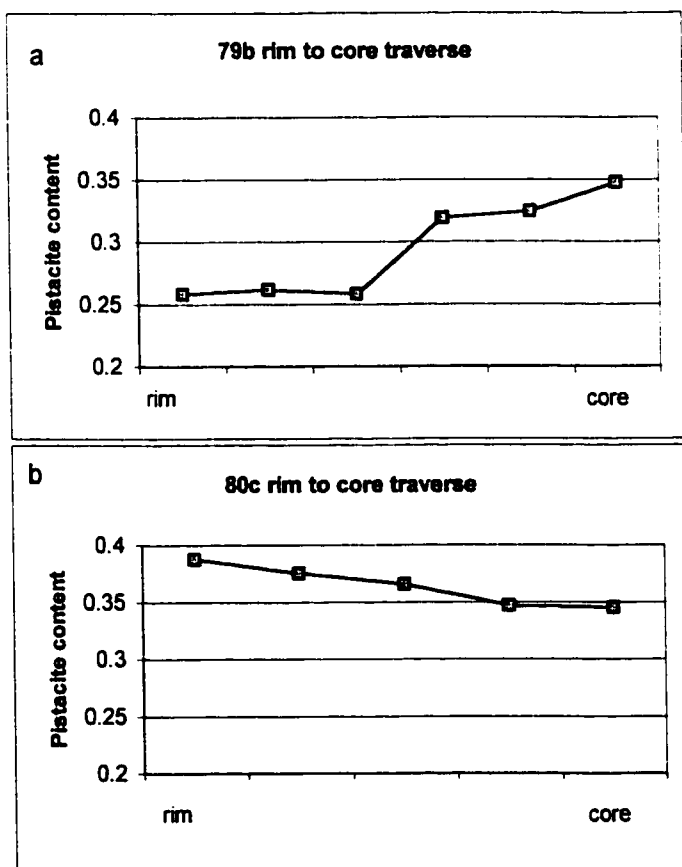


Figure 38. Pistacite content in traverses through epidote grains from rim (left) to core (right).

PRESSURE AND TEMPERATURE CONSTRAINTS ON PLUTON CRYSTALLIZATION

Constraints on Pressure From Magmatic Epidote

Quantitative barometry cannot be done with epidote, but the presence of magmatic epidote is believed to indicate a pressure of crystallization of at least 6 kbar (Zen and Hammarstrom, 1984). As discussed above, textural evidence suggests that much of the epidote in the Cardinal Peak pluton is magmatic. With the exception of one iron-rich grain, epidote falls between Ps_{24} and Ps_{33} , which is within the range found for magmatic epidote by Naney (1983); however, this is higher than the range of Ps_{20} - Ps_{25} given by Zen and Hammarstrom (1984) for high-pressure (> 6 kbar) magmatic epidote. The high pistacite content of some of the epidote in the pluton may mean that these grains formed at lower pressures than 6 kbar (Barth, 1990).

Al-in-Hornblende Barometry

The total amount of aluminum in hornblende has been correlated with pressures of crystallization (Hammarstrom and Zen, 1984; Hollister et al., 1987; Johnson and Rutherford, 1989; Rutter et al., 1989; Schmidt, 1992). The formulation of the Al-in-hornblende barometer used in this study is from Schmidt (1992), because he calibrated his thermometer using rocks similar in composition to Cardinal Peak tonalite. This barometer requires an eight-phase assemblage: hornblende, quartz, plagioclase, K-feldspar, apatite, biotite, sphene, and Fe-Ti oxides. Cardinal Peak samples containing

hornblende are lacking in one of the required phases, K-feldspar. This means that pressures obtained represent maximum values (Hollister et al., 1987).

Hornblende grains from six samples were analyzed; these six samples form a NW-SE traverse along the strike of the pluton from Hilgard Pass to Cardinal Peak (Fig. 5). Pressure results from this traverse can be used to test the hypothesis that the pluton is tilted downward to the SE, exposing a deeper section in the NW. At least three hornblende grains from each sample were analyzed by electron microprobe, with a minimum of six analysis points in each grain. Analyses were done on rims of hornblende within 20 μ of quartz, in order to ensure the hornblende was in equilibrium with the last crystallizing phases.

Results of the pressure determination are shown in Table 7. Pressures obtained range from 3.3 to 9.5 kbar, with a median value of 7.0 kbar. Most samples show least 2 kbar of variability within a single sample; this is due to changing Al content not only from one grain to another but also within individual hornblende grains.

A plot of the pressure results from NW to SE (Fig. 39) indicates that the NW part of the pluton does not represent a deeper exposure than the SE section; thus the pluton is not tilted along a NE-SW axis.

Hornblende-Plagioclase Thermometry

Crystallization temperatures were obtained using the hornblende-plagioclase thermometer of Blundy and Holland (1990). This thermometer uses the albite content of plagioclase, the Si content of hornblende, and the crystallization pressure derived from

Table 7. Al-in-hornblende (Al-in-hb) barometry (Schmidt, 1992) results. Also presented are plagioclase (Blundy and Holland, 1990), apatite (Harrison and Watson, 1984) and zircon (Watson and Harrison, 1983) thermometry results. Abbreviations as used in Figure 31. Sample locations are shown on Figure 5.

Plag. temp. (°C)	<u>84B-NBC</u>	<u>84A-NBC</u>	<u>53D-NMP</u>	<u>55a-NMP</u>	<u>86b-NMP</u>	<u>86A-NMP</u>	<u>88b-NMP</u>
Apatite temp. (°C)	767	865	770	831	895	928	824
Zircon temp. (°C)	769	764	837		808	779	
Al-in-hb pressure (kbar)				6.5			3.7
Plag. temp. (°C)	<u>17a-CBC</u>	<u>9-CBC</u>	<u>24a-CBC</u>	<u>24e-CBC</u>	<u>6a-CBC</u>	<u>5c-CBC</u>	<u>28a-CMP</u>
Apatite temp. (°C)	817	745	686	762	684	636	938
Zircon temp. (°C)	935	759	706	734	695	709	804
Al-in-hb pressure (kbar)	7.4						
Plag. temp. (°C)	<u>30-CMP</u>	<u>28b-CMP</u>	<u>80c-CMP</u>	<u>81b-CMP</u>	<u>81a-CMP</u>	<u>62-SMP</u>	<u>92-SMP</u>
Apatite temp. (°C)	938	912	926	816	909	929	920
Zircon temp. (°C)	803	788	804	813	804	808	797
Al-in-hb pressure (kbar)				7.1			
Plag. temp. (°C)	<u>67b-SMP</u>	<u>45-SMP</u>	<u>42e-SMP</u>	<u>76-SMP</u>	<u>PM171-SMP</u>		
Apatite temp. (°C)	935	900	822	826			
Zircon temp. (°C)	804	792	793				
Al-in-hb pressure (kbar)				8.7	7.7		

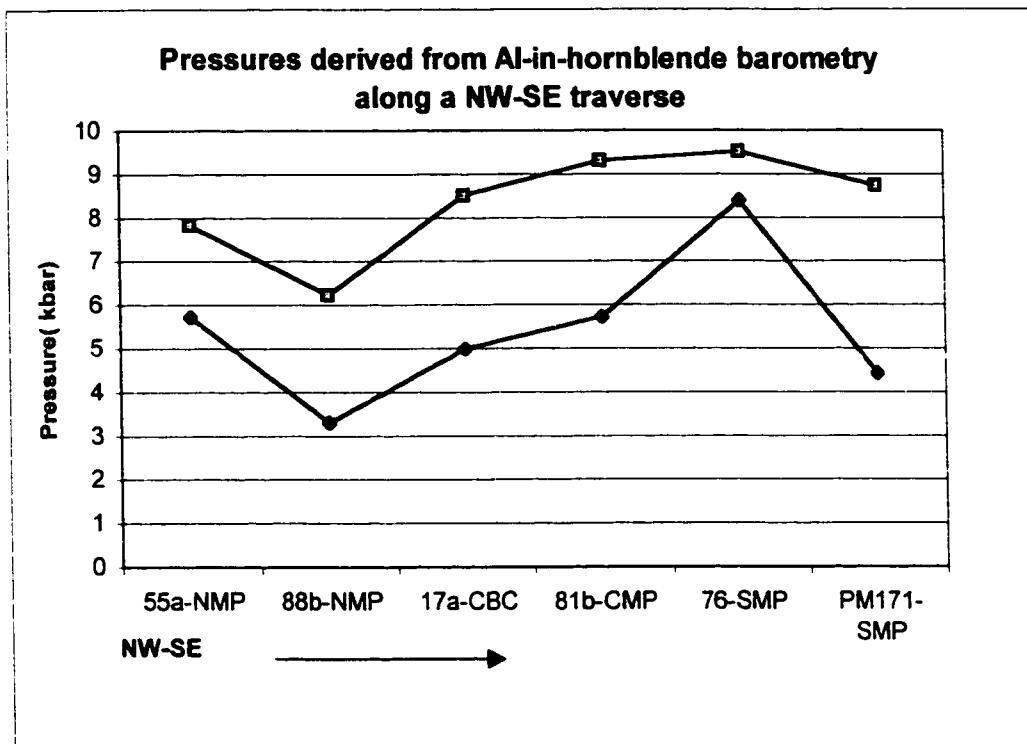


Figure 39. Maximum and minimum pressures derived from the Al-in-hornblende barometer for each sample analyzed, along a NW-SE traverse. Sample locations can be found on Figure 5. Abbreviations used as in Fig. 31.

Al-in-hornblende barometry to obtain the temperature at which these two minerals reached equilibration. This thermometer can only be used for rocks with the same restricted mineral composition as the Al-in-hornblende barometer. In addition, plagioclase must be more albitic than Ab_8 and hornblende must have less than 7.8 Si formula atoms. The Cardinal Peak samples used for this thermometer meet these criteria. Uncertainty is $\pm 75^\circ\text{C}$.

Temperatures were determined for five samples, and the results are shown in Table 7. The median temperature for all samples was 821°C . Temperatures are fairly uniform throughout the pluton: 817°C for the central Border Complex, 823°C for the NW Main Phase, 816°C for the central Main Phase and 826°C for the SE Main Phase.

Apatite Saturation Thermometry

The apatite saturation thermometer uses the equation

$$\ln D_p = \left[\frac{8400 + ((\text{SiO}_2 - 0.5)2.64 \times 10^4)}{T} \right] - [3.1 + (12.4(\text{SiO}_2 - 0.5))]$$

where D_p is the concentration ratio of P in stoichiometric apatite to that in the melt, T is the temperature at which apatite crystallized in the magma, and SiO_2 is the weight fraction of silica in the melt (Harrison and Watson, 1984). This thermometer is valid in the range 750°C to 1500°C (Wolf and London, 1994) and in peralkaline to metaluminous compositions between 45% and 75% SiO_2 . At this point, it should be noted that some Cardinal Peak samples are slightly peraluminous; however, most samples are metaluminous (Fig. 24). A critical assumption of this thermometer is that whole rock compositions are equivalent to melt compositions.

Apatite saturation temperatures for twenty-two samples are shown in Table 7. The average temperatures obtained were: 816°C for the NW Border Complex, 741°C for the central Border Complex, 864°C for the NW Main Phase, 922°C for the central Main Phase and 901°C for the SE Main Phase. The low temperatures obtained for the more mafic Border Complex samples is most likely due to apatite crystallizing later in these rocks than in the more felsic Main Phase samples. Central and SE Main Phase temperatures are also much higher than those obtained by the hornblende-plagioclase thermometer, and temperatures overall are more variable. This variability might be caused by the large range of rock compositions used for this thermometer, compared to the more limited range used in the hornblende-plagioclase thermometer.

Zircon Saturation Thermometry

Crystallization temperatures were also obtained using the zircon saturation thermometer. This thermometer uses the equation

$$\ln D_{Zr} = \{-3.80 - [0.85 (M-1)]\} + 12,900/T$$

where D_{Zr} is the concentration ratio of Zr in the stoichiometric zircon to that in the melt, T is the temperature at which zircon crystallized in the magma, and M is the cation ratio $(Na+K+2Ca)/(Al*Si)$ of the melt (Watson and Harrison, 1983). This thermometer is valid for non-alkaline compositions where $(Na+K)/Al$ is less than one (true for all Cardinal Peak samples), and for melts with greater than 2% H_2O . Calibration of the zircon thermometer to conventional thermometers has shown that it is valid to within $\pm 60^\circ C$ (Barrie, 1995). As with the apatite thermometer, it is assumed that whole rock

compositions are equal to melt compositions; and the presence of inherited zircons [confirmed in the Cardinal Peak pluton by Haugerud et al. (1991)] does not give substantial errors. A significant amount of inherited zircon would inflate the temperatures obtained (Barrie, 1995).

Zircon saturation temperatures for twenty-two samples are shown in Table 7. Average temperatures obtained were: 767°C for the NW Border Complex, 734°C for the central Border Complex, 808°C for the NW Main Phase, 803 °C for the central Main Phase and 799°C for the SE Main Phase. As with the apatite thermometer, lower temperatures were obtained for the Border Complex samples; this is most likely due to zircon crystallizing later in these rocks than in the more felsic Main Phase samples. Also, the temperatures of several of the central Border Complex samples are lower than the valid range for this thermometer. Overall these temperatures are lower than those obtained by apatite thermometry but are comparable to temperatures from hornblende-plagioclase thermometry.

Summary of temperature data

Zircon and hornblende-plagioclase thermometry yield similar temperatures, however, the apatite thermometer yields higher temperatures for most samples (Fig. 40). These high temperatures probably reflect the fact that apatite is an early crystallizing mineral; thus the apatite thermometer gives a temperature near the liquidus, while zircon and hornblende-plagioclase thermometry give temperatures closer to the solidus.

Temperatures obtained from the hornblende-plagioclase thermometer are

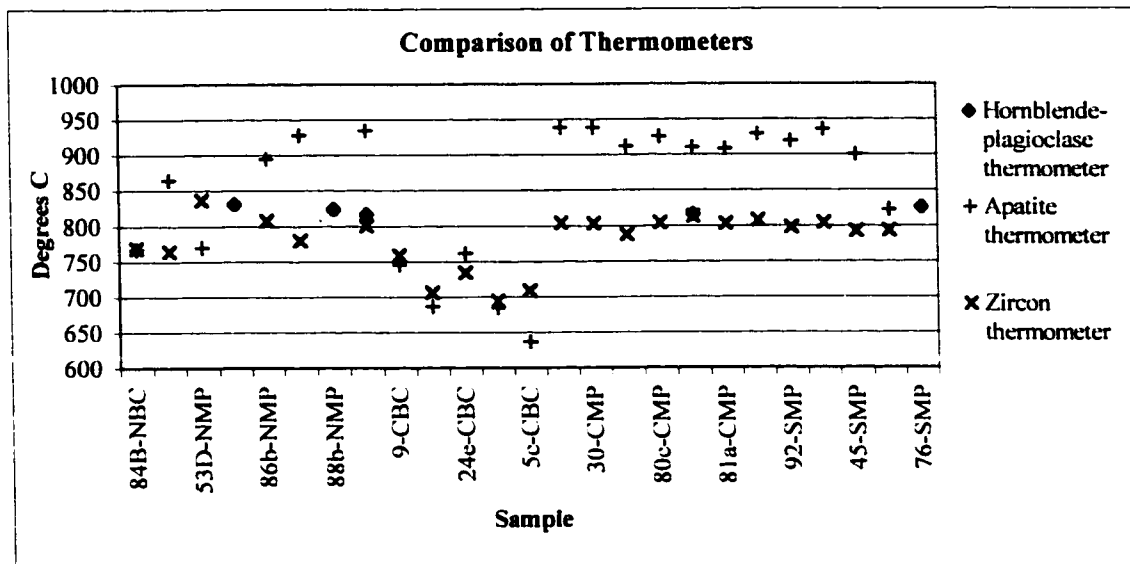


Figure 40. Comparison of temperatures obtained from hornblende-plagioclase, apatite and zircon thermometry. Sample locations displayed on Figure 5. Abbreviations used as in Figure 31.

probably the most reliable, since this method does not rely on the assumption that whole rock composition equals melt composition.

PETROLOGIC PROCESSES

The petrologic processes that may have been active in the formation of the Cardinal Peak pluton include mantle melting, lower-crustal melting, fractional crystallization, assimilation of crustal rocks, and magma mixing. This section discusses the contribution of each of these processes in the formation of the pluton.

Origin of the Mafic Rocks

Most workers agree that mafic magmas in continental arc systems are derived from partial melting of the ultramafic mantle (e.g., Yoder, 1976; Tatsumi and Eggins, 1995). The presence of mafic rocks in the Cardinal Peak pluton shows that mantle-derived magmas played a role in the formation of the pluton. However, except for hornblendite, these mafic rocks do not have the required chemistry to be considered primary compositions.

Mafic rocks in the Cardinal Peak pluton are present as gabbro and diorite in the NW section of the pluton and the central Border Complex, and throughout the pluton as mafic enclaves. Based on cross-cutting field relationships, the majority of the mafic magmatism in the NW and central Border Complex predated the felsic magmatism. However, the presence of mafic enclaves in the central and SE Main Phase tonalite suggests that mafic magmatism continued to some degree throughout the emplacement of the entire pluton.

It is informative to compare Cardinal Peak mafic rocks to calc-alkaline mafic rocks from two other Cordilleran arc plutons that have been recently studied in detail: the Chilliwack batholith, a 34 to 2 Ma epizonal intrusion located in the North Cascades, and the Onion Valley sill complex, a 92 Ma epizonal intrusion located in the Sierra Nevada, California. Both of these intrusions contain a range of mafic to felsic rocks, as does the Cardinal Peak pluton. Also, like the Cardinal Peak pluton, the Onion Valley sill complex contains hornblende. Tepper (1996) delineated two groups of mafic rocks from the Chilliwack batholith, a low-K, tholeiitic series (LKS) and a medium-K, calc-alkaline series (MKS); only the MKS is discussed here because it is the most similar to the Cardinal Peak mafic rocks.

Mafic rocks from the Onion Valley and MKS were plotted with Cardinal Peak gabbro, diorite and hornblende tonalite ($< 65\% \text{SiO}_2$) on several major and trace element Harker diagrams (Fig. 41). On these diagrams, Cardinal Peak mafic rocks most closely resemble MKS rocks in both major and trace elements, and are also similar to Onion Valley mafic rocks, but are slightly lower in K_2O and Sr and higher in Cr.

Mg# and Cr in samples from all three locations are too low to be considered primary compositions. A primary magma should have a Mg# $[(\text{MgO}/\text{MgO} + \text{FeO}) * 100]$ greater than 70 (Tatsumi and Eggins, 1995) and Cr greater than 400 ppm (Sato, 1977; Hart and Davis, 1978; Kinzler et al., 1990). The Mg# for samples from these locations ranges from 24-59 while Cr ranges from 2 to 218 ppm, except for one Cardinal Peak sample with Cr at 446 ppm. This high Cr sample also has a REE pattern suggestive of hornblende accumulation (Fig. 27b).

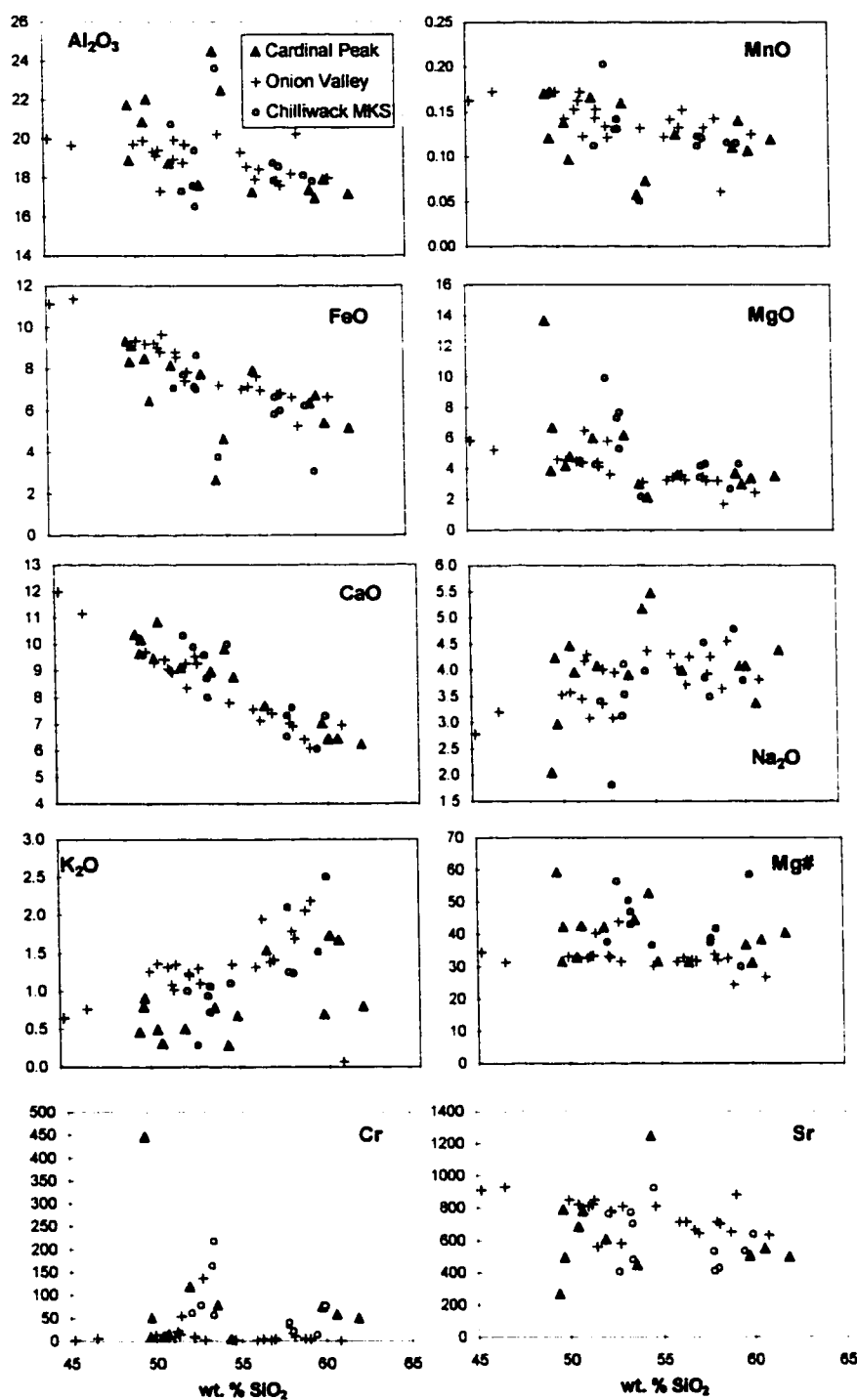


Figure 41. Harker diagrams for comparison of major elements for Cardinal Peak, Chilliwack Medium K-Series (Tepper et al., 1993), and Onion Valley mafic rocks (Sisson et al., 1996). Y-axis for oxides is weight percent, elements is ppm.

Comparative REE plots (Fig. 42) show that, as with the Harker diagrams, Cardinal Peak mafic rocks are most similar to MKS rocks, but are somewhat lower in LREE. Onion Valley mafic rocks are much higher in LREE from La through Eu than those from the Cardinal Peak, but have similar values for HREE.

One difference between the MKS and the Cardinal Peak and Onion Valley mafic rocks is that pyroxene is the major mafic mineral in the MKS, while the Cardinal Peak and Onion Valley mafic rocks are dominated by hornblende. This difference most likely reflects higher H₂O contents for Cardinal Peak and Onion Valley parental magmas (Cawthorn and O'Hara, 1976; Wyllie, 1977; Gill, 1981; Naney, 1983).

Since Cardinal Peak mafic rocks are so similar to MKS and Onion Valley mafic rocks, they can be inferred to have a similar origin. Tepper (1996) demonstrates that the most likely origin of the parental magma for the MKS is 9-27% partial melting of a mantle-composition spinel lherzolite with little or no garnet. Subsequent fractionation then produced the range of compositions seen in the MKS. The MKS is compositionally similar to non-primary calc-alkaline basalts and andesitic basalts from many continental arcs, and is interpreted by Tepper et al. (1993) to be their intrusive counterpart.

Melting experiments performed on hornblende picrite at high pressures (10 kbar) and 1120 to 1090°C result in hydrous high-alumina basaltic liquids (Ulmer, 1986, as cited by Sisson et al., 1996). Onion Valley mafic rocks are thought by Sisson et al. (1996) to have been formed by fractional crystallization of a similar hydrous magma.

Analogous to the Cardinal Peak pluton, hornblende cumulate rocks are found in the Onion Valley sill complex. Sisson et al. (1996) interpret these cumulates to be the

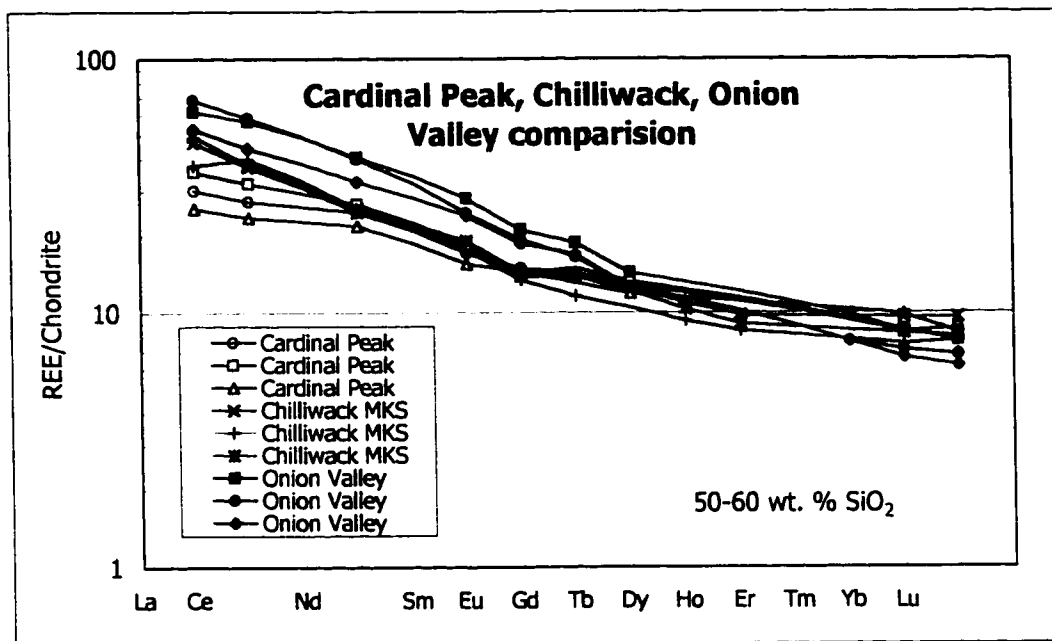


Figure 42. REE diagram comparing Cardinal Peak, Chilliwack Medium K-Series (Tepper et al. 1993) and Onion Valley mafic rocks (Sisson et al. 1996). MKS=Medium K-Series.

residue from the fractional crystallization of the hydrous primary magma that formed the Onion Valley mafic rocks.

In conclusion, Cardinal Peak mafic rocks likely originated by fractional crystallization of mafic, mantle-derived parental magmas. The hornblendites in the Cardinal Peak may represent the cumulate residue of this process.

Origin of the Tonalite: Fractional Crystallization

The sequence of rock compositions in the NW and central Cardinal Peak pluton; hornblendite, hornblende gabbro, hornblende-biotite diorite and hornblende-biotite tonalite, is considered a classic high-Al fractionation suite (e.g., Arth et al., 1978; Arth, 1979). In addition, the cumulate textures and REE patterns of the hornblendite and some gabbros suggest that fractional crystallization was an important process in the evolution of the pluton. In this section, the viability of fractional crystallization is modeled for tonalite from the NW and SE parts of the pluton. The central tonalite was not modeled because it is very similar to the SE tonalite.

In these models, major element fractionation is simulated using the computer program PETMIX (K. Laurent, U.S. Geological Survey), which is based on the least-squares analysis method of Bryan et al. (1969). Rare earth element fractionation was simulated using a spreadsheet program based on the Rayleigh equations for fractional crystallization.

The results of the model for major element fractionation of a NW Main Phase tonalite are shown in Table 8. The mineral assemblages used are those found in the parent

Table 8. Major element fractionation of a gabbro to produce a tonalite. Sample locations can be found on Figure 5.

Parent	Daughter	<u>Fractionation (+) or Accumulation (-) Phases</u>						Residual melt	r ²
		hornblende	plagioclase	biotite	sphene	magnetite	ilmenite		
Gabbro (53d)	Diorite (54)	29	25	0.03		-0.5	1	44	1.3
Diorite (54)	Tonalite (86a)	38	28	-9	-4		1	33	1.5

rock in each step, however, the proportions of minerals are different. The mineral compositions used are from a NW Main Phase diorite. The results show that a NW Main Phase tonalite (75% SiO₂) can be derived from a NW Main Phase gabbro (52% SiO₂) in two steps. The first step derives a NW Main Phase diorite (57% SiO₂) from the gabbro by fractional crystallization of 29% hornblende, 25% plagioclase, 0.03% biotite, and 1% ilmenite, and accumulation of 0.5% magnetite leaving 44% residual liquid. The second step derives the tonalite from the diorite by fractional crystallization of 38% hornblende, 28% plagioclase, and 1% ilmenite, and accumulation of 9% biotite and 4% sphene, leaving 33% residual melt.

The results for the REE fractionation model for the NW Main Phase tonalite are shown in Figure 43a and b. The partition coefficients used are from Martin (1987) and Tepper et al. (1993) for compositions similar to the Cardinal Peak rocks (Appendix C). Only plagioclase and hornblende are used as fractionating minerals because they have the largest impact on REE concentrations. The large Eu anomaly of the end member tonalite attests to the importance of plagioclase fractionation.

The same two steps that were used in the major element fractionation model are used in the REE model. For each step, there is a good fit between the model result and the daughter REE concentration. The first step requires fractional crystallization of 21% hornblende and 9% plagioclase leaving 70% residual liquid (Fig. 43a). The second step can be achieved with fractional crystallization of 24% hornblende and 36% plagioclase leaving 40% residual liquid (Fig. 43b). These values are not identical to those for major element fractionation. This is probably due to a difference between the REE partition

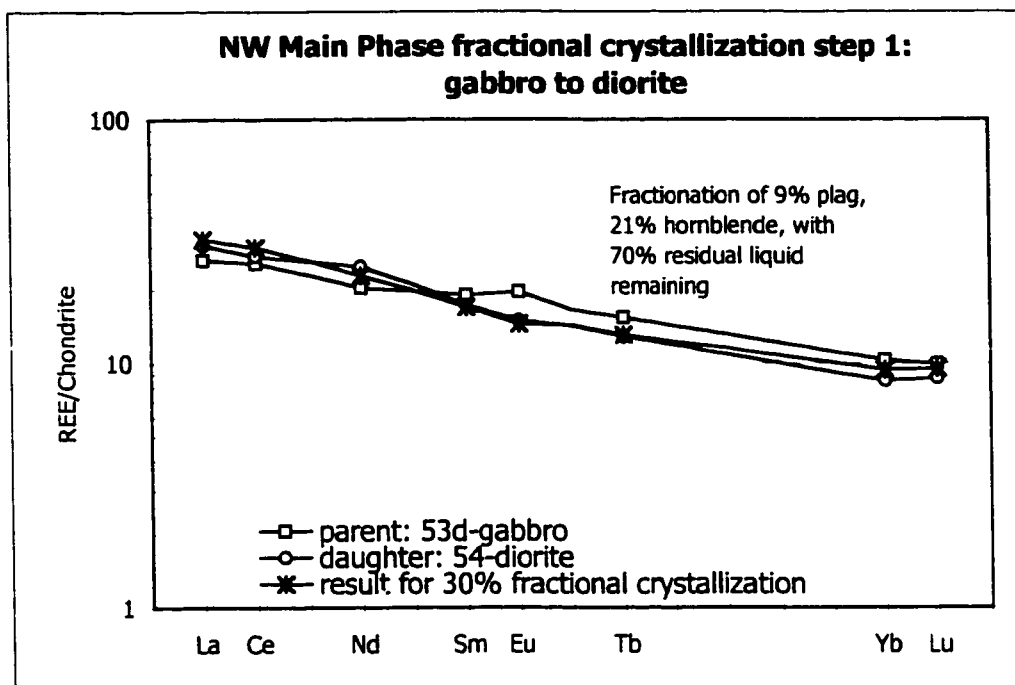


Figure 43a. Rayleigh fractional crystallization step 1. The parent composition is a gabbro (52% SiO₂), the daughter is a diorite (57% SiO₂). Sample locations shown on Figure 5.

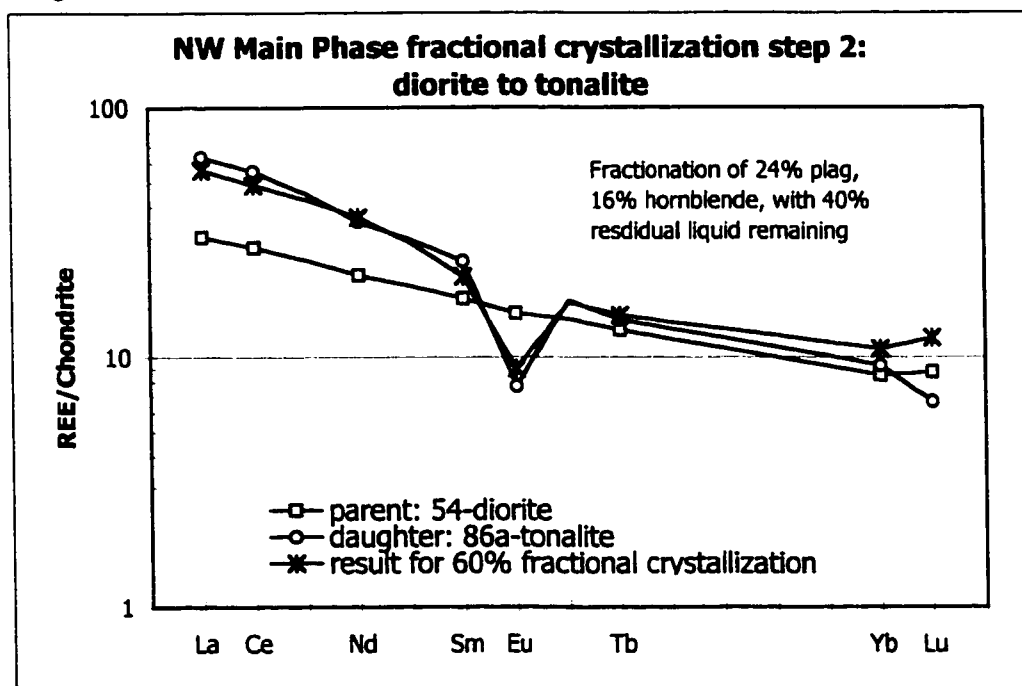


Figure 43b. Rayleigh fractional crystallization step 2. The parent composition is a diorite (58% SiO₂), the daughter is a tonalite (75% SiO₂). Sample locations shown on Figure 5.

coefficients used and the actual amount of REE partitioning in these rocks.

A REE fractionation model was also used to try to produce the HREE-depleted tonalite of the central and SE Main Phase from the same gabbroic parent (Fig. 44), but was unsuccessful. This model uses the same gabbroic parent as in the previous model. The REE model demonstrates that the large amount of HREE depletion of the tonalite cannot be produced by fractional crystallization of hornblende and plagioclase from the gabbro. In fact, fractional crystallization of any combination of the minerals found in mafic Cardinal Peak rocks does not produce the necessary amount of HREE depletion. Although the model shown employs a gabbroic parent, even a model using a relatively felsic parent, such as a hornblende tonalite, is unsuccessful. Another process must be responsible for the formation of the central and SE Main Phase tonalite.

The NW Main Phase tonalite shows several differences from the central and SE Main Phase tonalite that might indicate that these sets of rocks evolved differently. NW Main Phase tonalites display more scatter on Harker diagrams (Figs. 22 and 25), and exhibit different trends for several trace elements than those shown by the central and SE Main Phase tonalite. Y and Rb, for instance, are higher in most NW tonalites across all ranges of SiO₂, while REE patterns are more enriched in HREE than central and SE rocks at comparable SiO₂ values.

Harker diagrams also show similarities between Cardinal Peak mafic rocks and NW Main Phase tonalite. Similar to the NW Main Phase tonalite, mafic rocks exhibit much more scatter on Harker diagrams than central and SE Main Phase rocks, which

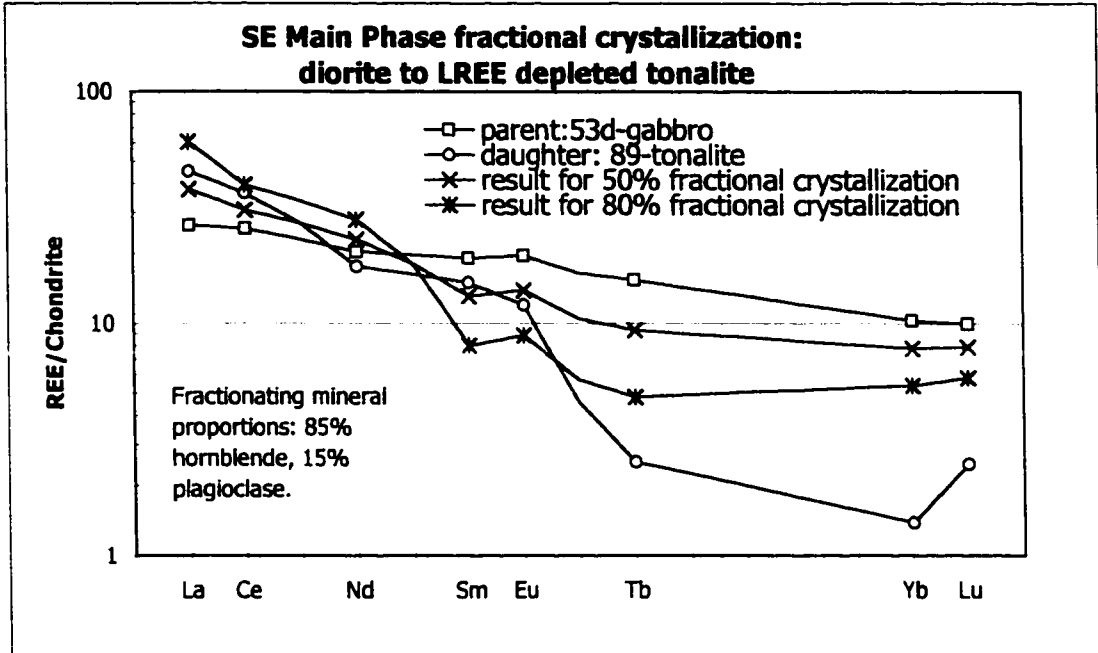


Figure 44. Rayleigh fractional crystallization model for SE Main Phase. The parent composition is a gabbro (52% SiO₂). The daughter is a SE Main Phase tonalite with depleted LREE (68% SiO₂). Sample locations are displayed on Figure 5.

tend to be tightly clustered. Y is higher in most mafic rocks from all locations and in most NW Main Phase tonalites than in central and SE tonalites. These relationships suggest that Cardinal Peak mafic rocks and NW Main Phase tonalite may be cogenetic, but central and SE tonalite are not related to the mafic rocks.

In summary, the results of the models suggest that fractional crystallization is a likely mechanism for producing the NW tonalite, but did not produce the large body of central and SE Main Phase tonalite. This is also supported by observations from the Harker and REE diagrams for Cardinal Peak rocks.

Origin of the Tonalite: Lower-Crustal Melting

Several recent studies have suggested that melting hydrous, mafic lower crust is an important method of producing tonalitic magmas in arcs (e.g., Beard, 1997). Recent experimental work (Beard and Lofgren, 1991; Sen and Dunn, 1994; Wolf and Wyllie, 1994; Winther, 1996) has shown that dehydration melting of amphibolites and greenstones at mid-to lower-crustal pressures can produce a melt similar in composition to an arc tonalite. This section discusses the applicability of lower-crustal melting to the formation of the central and SE Main Phase tonalites.

On a Sr/Y vs. Y diagram (Fig. 45), samples from the central and SE Main Phase, and a few from the NW Main Phase, plot in the adakite field. Adakites are high Mg dacites with high La/Yb that may have been derived by melting subducted oceanic crust (Drummond and Defant, 1990). Central and SE Main Phase tonalites have Mg values

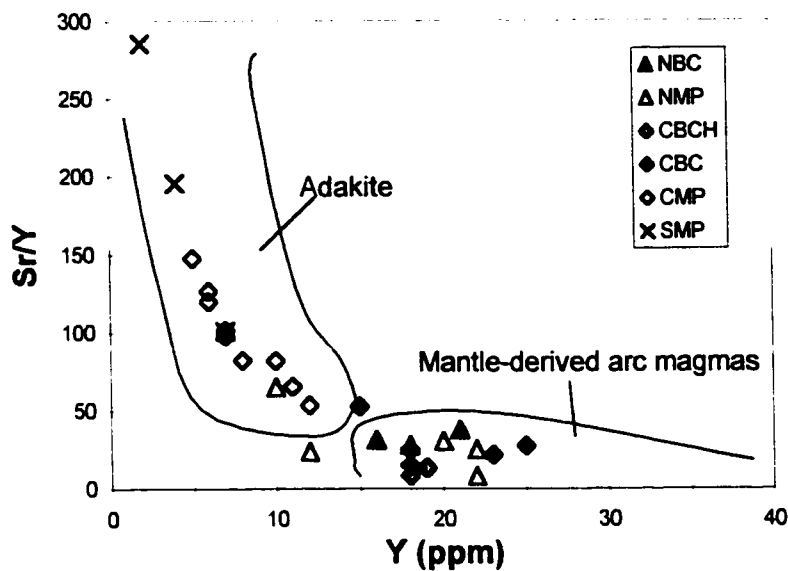


Figure 45. Sr/Y vs. Y discrimination diagram. Fields are from Drummond and Defant (1990). Abbreviations used as in Figure 31.

that are too low for adakites, but they share some of their characteristics, such as a high Sr/Y and high La/Yb. These features are thought to be distinctive of rocks derived from partial melting of a garnet-bearing basaltic source (e.g., Rapp et al., 1991; Drummond and Defant, 1990). The presence of garnet in the source implies that melting took place at pressures of at least 8 kbar, since garnet becomes stable in mafic rocks at this depth (Rapp et al., 1991; Wolf and Wyllie, 1991; Patino Douce and Beard, 1995). The fact that most NW Main Phase and Border Complex samples plot in the mantle-derived arc magma field on the Sr/Y vs. Y diagram suggests that their parental magma was most likely mantle-derived.

Cardinal Peak tonalites were plotted on major element Harker diagrams along with compositions from meta-basalt partial melting studies of Sen and Dunn (1994), Wolf and Wyllie (1994) and Winther (1996) (Fig. 46). The experimental melting pressures used in these studies ranged from 10 to 20 kbar, corresponding to lower-crustal conditions where garnet is stable. The crust in the area of the Cardinal Peak pluton was thickened by magma loading and/or thrusting in the Cretaceous (Brown and Walker, 1993; McGroder, 1991; Miller et al., 1993; Whitney et al., 1999); therefore 10-20 kbar are reasonable pressures for the lower crust underneath the pluton during its formation.

Cardinal Peak rocks are similar to the experimental melts in Al_2O_3 , FeO and MgO. Variations in TiO_2 , CaO, K_2O , and Na_2O are most likely due to differences in the melting source compositions. Table 9 shows the starting compositions for the experimental studies, and it can be seen that for those high in TiO_2 , CaO, K_2O and Na_2O , the melt compositions are also higher in these oxides.

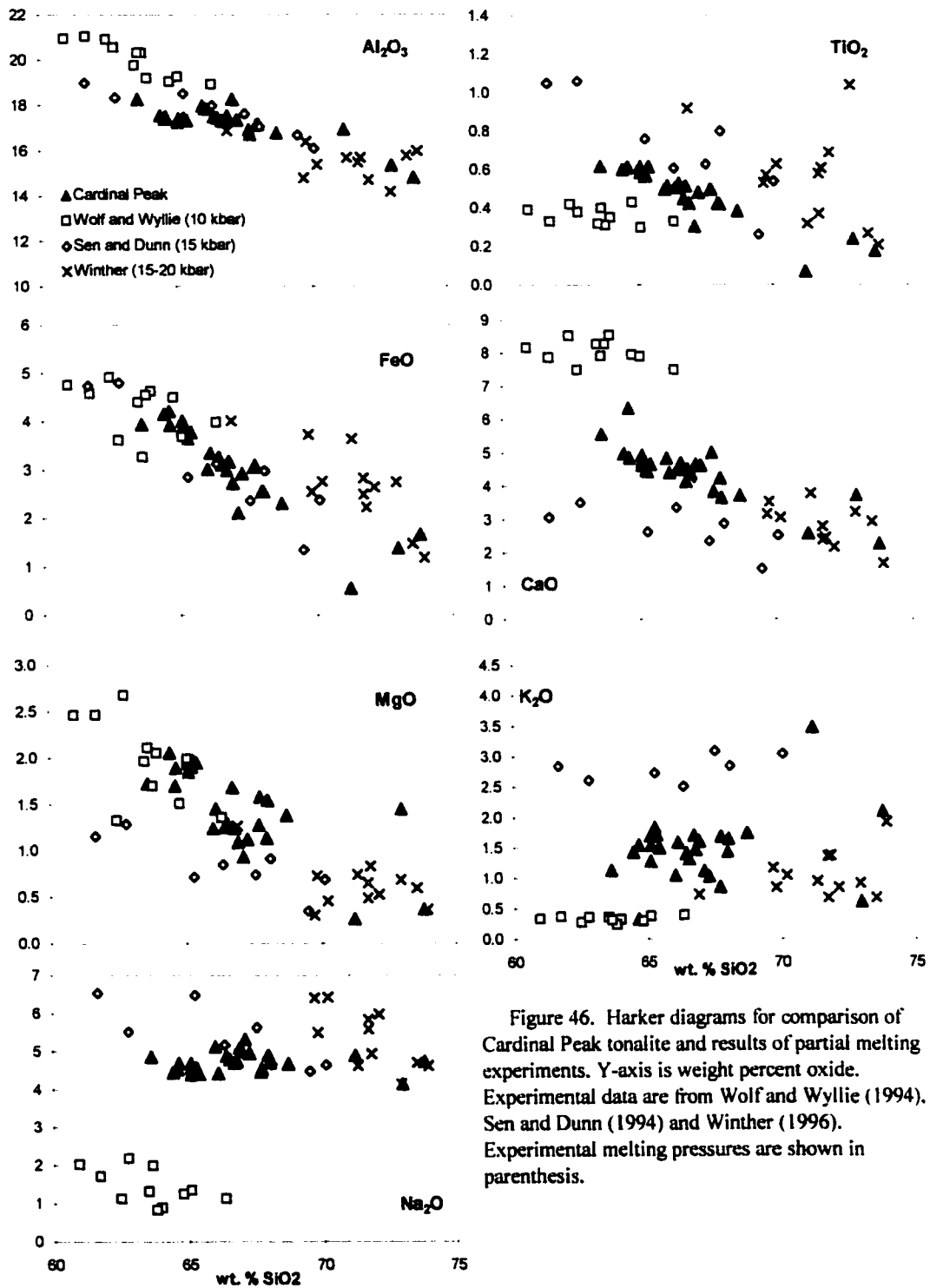


Figure 46. Harker diagrams for comparison of Cardinal Peak tonalite and results of partial melting experiments. Y-axis is weight percent oxide. Experimental data are from Wolf and Wyllie (1994), Sen and Dunn (1994) and Winther (1996). Experimental melting pressures are shown in parenthesis.

Table 9. Major element compositions of parent rocks for melting experiments

Reference: Melting pressure	Winther (1996) 15-20 kbar				Sen & Dunn (1994) 15 kbar	Wolf & Wyllie (1994) 10 kbar
Sample	aat5	aat3	aat1	aat3/2		
SiO₂	49.20	49.10	49.80	48.50	46.88	48.40
Al₂O₃	13.80	15.70	16.40	16.60	15.00	14.60
TiO₂	1.35	1.25	1.03	1.14	1.22	0.40
FeO*	14.80	13.70	12.70	13.40	13.09	8.40
MnO	0.18	0.18	0.13	0.09	0.26	0.20
CaO	12.10	10.60	9.88	10.50	11.28	14.30
MgO	6.19	6.86	7.09	7.42	8.25	10.70
K₂O	0.29	0.30	0.26	0.17	0.80	0.10
Na₂O	2.10	2.40	2.67	2.23	2.51	1.00

A lower-crustal melting origin for the tonalite rocks of the Cardinal Peak was tested using REE modeling. Although the composition of the lower crust under the Cardinal Peak pluton is not known, the exposed crust in much of the North Cascades consists of accreted island arcs. Therefore, the source rock in these models is based on a metamorphosed island arc basalt, with REE concentrations of 17x chondrite for LREE and 10x chondrite for HREE (e.g., Tatsumi and Eggins, 1995). The residual mineral proportions for the source rock are 44% hornblende, 22% garnet, 10% plagioclase and 24% clinopyroxene. These proportions were taken from partial melting studies of metabasalts at lower crustal pressures (10-15 kbar) (Sen and Dunn, 1994; Wolf and Wyllie, 1994). Partition coefficients from Martin (1987) (Appendix C) were used in the models, in order to be consistent with recent REE modeling studies that test a metabasalt partial melting origin for tonalite (e.g., Drummond and Defant, 1990; Barnes et al., 1996). Melting is assumed to take place under equilibrium conditions, and batch melting is also assumed.

The first model tests a lower-crustal melting origin for the NW Main Phase tonalite (Fig. 47). This model can only successfully produce a REE pattern similar to the NW tonalite with 60% melting of the source rock. Since 60% melting of a mafic rock is unlikely to produce a tonalite melt (Beard and Lofgren, 1991), the model cannot be considered successful.

The central Main Phase tonalite is tested for a lower-crustal melting origin in the second model. The best results for the second model were produced by 20% partial melting of the source rock (Fig. 48). The model result is closest to the least REE-enriched

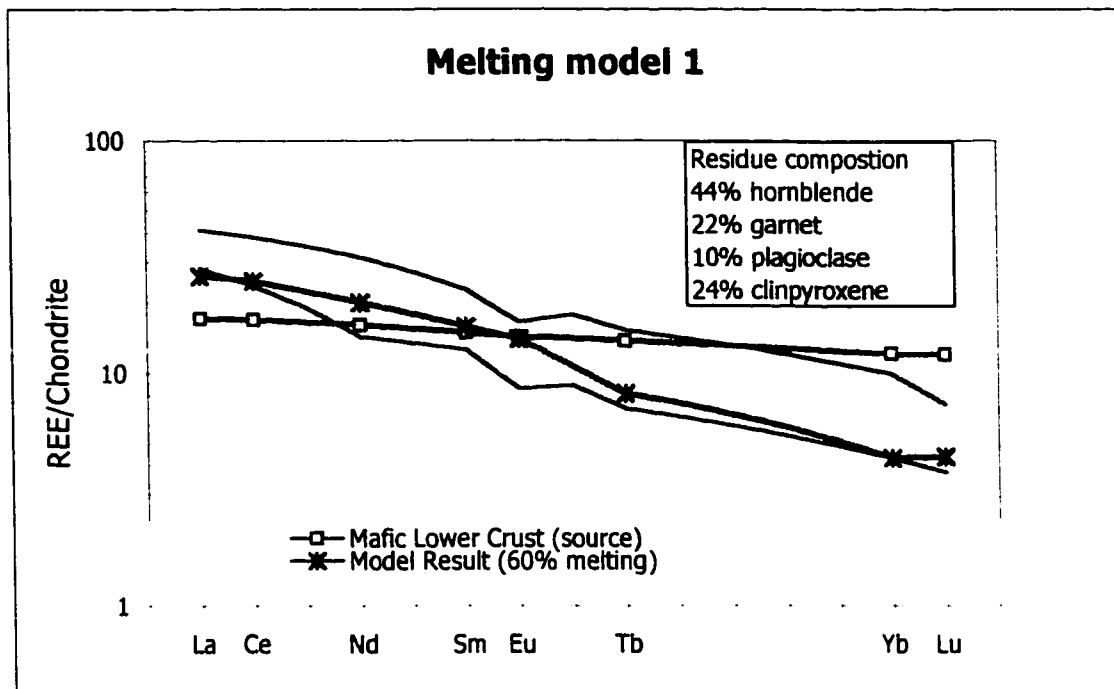


Figure 47. Melting model 1 to produce a NW tonalite during lower crustal melting of a garnet amphibolite source. Shaded area is range of NW tonalite (60-70% SiO₂).

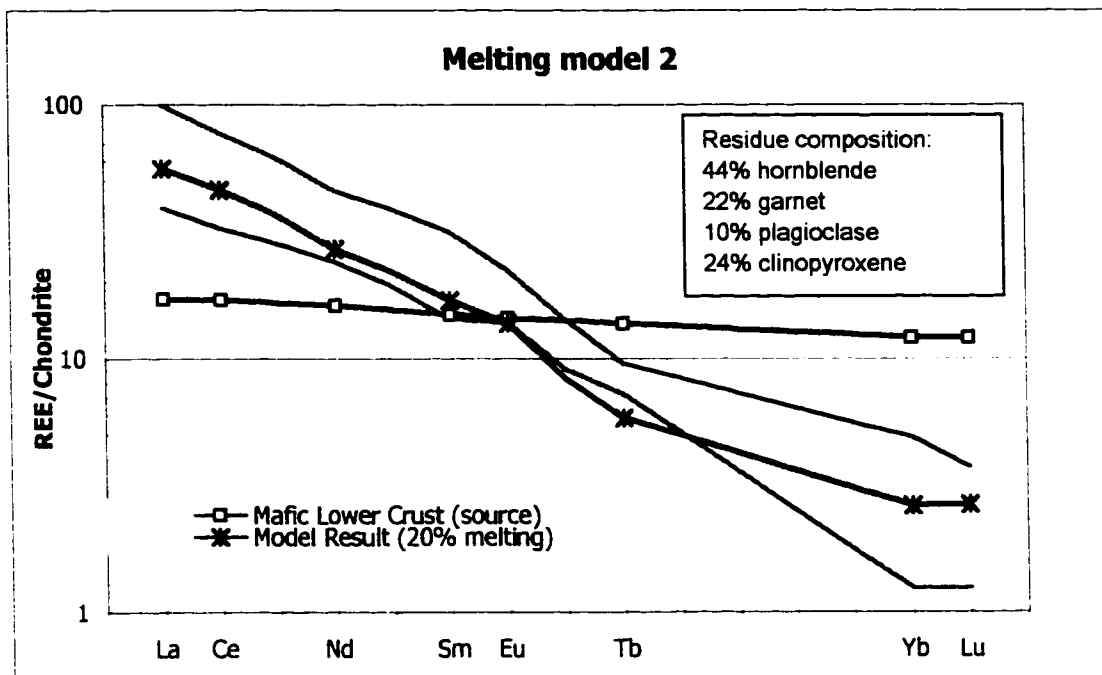


Figure 48. Melting model 2 to produce a central tonalite during lower crustal melting of a garnet amphibolite source. Shaded area is range of central tonalite (64-70% SiO₂).

pattern for the central tonalite. The more REE-enriched patterns of some of the central tonalites may have been produced by melting a more enriched source rock, or by fractional crystallization.

The third model tests the SE Main Phase tonalite. The best result for the third model is obtained by 15% partial melting of the source rock (Fig. 49). The model result is similar to the most REE-enriched pattern found in the SE tonalite. The less REE-enriched patterns of some of the rocks may have been produced by melting a less enriched source rock.

These results imply that lower crustal melting may have been an important mechanism in the formation of the central and SE Main Phase tonalite, but most likely did not produce the NW Main Phase tonalite.

Origin of the Tonalite: Magma Mixing

Magma mixing undoubtedly occurred to some extent in the Cardinal Peak pluton, as shown by the presence of schlieren in the central and SE Main Phase tonalite, but a mixing origin is unlikely for the bulk of the tonalite that makes up the pluton. Magma mixing produces well-defined linear trends on Harker diagrams, and except for CaO, the Harker diagrams for major and trace elements (Figs. 22 and 25) do not show such linear trends. In addition, central and SE tonalites are clustered on the Harker diagrams, whereas rocks produced by mixing would be expected to show a range of compositions.

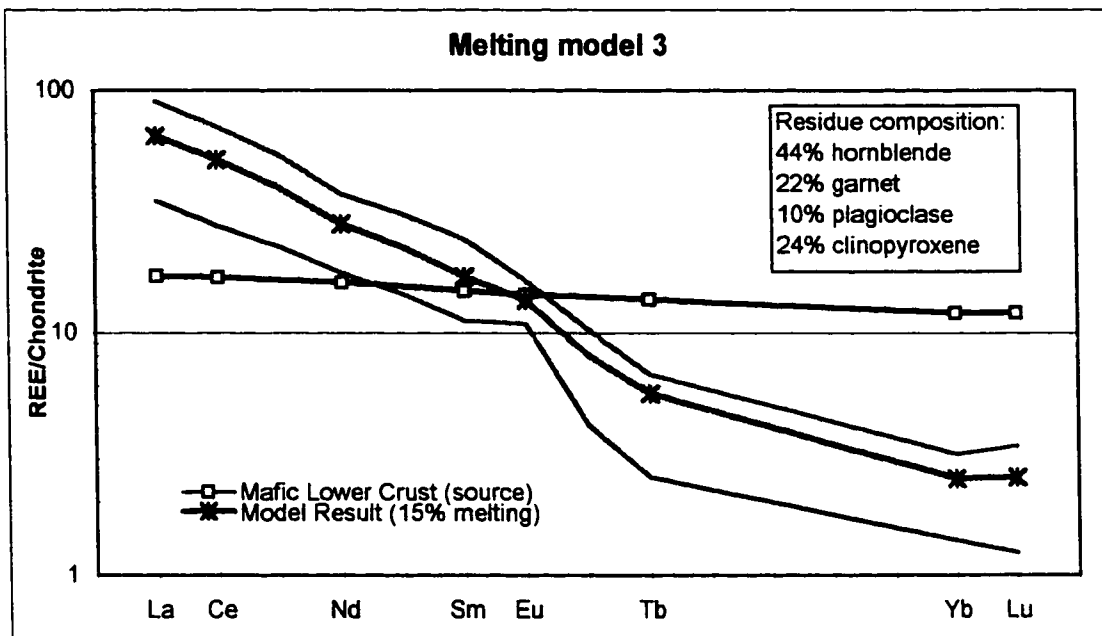


Figure 49. Melting model 3 to produce a SE tonalite during lower crustal melting of a garnet amphibolite source. Shaded area is range of SE tonalite (62-70% SiO₂) excepting hornblende-bearing enclaves.

Assimilation of Crustal Rocks

The presence of 2.0 Ga zircons in the Cardinal Peak pluton (Haugerud et al., 1991) shows that some assimilation of Precambrian crust took place during its formation. However, based on the discordance of U-Pb ages, only a minor amount (0.03% - 0.12%) of assimilation took place (Haugerud et al., 1991).

In addition, field evidence indicates that no significant assimilation took place at the level of emplacement. The contact aureole of the pluton shows no evidence of migmatization of the Holden Assemblage country rock, and most country rock inclusions within the pluton have sharp contacts with their host, indicating little or no melting.

MAGMA CHAMBER CONSTRUCTION

In this section, conceptual models are presented to explain the distinctive spatial characteristics of the Cardinal Peak pluton: the narrowness of the NW tip, the heterogeneity of the NW part and the homogeneity of the SE part of the pluton, and the mafic rim along the central section of the pluton. These models are evaluated using both field and chemical data.

In all models, mafic magmatism predates felsic magmatism, as it does in many I-type arc granitoid bodies (e.g., Pitcher, 1993). The models vary, however, in the geometry of the magma chamber, and its construction.

The first model assumes that the NW end represents a deeper, narrower section of the chamber than the SE end of the pluton. The NW end may even expose the feeder dikes for the magma chamber, preserving a range of rock compositions not seen in the SE and central parts of the pluton. The SE and central sections represent the shallower, wider, main magma chamber that was more homogenized than the NW section. A rim of mafic Border Complex was left in the central section, where homogenization was not complete.

The results of the aluminum-in-hornblende barometry from a NW-SE traverse of the pluton, presented above, do not support a greater depth for the NW part of the pluton. In fact, samples from the SE yield greater depths. In addition, although the NW part of the pluton contains some of the most felsic rocks in the intrusion, these rocks are rare, and there is a much larger proportion of mafic to felsic rocks than in the central or SE

tonalite. Therefore, homogenization of the compositions that formed the NW section of the pluton would result in a magma that was more mafic than the central and SE tonalite. In addition, none of the rocks in the NW part of the pluton show the depletion in HREE of many central and SE tonalites.

Instead of the NW part of the pluton exposing a deeper section, the mechanism by which the magma chamber was created, or the nature of the magmatism, may have changed from NW to SE. Miller and Paterson (1995) have suggested that the pluton was created by sheeting, which is the injection of multiple sheets of magma into a magma chamber. The NW tip of the pluton is clearly sheeted, consisting of hundreds of diorite to tonalite sheets, sub-parallel to the axis of the pluton. Sheets are also found in the central Border Complex. The NW Main Phase does not have numerous sub-parallel sheets, but rather consists of many discontinuous bodies, indicating it was also constructed by many pulses of magma. These bodies may have been sheets disaggregated by turbulent mixing during injection, similar to the way in which a mafic dike can be disaggregated in a felsic pluton to form enclaves (Hill, 1988; McNulty et al., 1996; Tobisch et al., 1996). However, the central and SE Main Phase are more homogenous, and do not show obvious sheeting.

The second and third models incorporate the sheeting hypothesis for the NW part of the pluton, while attempting to explain the lack of obvious sheeting in the SE and central Main Phase. The second model proposes that the central and SE Main Phase of the pluton were emplaced as one large, homogenous pulse of magma, instead of multiple sheets. The long, narrow shape of the pluton can be explained by NE-SW regional

contraction synchronous with emplacement, that forced the rising magma into a diapiric ridge (Talbot et al., 1991; Grujic and Mancktelow, 1998; Paterson and Miller, 1998).

The third model proposes that the SE and central Main Phase were also created by sheeting, but that the felsic magmas that make up this part of the pluton were similar enough that mixing easily took place and obscured the contacts between the sheets. These sheets are made up of compositions that are identical, or nearly identical, and impossible to distinguish in the field.

If the SE and central Main Phase consist of a single magma pulse as proposed in the second model, samples from NE-SW traverses across the pluton in these areas should show either geochemical homogeneity or random scatter. Multiple magma pulses, as proposed in the third model, could also result in random scatter, however, stepwise changes reflecting injection of different sheets might also be preserved.

Whole rock compositions from NE-SW traverses across the central and SE Main Phase were plotted on diagrams that show element or oxide amount versus location relative to the central axis of the pluton (Fig. 50 a, b). Most elements and oxides vary randomly along these traverses; SiO₂ is shown as an example (Fig.50a). However, the element Yb does show a systematic change across the pluton. In all NE-SW traverses, Yb is lowest in samples from nearest the central axis of the pluton (Fig.50b).

This systematic change in Yb supports the model of multiple, nearly homogenous, injections over the model of a single pulse formation for the central and SE Main Phase. However, this result is not conclusive, as only Yb displays this systematic change while all other oxides and elements show random scatter across the traverses.

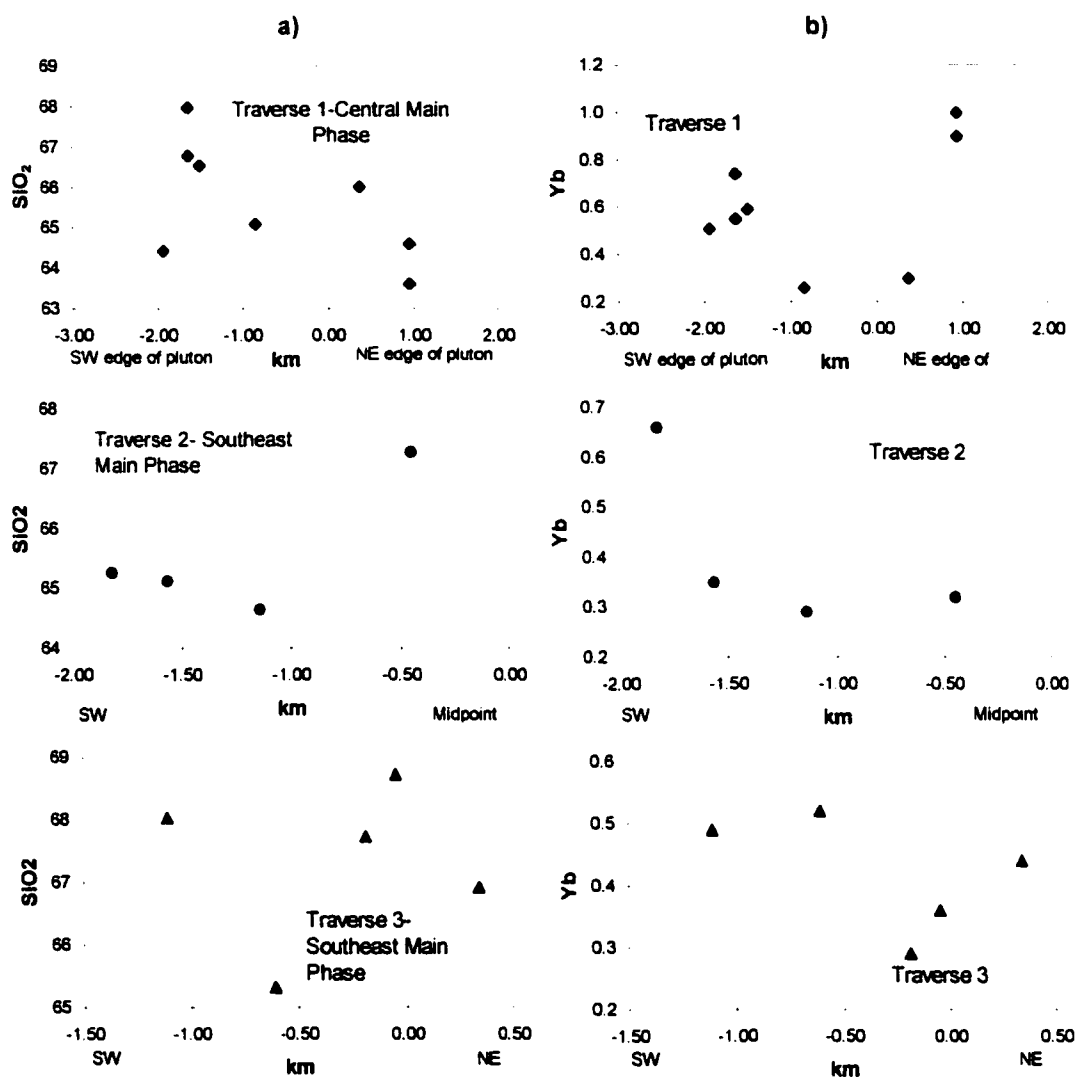


Fig 50. SW-NE traverses across the pluton. The x-axis denotes the distance of the sample from the midpoint of the pluton on a SW-NE line perpendicular to the long axis of the pluton. Negative distances are on the southwest side of the pluton, and positive distances are on the northeast side of the pluton. a) Traverses plotted for SiO₂ b) Traverses plotted for Yb.

The presence of a rim of Border Complex in the central part of the pluton may be explained by the following scenario, which is applicable to all three models. In this scenario, the Main Phase in the central part of the pluton was emplaced along the same conduit opened by the older- to coeval-Border Complex. The rising magma split the Border Complex apart, which isolated it along the margins.

CONCLUSIONS

The Late Cretaceous Cardinal Peak pluton is a mid-crustal, predominantly tonalitic intrusion located in the North Cascades core of Washington State, U.S.A. The pluton consists of hornblendite, gabbro, diorite, and tonalite, and shows an increase in heterogeneity from SE to NW. The pluton is divided into two phases, a voluminous tonalitic Main Phase and a mafic Border Complex. The Border Complex dominates the NW region and rims the central part of the pluton, but is absent in the southern portion of the pluton.

Variations in mineral chemistry can generally be correlated with increasing whole-rock differentiation. Whole-rock analyses for Cardinal Peak rocks define a calc-alkaline trend, and fall within the medium-K series of Peccerillo and Taylor (1976). On major and trace element Harker diagrams, central and SE tonalites are clustered and tend to follow clear trends, while NW and mafic rocks show more scatter. Rare earth element diagrams show that many mafic central Border Complex rocks have been affected by hornblende accumulation. They also show that central and SE tonalites are much more depleted in LREE than NW tonalites.

Thermometry and barometry on Cardinal Peak samples yield temperatures of approximately 820°C and pressures of approximately 7 kbar.

Any petrologic model for the Cardinal Peak pluton must be able to explain both the range and spatial distribution of rock compositions found in the pluton. From the evidence presented in this study, the following model is favored for the formation of the pluton, as illustrated in Figure 51. The sequence of events is as follows: 1) Evolved

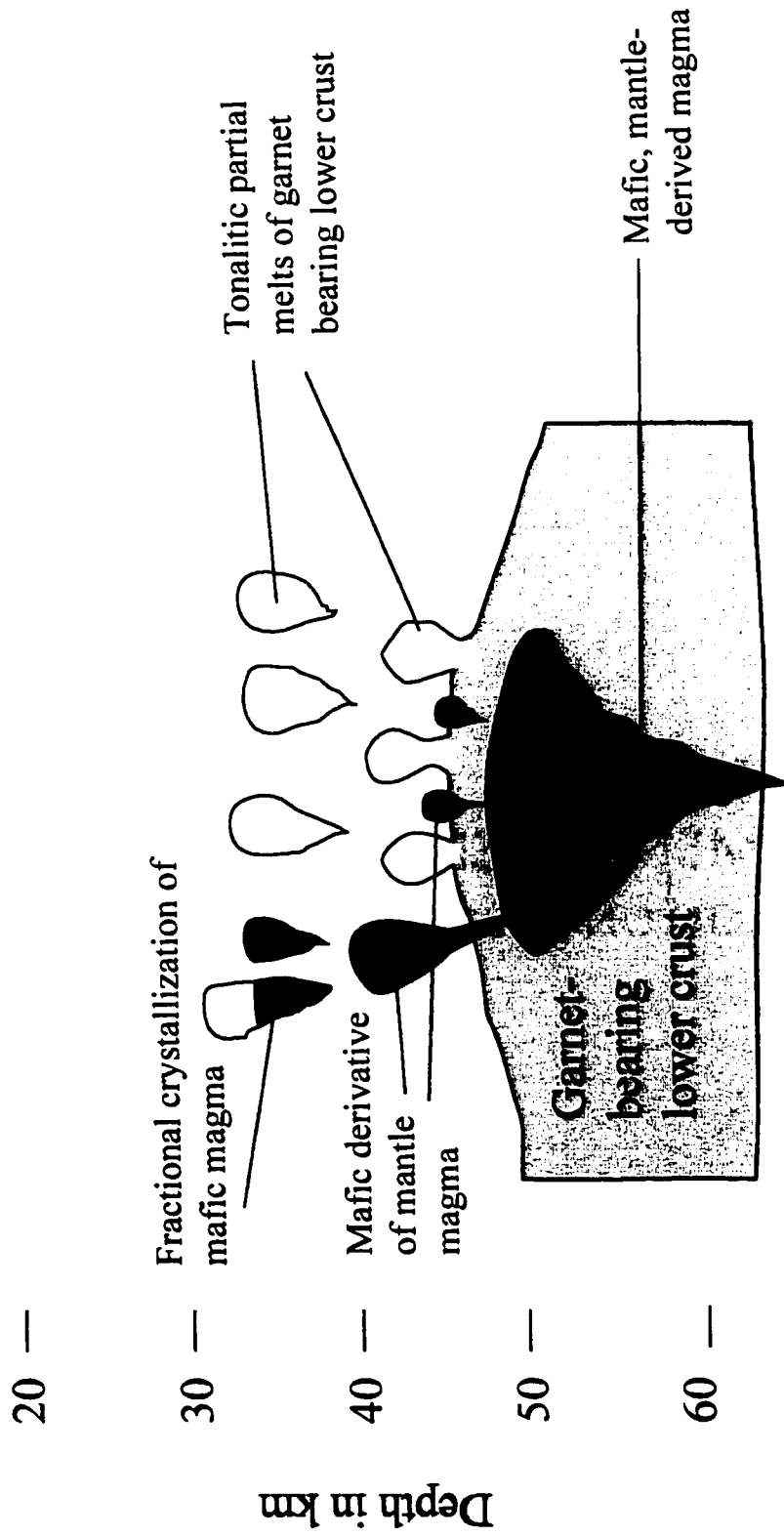


Figure 51. Cartoon illustrating petrogenesis of the tonalitic and mafic rocks of the Cardinal Peak pluton.

mantle-derived magmas were emplaced as the NW and central Border Complex and some of the NW Main Phase. Fractional crystallization of these mafic magmas produced most of the NW Main Phase tonalite. 2) Some of the mantle-derived magmas stalled in the lower crust, causing partial melting of a mafic lower crust and subsequent production of tonalitic magma. These lower-crustal melts then rose along the same conduits previously utilized by the mafic magmas and formed the central and SE Main Phase. Some assimilation of Precambrian crust also took place at this time, as shown by the 2.0 Ga zircons found in the Cardinal Peak pluton (Haugerud et al., 1991). 3) Mafic magmatism continued throughout pluton emplacement, evidence of which is found in mafic enclaves from the central and SE Main Phase. Some mixing of mafic and felsic magmas may have occurred; however, mixing was not extensive. The favored model for magma chamber construction requires that the pluton was created by a series of pulses, consisting of mafic to felsic magmas in the NW and central Border Complex, but predominantly tonalitic magma in the central and SE Main Phase.

References

- Armstrong, J. T., 1995, CITZAF: A package of correction programs for the quantitative electron microbeam x-ray analysis of thick polished materials, thin films, and particles: *Microbeam Analysis*, v. 4, p. 177-200.
- Arth, J. G., 1979, Some trace elements in trondhjemites: their implications to magma genesis and paleotectonic setting, *in* Barker, F. (editor), *Trondhjemites, dacites, and related rocks*: Elsevier, New York, p. 123-132.
- Arth, J. G., Barker, F., Peterman, Z. E., and Friedman, I., 1978, Geochemistry of the gabbro-diorite-tonalite-trondhjemite suite of Southwest Finland and its implications for the origin of tonalitic and trondhjemitic magmas: *Journal of Petrology*, v. 19, p. 289-316.
- Barker, F., 1979, Trondhjemite; definition, environment and hypotheses of origin, *in* Barker, F. (editor), *Trondhjemites, dacites, and related rocks*: Elsevier, Amsterdam, p. 1-12.
- Barker, F., and Arth, J. G., 1976, Generation of trondhjemitic-tonalitic liquids and Archean bimodal trondhjemite-basalt suites: *Geology*, v. 4, p. 596-600.
- Barker, F., Arth, J. G., and Hudson, T., 1981, Tonalites in crustal evolution: *Philosophical Transactions of the Royal Society of London, Series A: Mathematical and Physical Sciences*, v. 301, p. 293-303.
- Barnes, C. G., Petersen, S. W., Kistler, R. W., Murray, R. W., and Kays, M. A., 1996, Source and tectonic implications of tonalite-trondhjemite magmatism in the Klamath Mountains: *Contributions to Mineralogy and Petrology*, v. 123, p. 40-60.
- Barrie, C. T., 1995, Zircon thermometry of high-temperature rhyolites near volcanic-associated massive sulfide deposits, Abitibi Subprovince, Canada: *Geology*, v. 23, p. 169-172.
- Barth, A. P., 1990, Mid-crustal emplacement of Mesozoic plutons, San Gabriel Mountains, California, and implications for the geologic history of the San Gabriel Terrane, *in* Anderson, J. L. (editor), *The nature & origin of Cordilleran magmatism: Memoir - Geological Society of America*, v. 174, p. 33-45.
- Beard, J. S., 1997, Geochemistry and petrogenesis of tonalite dikes in the Smith River allochthon, south-central Virginia, *in* Sinha, A.K., Whalen, J.B., and Hogan, J.P.

- (editors), *The Nature of Magmatism in the Appalachian Orogen: Geological Society of America Memoir 191*, p. 75-86.
- Beard, J., and Lofgren, G., 1991, Dehydration melting and water saturated melting of basaltic and andesitic greenstones and amphibolites at 1, 3, and 6-9 kb: *Journal of Petrology*, v. 32, p. 365-401.
- Blundy, J. D., and Holland, T. J. B., 1990, Calcic amphibole equilibria and a new amphibole-plagioclase geothermometer: *Contributions to Mineralogy and Petrology*, v. 104, p. 208-224.
- Bowen, N. L., 1956, *The evolution of the igneous rocks*: Princeton University Press, Princeton, N.J., 336 p.
- Brown, E. H., and Walker, N. W., 1993, A magma-loading model for Barrovian metamorphism in the southeast Coast plutonic complex, British Columbia and Washington: *Geological Society of America Bulletin*, v. 105, p. 479-500.
- Bryan, W. B., Finger, L. W., and Chayes, F., 1969, Estimating proportions in petrographic mixing equations by least-squares approximation: *Science*, v. 163, p. 926-927.
- Cater, F., 1982, *Intrusive rocks of the Holden and Lucerne quadrangles*, Washington: U. S. G. S. Prof. Paper 1220, 108 p.
- Cater, F. W., and Crowder, D. F., 1967, *Geologic map of the Holden Quadrangle, Snohomish and Chelan counties, Washington*, Geologic Quadrangle Map 0646: U. S. Geological Survey, Reston, VA.
- Cater, F. W., and Wright, T. L., 1967, *Geologic map of the Lucerne Quadrangle, Chelan County, Washington*, Geologic Quadrangle Map 0647: U. S. Geological Survey, Reston, VA.
- Cawthorn, R. G., and O'Hara, M. J., 1976, Amphibole fractionation in calc-alkaline magma genesis: *American Journal of Science*, v. 276, p. 309-329.
- Cui, Y., and Russell, J. K., 1995, Magmatic origins of calc-alkaline intrusions from the Coast Plutonic Complex, southwestern British Columbia: *Canadian Journal of Earth Sciences*, v. 32, p. 1643-1667.
- Dawes, R. L., 1993, *Mid-crustal, Late Cretaceous plutons of the North Cascades; petrogenesis and implications for the growth of continental crust [Ph. D. Dissertation]*: University of Washington, Seattle, WA, 273 p.

- Dragovich, J. D., Cary, J.A., and Brown, E. H., 1989, Stratigraphic and structural relations of the Cascade River Schist, North Cascades, Washington: G. S. A. Abstracts with Programs 1989, v. 21, p. 74.
- Drummond, M. S., and Defant, M. J., 1990, A model for trondhjemite-tonalite-dacite genesis and crustal growth via slab melting; Archean to modern comparisons: *Journal of Geophysical Research, B, Solid Earth and Planets*, v. 95, p. 21,503-21,521.
- Flanagan, F. J., 1976, Nineteen seventy two (1972) compilation of data on USGS standards, *in* Flanagan, F. J. (editor), Description and analyses of eight new USGS rock standards: US Geological Survey Professional Paper 840, p 131-183.
- Gill, J.B., 1981, *Orogenic andesites and plate tectonics*: Springer-Verlag, New York, 90 p.
- Grujic, D., and Mancktelow, N. S., 1998, Melt-bearing shear zones: analogue experiments and comparison with examples from southern Madagascar: *Journal of Structural Geology*, v. 20, p. 673-680.
- Hammarstrom, J. M., and Zen, E., 1986, Aluminum in hornblende; an empirical igneous Geobarometer: *American Mineralogist*, v. 71, p. 1297-1313.
- Harrison, T. M., and Watson, E. B., 1984, The behavior of apatite during crustal anatexis: equilibrium and kinetic considerations: *Geochimica et Cosmochimica Acta*, v. 48, p. 1467-1477.
- Hart S.R., and Davis, K.E., 1978, Nickel partitioning between olivine and silicate melt: *Earth and Planetary Science Letters*, v. 44, p. 159-161.
- Haugerud, R. A., Van der Heyden, P., Tabor, R. W., Stacey, J. S., and Zartman, R. E. 1991, Late Cretaceous and early Tertiary plutonism and deformation in the Skagit gneiss complex, North Cascade Range, Washington and British Columbia: *Geological Society of America Bulletin*, v. 103, p.1297-1307.
- Hill, R. I., 1988, San Jacinto intrusive complex; 1, Geology and mineral chemistry, and a model for intermittent recharge of tonalitic magma chambers: *Journal of Geophysical Research, B, Solid Earth and Planets*, v. 93, p. 10,325-10,348.
- Hollister, L. S., Grissom, G. C., Peters, E. K., Stowell, H. H., and Sisson, V. B. , 1987, Confirmation of the empirical correlation of A in hornblende with pressure of solidification of calc-alkaline plutons: *American Mineralogist*, v. 72, p. 231-239.
- Hopson, C., A., and Mattinson, J. M., 1994, Chelan Migmatite Complex, Washington: Field evidence for mafic magmatism, crustal anatexis, mixing and protodiapric

- emplacement, in Swanson, D.A., and Haugerud, R.A., (editors), *Geologic Field Trips in the Pacific Northwest: Geological Society of America, Chapter 2K*, p.1-21.
- Hurban, G. K., 1991, Fabric study and structural history of deformed plutonic and metamorphic rocks in the Holden area, North Cascades, Washington [M.S. Thesis]: Western Washington University, Bellingham, WA, p. 118.
- Irvine, T. N., and Baragar, W.R.A., 1971, A guide to the chemical classification of common volcanic rocks: *Canadian Journal of Earth Sciences*, v. 8, p. 523-548
- Johnson, D.M., Hooper, P.R., and Conrey, R.M., 1998, XRF Analysis of rocks and minerals for major and trace elements on a single low dilution Li-tetraborate fused bead: *Advances in X-ray Analysis*, v. 41 (in press).
- Johnson, M.C., and Rutherford, M. J., 1989, Experimental calibration of the aluminum-in-hornblende geobarometer with application to Long Valley Caldera (California) volcanic rocks: *Geology*, v. 17, p. 837-841.
- Kinzler, B. J., Grove, T. L., and Recca, S. I., 1990, An experimental study on the effect of temperature and melt composition on the partitioning of nickel between olivine and silicate melt: *Geochimica et Cosmochimica Acta*, v. 54, p. 1255-1265.
- Krauskopf, K. B., and Bird, D. K., 1995, *Introduction to Geochemistry*: McGraw-Hill, New York, 647 p.
- Leake, B. E. , 1978, Nomenclature of amphiboles: *American Mineralogist*, v. 63, p. 1023-1052.
- Martin, H., 1987, Petrogenesis of Archaean trondhjemites, tonalites and granodiorites from eastern Finland; major and trace element geochemistry: *Journal of Petrology*, v. 28, p. 921-953.
- McGroder, M. F., 1991, Reconciliation of two-sided thrusting, burial metamorphism, and diachronous uplift in the Cascades of Washington and British Columbia: *Geological Society of America Bulletin*, v. 103, p. 189-209.
- McNulty, B. A., Vernon, R. H., and Tobisch, O. T., 1996, Heterogeneous microgranitoid enclave swarms; possible mechanisms of formation: *Abstracts with Programs, Cordilleran Section, Geological Society of America*, v. 28, p. 90.
- Miller, R.B., Bowring, S.A., and Hoope, W.J., 1989, Paleocene plutonism and its tectonic implications, North Cascades, Washington: *Geology*, v. 17, p. 846-849.

- Miller, R. B., Brown, E. H., McShane, D. P., and Whitney, D. L., 1993, Intra-arc crustal loading and its tectonic implications, North Cascades crystalline core, Washington and British Columbia: *Geology*, v. 21, p. 255-258.
- Miller, R. B., Haugerud, R. A., Murphy, F., and Nicholson, L. S., 1994, Tectonostratigraphic framework of the northeastern Cascades: Washington Division of Geology and Earth Resources, v. 80, p. 73-92.
- Miller, R. B., and Paterson, S. R., 1995, Structure and magma chamber dynamics of mid- to lower-crustal sheeted plutons, North Cascades, Washington: GSA Abstracts with Programs 1995, Cordilleran Section, v. 27, p. 65.
- Miller, R. B., and Paterson, S. R., 1998, Mid-crustal magmatic sheets in the Cascades Mountains, Washington: implications for magma ascent: *Journal of Structural Geology*, v. 20, p. 1345-1363.
- Misch, P., 1966, Tectonic evolution of the NW Cascades of Washington State: a west-cordilleran case history: *Canadian Institute of Mining and Metallurgy*, v. 8, p. 101-148.
- Misch, P., 1988, Tectonic and metamorphic evolution of the North Cascades; an overview, *in* Ernst, W. G. (editor), *Metamorphism and crustal evolution of the Western United States (Rubey Volume 7)*: Prentice Hall, Englewood Cliffs, N.J. p. 179-195.
- Murphy, F., 1996, Metamorphism and protoliths of the younger gneissic rocks of the Holden area, North Cascades crystalline core, Washington: Abstracts with Programs, Cordilleran Section Geological Society of America, v. 28, p. 94.
- Naney, M. T., 1983, Phase equilibria of rock-forming ferromagnesian silicates in granitic systems: *American Journal of Science*, v. 283, p. 993-1033.
- Paterson, S. R., Fowler, T. K., Schmidt, K. L., Yoshinobu, A. S., Yuan, E. S., and Miller, R. B., 1998, Interpreting magmatic fabric patterns in plutons: *Lithos*, v. 44, p. 53-82.
- Paterson, S. R., and Miller, R. B., 1998, Mid-crustal magmatic sheets in the Cascades Mountains, Washington: implications for magmatic ascent: *Journal of Structural Geology*: v. 20, p. 1345-1363
- Patino Douce, A. E., and Beard, J. S., 1995, Dehydration-melting of biotite gneiss and quartz amphibolite from 3 to 15 kbar: *Journal of Petrology*, v. 36, p. 707-738.

- Peccerillo, A., and Taylor, S. R., 1976, Geochemistry of Eocene calc-alkaline volcanic rocks from the Kastamonu area, NW Turkey: *Contributions to Mineralogy and Petrology*, v. 58, p. 63-81.
- Pitcher, W. 1993, *The Nature and Origin of Granite*: Blackie Academic and Professional, London, 321 p.
- Rapp, R. P., Watson, E. B., and Miller, C. F., 1991, Partial melting of amphibolite/eclogite and the origin of Archean trondhjemites and tonalites: *Precambrian Research*, v. 51, p. 1-25.
- Rutter, M. J., Van der Laan, S. R., and Wyllie, P. J., 1989, Experimental data for a proposed empirical igneous geobarometer; aluminum in hornblende at 10 kbar pressure: *Geology*, v. 17, p. 897-900.
- Sato, H., 1977, Nickel content of basaltic magma: Identification of primary magmas and measure of the degree of olivine fractionation: *Lithos*, v. 10, p. 113-120.
- Schmidt, M. W., 1992, Amphibole composition in tonalite as a function of pressure; an experimental calibration of the Al-in-hornblende barometer: *Contributions to Mineralogy and Petrology*, v. 110, p. 304-310.
- Sen, C., and Dunn, T., 1994, Dehydration melting of a basaltic composition amphibolite at 1.5 and 2.0 Gpa: implications for the origin of adakites: *Contributions to Mineralogy and Petrology*, v. 117, p. 394-409.
- Sisson, T. W., Grove, T. L., and Coleman, D. S., 1996, Hornblende gabbro sill complex at Onion Valley, California, and a mixing origin for the Sierra Nevada batholith: *Contributions to Mineralogy and Petrology*, v. 126, p. 81-108.
- Streckeisen, A., 1976, To each plutonic rock its proper name: *Earth Science Reviews*, v. 12, p. 1-33.
- Tabor, R., Haugerud, R., Miller, R., Brown, E., and Babcock, R., 1989, *Accreted terranes of the North Cascades range, Washington*: American Geophysical Union Field Trip Guidebook T307, 62 p.
- Talbot, C. J., Ronnlund, P., Schmeling, H., Koyi, H. and Jackson, M. P. A., 1991, Diapiric spoke patterns: *Tectonophysics*, v. 188, p. 187-201
- Tatsumi, Y., 1989, Migration of fluid phases and genesis of basalt magmas in subduction zones: *Journal of Geophysical Research*, v. 94, p. 4697-4707
- Tatsumi, Y., and Eggins, S., 1995, *Subduction Zone Magmatism*: Blackwell Science, Cambridge, MA, 211 p.

- Tepper, J. H., 1996, Petrology of mafic plutons associated with calc-alkaline granitoids, Chilliwack batholith, North Cascades, Washington: *Journal of Petrology*, v. 37, p. 1409-1436.
- Tepper, J. H., Nelson, B. K., Bergantz, G. W., and Irving, A. J., 1993, Petrology of the Chilliwack batholith, North Cascades, Washington; generation of calc-alkaline granitoids by melting mafic lower crust with variable water fugacity: *Contributions to Mineralogy and Petrology*, v. 113, p. 333-351.
- Tobisch, O. T., McNulty, B. A., and Vernon, R. H., 1996, Geometry of heterogeneous microgranitoid enclave swarms with special reference to "layering dikes," central Sierra Nevada, California: *Abstracts with Programs, Cordilleran Section, Geological Society of America*, v. 28, p. 118.
- Ulmer, P., 1986, *Basisch und ultrabasische Gesteine des Adamele*: [Ph.D. Dissertation], ETH Surich, Switzerland.
- Vance, J. A., 1957, The geology of the Sauk River area in the northwest Cascades of Washington: [Ph.D. Dissertation], University of Washington, Seattle, WA, 312 p.
- Watson, E. B., and Harrison, T. M., 1983, Zircon saturation revisited; temperature and composition effects in a variety of crustal magma types: *Earth and Planetary Science Letters*, v. 64, p. 295-304.
- White, L.D., Maley, C. A., Barnes, I., and Ford, A.B., 1988, Oxygen isotopic data for plutonic rocks and gneisses of the Glacier Peak Wilderness and vicinity, northern Cascades, Washington: U.S.G.S. OFR 86-76, 35 p.
- Whitney, D.L., Miller, R. B., and Paterson, S.R., 1999, P-T-t evidence for mechanisms of vertical tectonic motion in a contractional orogen: north-western US and Canadian Cordillera: *Journal of Metamorphic Geology*, v. 17, p. 75-90.
- Wilson, M., 1989, *Igneous Petrogenesis*: Unwin Hyman, London, 466 p.
- Winther, K. T., 1996, An experimentally based model for the origin of tonalitic and trondhjemitic melts: *Chemical Geology*, v. 127, p. 43-59.
- Wolf, M. B., and London, D., 1994, Apatite dissolution into peraluminous haplogranitic melts; an experimental study of solubilities and mechanisms: *Geochimica et Cosmochimica Acta*, v. 58, p. 4127-4145.
- Wolf, M. B., and Wyllie, P. J., 1991, Dehydration-melting of solid amphibolite at 10 kbar; textural development, liquid interconnectivity and applications to the segregation of magmas: *Mineralogy and Petrology*, v. 44, p. 151-179.

- Wolf, M. B., and Wyllie, P. J., 1994, Dehydration melting of amphibolite at 10 kbar: the effects of temperature and time: *Contributions to Mineralogy and Petrology*, v. 115 p. 369-383.
- Wyllie, P. J., 1977, Crustal anatexis; an experimental review: *Tectonophysics*, v. 43, p. 41-71.
- Yoder, H. S., Jr., 1976, *Generation of basaltic magma*: National Academy of Sciences, Washington D.C., 265 p.
- Zen, E., and Hammarstrom, J., 1984, Magmatic epidote and its petrologic significance: *Geology*, v. 12, p. 515-518.

APPENDIX A
CHEMICAL ANALYSES FROM CATER (1982)

Analyses of two Cardinal Peak hornblende-biotite tonalites from Cater (1982)

Sample	1	2
Chemical analyses (percent)		
SiO ₂	66.9	65.3
Al ₂ O ₃	16.5	18.5
Fe ₂ O ₃	1.26	1.38
FeO	2.21	2.44
MgO	0.96	0.93
CaO	4.1	5
Na ₂ O	4.36	4.55
K ₂ O	1.61	1.17
Mn	0.061	0.092

Semiquantitative spectrographic analyses (parts per million)

Ba	1000	700
Co	15	15
Cr	50	7
Cu	100	100
Ga	50	30
Ni	20	n.d.
Sc	10	15
Sr	1500	1000
V	100	100
Y	10	15
Yb	1.5	1.5
Zr	70	50

APPENDIX B
WHOLE ROCK CHEMICAL ANALYSES

Acronyms and abbreviations used:

Methods: WSU=Washington State University, SJSU=San Jose State University,

UM=University of Michigan.

Minerals: hb=hornblende, bt=biotite, qz=quartz.

Locations: First letter: N=NW, C=central, S=SE.

Second and third letters: BC=Border Complex, MP=Main Phase.

Sample:	1	15	10	9	84B	53D
Rock Type:	hornblende	hornblende	hb gabbro	hb gabbro	hb gabbro	hb gabbro
Location:	CBC	CBC	CBC	CBC	NBC	NMP
Latitude:	48.1192	48.1231	48.1230	48.1229	48.2340	48.2067
Longitude:	120.6567	120.6660	120.6677	120.6619	120.7914	120.7611
Method:	WSU XRF	WSU ICP-MS	WSU ICP-MS	WSU XRF	WSU XRF	WSU XRF
Normalized Oxides (Wt. %), all Fe reported as FeO						
SiO₂	52.16	59.70	49.37	50.43	49.61	51.90
Al₂O₃	10.48	7.60	13.65	20.87	21.74	18.75
TiO₂	0.81	0.47	0.89	1.27	1.37	1.10
FeO	7.74	7.91	9.34	8.50	8.34	8.17
MnO	0.16	0.18	0.17	0.14	0.12	0.17
CaO	12.63	10.87	10.37	9.46	9.66	9.11
MgO	14.00	12.33	13.62	4.17	3.83	5.99
K₂O	0.35	0.27	0.46	0.49	0.79	0.50
Na₂O	1.54	0.63	2.04	4.46	4.24	4.08
P₂O₅	0.14	0.04	0.09	0.23	0.31	0.23
Trace Elements (ppm)						
Ni	198	107	152	2	3	32
Cr	975	788	446	10	10	118
Sc	43	40	37	24	23	28
V	226	185	246	235	198	210
Ba	152	98	120	158	306	230
Rb	4	5	9	8	14	12
Sr	249	151	264	683	788	606
Zr	48	50	51	119	133	297
Y	19	18	18	25	21	20
Nb	1.40	2.10	2.90	3.62	5.00	4.07
Ga	11	8	15	20	24	19
Cu	95	47	47	99	43	15
Zn	78	83	76	86	92	103
Pb	3	2	2	6	4	3
Th	0	2	0	2	0	0
Method:	OSU INAA	WSU ICPMS	WSU ICPMS	OSU INAA	OSU INAA	OSU INAA
Rare Earth Elements (ppm)						
La	4.7	4.22	3.14	5.1	7.8	8.2
Ce	12.6	10.37	7.65	14.2	20.6	20.7
Pr		1.61	1.28			
Nd	12	8.20	6.69	14.7	15.1	14.6
Sm	3.11	2.73	2.39	4.43	4.15	3.72
Eu	0.91	0.80	0.88	1.52	1.41	1.44
Gd		3.13	2.77			
Tb	0.46	0.53	0.48	0.91	0.64	0.73
Dy		3.27	3.13			
Ho		0.65	0.65			
Er		1.70	1.77			
Tm		0.23	0.25			
Yb	1.8	1.41	1.52	2.5	1.9	2.15
Lu	0.24	0.22	0.23	0.35	0.21	0.32

Sample:	7	24a	6a	53c	5c	55a
Rock Type:	hb gabbro	qz hb/bt gabrro	hb diorite	hb diorite	hb diorite	qz hb/bt diorite
Location:	CBC	CBC	CBC	NMP	CBC	NMP
Latitude:	48.1229	48.1340	48.1229	48.2067	48.1225	48.2014
Longitude:	120.6628	120.6493	120.6640	120.7611	120.6634	120.7621
Method:	no majors	WSU XRF	WSU XRF	SJSU XRF	WSU XRF	SJSU XRF
SiO ₂		49.69	50.66	54.84	54.36	56.54
Al ₂ O ₃		18.89	22.03	22.49	24.47	17.26
TiO ₂		1.25	0.73	0.64	0.14	1.03
FeO		9.13	6.46	4.63	2.66	7.92
MnO		0.17	0.10	0.07	0.06	0.12
CaO		10.17	10.83	8.75	9.83	7.68
MgO		6.68	4.80	2.13	2.99	3.59
K ₂ O		0.90	0.31	0.68	0.29	1.54
Na ₂ O		2.96	3.96	5.48	5.17	3.99
P ₂ O ₅		0.15	0.13	0.30	0.04	0.33
Ni		23	5		5	
Cr	4	51	15	4	4	19
Sc	24	31	25	7.50	10	17.3
V		290	141		32	
Ba	131	264	128	226	141	4.66
Rb	6	18	4	7	4	23
Sr		493	784		1247	
Zr		68	52		51	
Y		23	15		1	
Nb		3.45	1.56		0.62	
Ga		22	24		21	
Cu		0	64		19	
Zn	116	95	62	50	31	99
Pb		1	2		2	
Th	nd	2	0	0.1	0	1.37
Method:	OSU INAA	OSU INAA	OSU INAA	OSU INAA	OSU INAA	OSU INAA
La	4	5.7	4.1	6.7	2.6	11.1
Ce	12.2	15.0	11.2	16.0	5.3	26.1
Pr						
Nd	12.6	10.2	9	10.3	3.4	16.1
Sm	4.1	3.49	2.87	2.46	0.6	3.59
Eu	1.39	1.25	1.06	1.03	0.54	1.05
Gd						
Tb	0.87	0.69	0.6	0.36	0.09	0.63
Dy						
Ho						
Er						
Tm						
Yb	2	2.0	1.4	0.8	0.2	1.8
Lu	0.32	0.30	0.06	0.12	0.03	0.25

Sample:	24e	54	88b	86b	84A	81B
Rock Type:	qz hb/bt diorite	qz hb/bt diorite	qz hb/bt diorite	qz hb/bt diorite	hb tonalite	hb tonalite
Location:	CBC	NMP	NMP	NMP	NBC	SMP
Latitude:	48.1340	48.2072	48.1918	48.1863	48.2346	48.1242
Longitude:	120.6493	120.7628	120.7428	120.7364	120.7914	120.6122
Method:	WSU XRF	WSU XRF	SJSU XRF	WSU XRF	WSU XRF	WSU XRF
SiO2	53.56	59.72	60.06	60.56	61.87	64.61
Al2O3	17.61	17.36	16.94	17.91	17.15	17.41
TiO2	0.93	0.822	0.71	0.95	0.65	0.61
FeO	7.72	6.34	6.70	5.39	5.15	4.22
MnO	0.16	0.110	0.14	0.11	0.12	0.07
CaO	8.97	7.01	6.41	6.44	6.22	6.34
MgO	6.18	3.69	3.01	3.36	3.51	1.70
K2O	0.78	0.69	1.72	1.67	0.80	0.33
Na2O	3.90	4.07	4.08	3.37	4.38	4.53
P2O5	0.17	0.187	0.23	0.24	0.16	0.18
Ni	29	22		12	13	3
Cr	79	74	5	58	49	6
Sc	24	23	18.60	14	16	13
V	212	149		107	113	69
Ba	247	320	611	618	295	221
Rb	24	11	47	40	15	8
Sr	444	500		546	498	818
Zr	93	115		153	96	159
Y	18	18		22	16	10
Nb	4.33	5.6		7.18	4.76	3.37
Ga	16	21		22	18	19
Cu	32	16		1	0	12
Zn	75	80	80	77	73	40
Pb	1	3		5	4	1
Th	1	3	1.4	3	1	1
Method:	OSU INAA	OSU INAA	OSU INAA	OSU INAA	OSU INAA	OSU INAA
La	8.0	9.4	6.8	12.7	11.1	14.4
Ce	19.1	22.2	15.4	31.1	26.9	31.2
Pr						
Nd	13.2	14.9	9.3	19.0	14.8	16.8
Sm	3.04	3.36	2.57	4.46	3.09	3.20
Eu	1.07	1.1	0.89	1.22	1.00	1.11
Gd						
Tb	0.56	0.61	0.51	0.72	0.45	0.38
Dy						
Ho						
Er						
Tm						
Yb	2.1	1.77	1.9	2.1	1.6	0.9
Lu	0.27	0.28	0.25	0.24	0.20	0.10

Sample:	81A	PM164	PM171	17a	86c	77
Rock Type:	hb/bt tonalite	hb/bt tonalite	hb/bt tonalite	bt/hb tonalite	bt tonalite	bt tonalite
Location:	SMP	SMP	SMP	CBC	NMP	SMP
Latitude:	48.1242	48.0866	48.0898	48.1229	48.1863	48.1002
Longitude:	120.6122	120.5809	120.5878	120.6606	120.7364	120.6287
Method:	WSU XRF	SJSU XRF	no majors	WSU XRF	WSU XRF	SJSU XRF
SiO ₂	63.62	62.08		67.69	66.12	64.43
Al ₂ O ₃	18.28	17.73		16.93	17.87	17.55
TiO ₂	0.62	0.57		0.49	0.516	0.60
FeO	3.94	5.04		3.06	3.36	4.16
MnO	0.07	0.10		0.05	0.068	0.08
CaO	5.57	6.34		5.01	4.40	4.98
MgO	1.73	2.09		1.28	1.45	2.06
K ₂ O	1.13	1.03		0.85	1.59	1.42
Na ₂ O	4.86	4.75		4.47	4.42	4.45
P ₂ O ₅	0.20	0.28		0.17	0.204	0.26
Ni	6			4	6	
Cr	6	5.09	9.95	3	10	
Sc	9	8.92	13.10	7	13	
V	76			54	69	
Ba	501	290	783.00	493	618	
Rb	33	18.60	27.40	19	70	
Sr	716			708	646	
Zr	139			125	109	
Y	11			7	10	
Nb	5.42			3.59	6.6	
Ga	21			20	23	
Cu	6			0	9	
Zn	64	67.10	69.80	70	71	
Pb	7			4	7	
Th	2	0.29	2.70	3	1	
Method:	OSU INAA	OSU INAA		OSU INAA	OSU INAA	UM INAA
La	12.1	5.1		21	8.7	14.41
Ce	28.5	11.4		42		29.07
Pr						
Nd	17.2			19.9	8.6	12.8
Sm	3.59	2.48		3.45	2.45	3.37
Eu	1.16	1.06		1.04	0.85	1.09
Gd						
Tb	0.44	<8		0.42	0.33	0.29
Dy						1.59
Ho						
Er						
Tm						
Yb	1.0	1.1		0.6	0.9	0.51
Lu	0.08	0.13		0.11	0.12	0.11

Sample:	61	79b	60	40a	21b	58
Rock Type:	bt tonalite	bt tonalite	bt tonalite	bt tonalite	bt tonalite	bt tonalite
Location:	SMP	SMP	SMP	SMP	CBC	SMP
Latitude:	48.0824	48.1102	48.0812	48.0500	48.1271	48.0792
Longitude:	120.5866	120.6240	120.5926	120.5267	120.6563	120.5942
Method:	SJSU XRF	SJSU XRF	SJSU XRF	SJSU XRF	SJSU XRF	SJSU XRF
SiO2	64.65	65.10	65.12	65.32	65.43	65.26
Al2O3	17.52	17.30	17.42	17.44	17.34	17.36
TiO2	0.61	0.59	0.59	0.57	0.61	0.56
FeO	3.93	3.85	3.83	3.66	3.78	3.78
MnO	0.07	0.07	0.07	0.07	0.06	0.07
CaO	4.84	4.93	4.75	4.45	4.66	4.48
MgO	1.90	1.94	1.86	1.97	1.95	1.91
K2O	1.55	1.28	1.54	1.72	1.50	1.84
Na2O	4.69	4.69	4.56	4.57	4.41	4.50
P2O5	0.24	0.25	0.26	0.24	0.25	0.23
Ni						
Cr				3.00	3.00	
Sc				3.73	4.13	
V						
Ba				618.00	825.00	
Rb				34.00	30.00	
Sr						
Zr						
Y						
Nb						
Ga						
Cu						
Zn				57.00	53.00	
Pb						
Th				1.30	1.40	
Method:	UM INAA	UM INAA	UM INAA	OSU INAA	OSU INAA	UM INAA
La	17.08	14.11	17.03	12.3	13	11.82
Ce	34	32.17	32.62	25.4	26.2	24.25
Pr						
Nd	11.86	15.62	10.06	13.4	14.4	8.55
Sm	3.31	2.78	3.55	2.81	2.91	2.6
Eu	0.98	1.04	1.02	0.88	1.01	0.91
Gd						
Tb	0.21	0.21	0.23	0.32	0.34	0.24
Dy	1.01	0.9	1.61			2.09
Ho						
Er						
Tm						
Yb	0.29	0.26	0.35	0.52	0.45	0.66
Lu	0.07	0.05	0.06	0.08	0.11	0.11

Sample:	23	89	80C	42f	30	28a
Rock Type:	bt tonalite	bt tonalite	bt tonalite	bt tonalite	bt tonalite	bt tonalite
Location:	CBC	SMP	SMP	SMP	CMP	CMP
Latitude:	48.1328	48.0484	48.1193	48.0546	48.1086	48.1080
Longitude:	120.6493	120.5165	120.6152	120.5315	120.6336	120.6351
Method:	SJSU XRF	SJSU XRF	WSU XRF	SJSU XRF	WSU XRF	WSU XRF
SiO ₂	65.10	67.74	66.02	66.72	66.55	66.79
Al ₂ O ₃	17.26	16.73	17.97	17.34	17.46	17.30
TiO ₂	0.61	0.49	0.50	0.45	0.53	0.51
FeO	4.01	3.12	3.01	2.99	3.11	3.17
MnO	0.08	0.07	0.05	0.06	0.06	0.06
CaO	4.63	3.84	4.84	4.13	4.70	4.51
MgO	1.98	1.58	1.25	1.69	1.29	1.24
K ₂ O	1.69	1.68	1.05	1.70	1.32	1.48
Na ₂ O	4.39	4.53	5.13	4.70	4.79	4.75
P ₂ O ₅	0.24	0.21	0.18	0.21	0.19	0.19
Ni			5		3	3
Cr	3.48		2	3.00	3	6
Sc	5.92		6	2.95	8	8
V			49		56	47
Ba	841.00		626	642.00	663	686
Rb	33.60		28	27.00	30	37
Sr			758		682	640
Zr			132		130	130
Y			6		7	12
Nb			3.43		4.67	6.86
Ga			21		22	21
Cu			3		0	2
Zn	83.10		87	58.00	83	89
Pb			8		7	7
Th	3.21		2	1.80	4	1
Method:	OSU INAA	UM INAA	UM INAA	OSU INAA	OSU INAA	UM INAA
La	17.6	14.02	18.72	10.8	26.2	30.81
Ce	38.7	29.4	40.52	22.3	54.9	62.33
Pr						
Nd	17.0	10.55	12.8	13	27.4	25.18
Sm	3.71	2.92	3.42	2.19	4.71	6.15
Eu	1.07	0.88	1.06	0.82	1.16	1.63
Gd						
Tb	0.37	0.12	0.21	0.2	0.45	0.43
Dy			1.95			2.56
Ho						
Er						
Tm						
Yb	0.8	0.29	0.3	0.47	0.59	0.74
Lu	0.12	0.08	0.04	0.07	0.11	0.09

Sample:	62	92	67B	45	90	28B
Rock Type:	bt tonalite	bt tonalite	bt tonalite	bt tonalite	bt tonalite	bt tonalite
Location:	SMP	SMP	SMP	SMP	SMP	CMP
Latitude:	48.0802	48.0487	48.0957	48.0638	48.0477	48.1080
Longitude:	120.5843	120.5071	120.5942	120.5488	120.5127	120.6351
Method:	WSU XRF	WSU XRF	WSU XRF	WSU XRF	SJSU XRF	WSU XRF
SiO2	66.43	66.92	67.27	67.10	68.72	67.98
Al2O3	17.52	17.53	17.38	18.28	16.81	17.16
TiO2	0.51	0.42	0.48	0.30	0.38	0.42
FeO	3.26	2.73	2.93	2.12	2.31	2.55
MnO	0.05	0.05	0.04	0.04	0.07	0.04
CaO	4.51	4.38	4.62	4.66	3.72	4.24
MgO	1.26	1.09	1.12	0.93	1.38	1.14
K2O	1.41	1.61	1.03	1.13	1.74	1.44
Na2O	4.87	5.10	4.95	5.32	4.67	4.90
P2O5	0.18	0.16	0.17	0.13	0.20	0.13
Ni	4	6	4	4		4
Cr	5	4	4	0		4
Sc	10	7	8	3		5
V	42	44	48	29		39
Ba	711	677	642	619		723
Rb	32	34	23	24		29
Sr	717	704	737	782		656
Zr	136	122	129	113		106
Y	6	7	5	4		8
Nb	4.43	5.57	3.42	4.09		4.58
Ga	21	21	19	20		19
Cu	1	0	0	0		0
Zn	99	78	80	63		74
Pb	6	7	7	7		6
Th	2	2	2	3		2
Method:	UM INAA	UM INAA	UM INAA	OSU INAA	UM INAA	UM INAA
La	27.94	18.57	20.01	20.4	15.65	20.04
Ce	57.34	38.8	37.37	42.1	32.02	40.01
Pr						
Nd	25.39	16.14	17.39	22.4	21.2	15.24
Sm	4.76	3.34	3.69	3.55	3.06	3.87
Eu	1.21	1.02	1.01	1.1	0.8	1.12
Gd						
Tb	0.36	0.25	0.2	0.23	0.22	0.34
Dy	0.91	0.99	0.72		2.06	3.06
Ho						
Er						
Tm						
Yb	0.32	0.44	0.32	0.5	0.36	0.55
Lu	0.07	0.05	0.05	0.08	0.04	0.07

Sample:	50d	39	15f	42E	86A
Rock Type:	bt tonalite	bt tonalite	leucotonalite	leucotonalite	bt tonalite
Location:	NMP	SMP	CBC	SMP	NMP
Latitude:	48.2031	48.0417	48.1231	48.0546	48.1863
Longitude:	120.7588	120.5232	120.6609	120.5315	120.7364
Method:	WSU XRF	SJSU XRF	SJSU XRF	WSU XRF	WSU XRF
SiO₂	73.76	68.03	72.94	71.19	75.11
Al₂O₃	14.81	17.18	15.34	16.94	13.62
TiO₂	0.177	0.42	0.24	0.07	0.18
FeO	1.66	2.55	1.38	0.56	1.29
MnO	0.034	0.06	0.03	0.01	0.03
CaO	2.27	3.66	3.74	2.57	1.27
MgO	0.37	1.54	1.45	0.26	0.50
K₂O	2.10	1.65	0.62	3.48	4.31
Na₂O	4.73	4.72	4.14	4.89	3.62
P₂O₅	0.079	0.19	0.12	0.04	0.08
Ni	9			6	9
Cr	3	3.00	3.00	3	1
Sc	4	2.63	1.16	5	2
V	18			0	13
Ba	1004	737.00	237.00	3326	846
Rb	56	34.00	9.00	36	103
Sr	281			571	168
Zr	88			106	86
Y	12			2	22
Nb	6.9			1.54	9.14
Ga	17			21	16
Cu	4			0	1
Zn	30	48.00	14.00	15	36
Pb	13			18	20
Th	4	1.80	0.50	0	10
Method:	OSU INAA	OSU INAA	OSU INAA	OSU INAA	OSU INAA
La	12.8	11.6	1.6	3.2	19.6
Ce	26.8	23.3	3.8	6.3	44.8
Pr					
Nd	13.4	12.2	1.5	<3	20.9
Sm	2.62	2.37	0.44	0.56	4.74
Eu	0.63	0.77	0.33	0.41	0.56
Gd					
Tb	0.39	0.22	0.05	0.15	0.67
Dy					
Ho					
Er					
Tm					
Yb	1	0.49	0.17	0.5	1.9
Lu	0.16	0.08	0.02	0.08	0.21

APPENDIX C
PARTITION COEFFICIENTS

**Partition coefficients used in fractional crystallization models,
from Tepper et al. (1993) and Martin (1987).**

	Ilmenite	Plagioclase	Hornblende
La	0.005	0.148	0.600
Ce	0.006	0.082	0.800
Nd	0.008	0.055	1.400
Sm	0.010	0.039	1.900
Eu	0.007	1.126	2.200
Tb	0.021	0.027	2.100
Yb	0.075	0.023	1.800
Lu	0.100	0.019	1.600

Partition coefficients used in melting models, from Martin (1987).

	Clinopyroxene	Garnet	Plagioclase	Hornblende
La	.100	.040	0.130	0.200
Ce	.200	.080	0.110	0.300
Nd	.400	.200	0.070	0.800
Sm	.600	1.000	0.050	1.100
Eu	.600	.980	1.300	1.300
Tb	.700	7.500	0.037	2.000
Yb	.600	21.000	0.024	1.700
Lu	.600	21.000	0.023	1.500